

**OPTIMIZATION OF EXPERIMENTAL CONDITIONS AND ANALYSIS TOOLS
FOR THE STUDY OF PHOSPHODIESTERASE-5 IN A MODEL OF CULTURED
ADULT RAT CARDIOMYOCYTES**

by
Anél Botha

*Thesis presented in fulfilment of the requirements for the degree of
Master of Science in the Faculty of Biomedical Sciences at
Stellenbosch University*



Supervisor: Dr John Lopes

March 2017

DECLARATION

By submitting this thesis electronically, I declare that the entirety of the work contained therein is my own, original work, that I am the sole author thereof (save to the extent explicitly otherwise stated), that reproduction and publication thereof by Stellenbosch University will not infringe any third party rights and that I have not previously in its entirety or in part submitted it for obtaining any qualification.

Signature:

Date: March 2017

ABSTRACT

Part 1

Introduction: Phosphodiesterases (PDEs) hydrolyse cyclic nucleotides that regulate ischemia-reperfusion injury (IRI) in the heart. Phosphodiesterases-5 (PDE5) inhibition increases cyclic guanosine monophosphate (cGMP) levels and thereby promotes cardioprotection. Cannabidiol is a cannabinoid that can alter cGMP levels and induced protection in whole hearts. Cannabidiol-mediated cardioprotection might be controlled by specific PDEs, possibly PDE5.

This study aimed to:

- Evaluate the role of PDE5 inhibition in IRI.
- Determine whether PDE5 plays a role in cannabidiol-mediated protection.

Methods: Cultured adult rat cardiomyocytes were subjected to 20 minutes ischemia, 60 minutes reperfusion, which included mitochondrial staining to measure mitochondrial function with JC-1, followed by fluorescence microscopy and image analysis. A cardioprotective dose of cannabidiol and time of intervention was sought by administration of cannabidiol (0.001 μ M, 1 μ M and 100 μ M) during ischemia and reperfusion, only ischemia, and only reperfusion, respectively. 10 μ M Sildenafil was administered during ischemia only to inhibit PDE5.

Results: Ischemia-reperfusion reduced cell viability according to morphology by 79 % and mitochondrial function by 50 %. None of the treatments induced cardioprotection.

Conclusion: The lack of cardioprotection from cannabidiol and sildenafil might have been due to (1) the ischemic conditions being too harsh, (2) the analysis program being faulty, or (3) unreliable data from morphology analysis. These three points of concern became the basis for the new objectives investigated in Part 2 of this thesis.

Part 2

Introduction: Cell viability and mitochondrial function are parameters normally evaluated in cardiomyocytes, and were also used in this study, but cardioprotection could not be found. This raised concerns about the reliability of the image analysis program (ImageJ), the severity of ischemia, and the reliability of the parameters measured. The method used to determine cell viability was especially questioned, because it relies on the researcher to classify rod cells as viable and round cells as dead, which is thus subjective. Morphometry analysis with length over width (L/W) removes the human aspect, allowing cell viability to be determined by classifying cardiomyocytes with $L/W \geq 1.5$ as viable. Length on its own is also a morphometric measurement, but is seldom used.

Part 2 of this study aimed to:

- Compare image analysis of ImageJ with that of CellProfiler.
- Optimize conditions for ischemia-reperfusion and hypoxia-reperfusion.
- Compare morphology analysis with morphometry analysis.

Methods: The sildenafil experimental images from Part 1 were reanalyzed using CellProfiler and the data compared with that found with ImageJ. Ischemia-reperfusion was induced with less harsh conditions for 1 hour, and compared to hypoxia-reperfusion, using cell viability and mitochondrial function. Cell viability was determined by selecting viable cells by rod shape, compared to $L/W \geq 1.5$, and length $\geq 55 \mu\text{m}$. The average length for hypercontracted cells in the normoxic population was determined, and found to be consistently below $55 \mu\text{m}$. Length $\geq 55 \mu\text{m}$ was chosen as morphometry selection to identify viable cells.

Results: Both ImageJ and CellProfiler provided similar data. Cell viability for $L/W \geq 1.5$ and length $\geq 55 \mu\text{m}$ were similar, but higher than morphology, especially for hypoxia-reperfusion, but not for ischemia-reperfusion. $L/W \geq 1.5$ and length $\geq 55 \mu\text{m}$ found differences between normoxia and hypoxia-reperfusion, unlike morphology. The differences can be explained by morphology selecting fewer cells that are perfectly healthy, while morphometry selects more cells with varying degrees of cell injury. Only for ischemia-reperfusion did all parameters provide similar knockdown. This can be explained by ischemia-reperfusion that induced severe injury and hypoxia-reperfusion that induced less injury.

Conclusion: The lack of cardioprotection by PDE5 inhibition and cannabidiol was not due to an image analysis error by the program, but might rather be due to ischemia-reperfusion that was too harsh. Conversely, hypoxia-reperfusion induced injury that was not harsh enough. Morphometry selection is biased and unreliable, and morphometry selection should rather be used to evaluate an injured cardiomyocyte population.

OPSOMMING

Deel 1

Inleiding: Fosfodiesterases (FDEs) hidroliseer sikliese nukleotiedes wat iskemie-herperfusie besering (IRB) in die hart reguleer. Fosfodiesterases-5 (FDE5) inhibisie verhoog sikliese guanosien monofosfaat (sGMF) vlakke en bevorder daardeur kardiobeskerming. Cannabidiol is 'n cannabinoïde wat sGMF vlakke kan verander en induseer beskerming in heel harte. Cannabidiol-bemiddelde kardiobeskerming word moontlik beheer deur spesifieke FDEs, waarskynlik FDE5.

Die doelwitte van hierdie studie was om:

- Die rol van FDE5 inhibisie in IRB te evalueer.
- Te bepaal of FDE5 'n rol speel in cannabidiol-bemiddelde beskerming.

Metodes: Gekultuurde volwasse rotkardiomiosiete was onderwerp aan 20 minute iskemie, 60 minute herperfusie, insluitend mitokondriale kleuring om mitokondriale funksie te meet met JC-1, gevolg deur fluoressensie mikroskopie asook beeldanalise. 'n Kardiobeskermdende dosis van cannabidiol en intervensietyd was bepaal deur die administrasie van cannabidiol (0.001 μ M, 1 μ M en 100 μ M) gedurende iskemie en herperfusie, slegs iskemie, en slegs herperfusie, afsonderlik. 10 μ M Sildenafil was geadministreer gedurende iskemie alleenlik om FDE5 te inhibeer.

Resultate: Iskemie-herperfusie het sellewensvatbaarheid volgens morfologie met 79 % en mitokondriale funksie met 50 % verminder. Geen van die behandelinge het kardiobeskerming geïnduseer nie.

Gevolgtrekking: Die gebrek aan kardiobeskerming van cannabidiol en sildenafil is moontlik as gevolg van (1) die iskemie kondisies was te skadelik, (2) die analise program was foutief, of (3) die data van morfologie analise was onbetroubaar. Hierdie drie punte van kommer het die basis geword vir die nuwe objektiewe geëvalueer in Deel 2 van hierdie tesis.

Deel 2

Inleiding: Sellewensvatbaarheid en mitokondriale funksie is die parameters wat normaalweg geëvalueer word in kardiomiosiete. Hierdie studie het ook die parameters gebruik, maar kardiobeskerming kon nie gevind word nie. Dit het onsekerheid veroorsaak oor die betroubaarheid van die beeldanalise program (ImageJ), die intensiteit van iskemie, en die betroubaarheid van die geëvalueerde parameters. Die metode wat gebruik was om sellewensvatbaarheid te bepaal was veral bevraagteken, want dit is afhanklik van die navorser om staaf-vormige selle as lewendig en ronde selle as dood te klassifiseer, en is dus subjektief. Morfometrie analise met lengte oor wydte (L/W)

verwyder die menslike aspek, en laat toe dat sellewensvatbaarheid bepaal word deur kardiomiosiete met $L/W \geq 1.5$ as lewendig te klassifiseer. Lengte op sy eie is ook 'n morfometrie meting, maar word selde gebruik.

Die doel van Deel 2 van hierdie studie was om:

- Beeldanalise van ImageJ met die van CellProfiler te vergelyk.
- Die kondisies vir iskemie-herperfusie en hipoksie-herperfusie te optimaliseer.
- Morfologie analise met morfometrie analise te vergelyk.

Metodes: Die sildenafil eksperimentele beelde van Deel 1 is geherevalueer met CellProfiler en die data is vergelyk met die data gevind met ImageJ. Iskemie-herperfusie was geïnduseer met minder skadelike kondisies vir 1 uur, en was toe vergelyk met hipoksie-herperfusie, asook met die gebruik van sellewensvatbaarheid en mitokondriale funksie. Sellewensvatbaarheid was bepaal deur lewendige selle met staaf vorm te kies, en is toe vergelyk met $L/W \geq 1.5$, en lengte $\geq 55 \mu\text{m}$. Die gemiddelde lengte vir hiper-gekontraakteerde selle in die normoksiese populasie was bepaal, en is gevind om konstant onder $55 \mu\text{m}$ te wees. Lengte was gekies as morfometriese seleksie ten einde lewendige selle te identifiseer.

Resultate: Beide ImageJ en CellProfiler het dieselfde data gehad. Sellewensvatbaarheid vir $L/W \geq 1.5$ en lengte $\geq 55 \mu\text{m}$ was ooreenstemmend, maar hoër as morfologie, spesifiek vir hipoksie-herperfusie, maar nie vir iskemie-herperfusie nie. $L/W \geq 1.5$ en lengte $\geq 55 \mu\text{m}$ het verskille tussen normoksie en hipoksie-herperfusie gevind, anders as morfologie. Die verskille kan verduidelik word deur morfologie wat minder selle selekteer wat net perfek gesond is, terwyl morfometrie selle selekteer wat verskillende grade van selskade toon. Slegs vir iskemie-herperfusie het alle parameters dieselfde besering getoon. Dit kan verduidelik word deur iskemie-herperfusie wat intense skade induseer en hipoksie-herperfusie wat gevolglik minder skade induseer.

Gevolgtrekking: Die tekort aan kardiobeskerming deur FDE5 inhibisie en cannabidiol was nie as gevolg van 'n beeldanalise fout deur die program nie, maar moontlik eerder weens iskemie-herperfusie wat te skadelik was. Inteenstelling, hipoksie-herperfusie het skade geïnduseer wat nie skadelik genoeg was nie. Morfologie seleksie is bevooroordeelend en onbetroubaar, en morfometrie seleksie moet eerder gebruik word om 'n beseerde kardiomiosiet populasie te evalueer.

ACKNOWLEDGEMENTS

I acknowledge Dr John Lopes for exceeding what is expected of a supervisor, and for his broad insight, guidance and support.

Thank you to Dr Ebrahim Samodien for the continuous support and assistance in the laboratory, and specifically for his great contribution to Part 2 of this study.

I acknowledge the Department of Medical Physiology for the privilege to partake in this study, including my colleagues, for the endless encouragement and the wonderful friendships made.

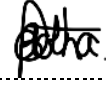
A special thanks to the Harry Crossley Foundation, for project funding in 2015, and both the National Research Foundation and Stellenbosch University, for personal funding throughout my Master's study.

DISCLOSURE OF INTEREST

Signed on the 5th day of December 2016 at Stellenbosch University

.....

(Dr John Lopes)



.....

(Anél Botha)

TABLE OF CONTENTS

DECLARATION	II
ABSTRACT.....	III
OPSOMMING	V
ACKNOWLEDGEMENTS	VII
DISCLOSURE OF INTEREST	VIII
TABLE OF CONTENT	IX
LIST OF FIGURES	XIII
LIST OF TABLES.....	XIV
LIST OF ABBREVIATIONS.....	XV
Chapter 1 LITERATURE REVIEW	1
1.1 Acute myocardial infarction.....	1
1.2 Pathology associated with acute myocardial ischemia.....	1
1.3 Pathology associated with reperfusion.....	2
1.4 Conditioning as protective intervention	5
1.5 The isolated cardiomyocyte model.....	5
1.6 Signaling pathways that promote ischemic damage or protection	6
1.6.1 β -ARs signaling	6
1.6.2 Cannabinoid signaling.....	9
1.7 CN mediated signaling during I/R.....	12
1.8 Compartmentation of cAMP and cGMP	13
1.9 Role of PDEs in regulating CN levels.....	14
1.10 PDE5: cGMP specific enzymes	15
1.10.1 The role and expression of PDE5 under normal physiological conditions.....	15
1.10.2 The role and expression of PDE5 in acute myocardial ischemia	16
1.11 Cardiomyocyte cAMP and cGMP cross-talk with PDE5	19
1.12 PDE2: cGMP stimulated to hydrolyse cAMP and cGMP	21
1.12.1 The role and expression of PDE2 under normal physiological conditions.....	21

1.12.2	The role and expression of PDE2 in acute myocardial ischemia	22
1.13	PDE3: cGMP-inhibited cAMP-hydrolysing enzymes.....	23
1.13.1	The role and expression of PDE3 under normal physiological conditions.....	23
1.13.2	The role and expression of PDE3 in acute myocardial ischemia	24
Chapter 2	HYPOTHESIS, AIMS, OBJECTIVES AND VALUE OF RESEARCH	27
2.1	Hypothesis.....	27
2.2	Aims	27
2.3	Objectives.....	27
2.4	Value research contributes to society	28
Chapter 3	MATERIALS AND METHODS.....	29
3.1	Animals.....	29
3.2	Ethical approval	29
3.3	Reagents	29
3.4	Coating culture surface with Laminin-Entactin adhesive	29
3.5	Isolation of adult rat ventricular cardiomyocytes.....	29
3.6	I/R and JC-1 staining	30
3.7	Drug concentrations.....	31
3.8	Data collection and analysis.....	32
3.9	Statistics	32
Chapter 4	RESULTS.....	33
4.1	The effect that different CBD concentrations exert during normoxia, ischemia and I/R on isolated ventricular cardiomyocytes survival	34
4.1.1	Average cell viability in percentage according to morphology	36
4.1.2	Average R/G fluorescence of JC-1 in percentage as an early apoptosis indicator.....	37
4.2	The effect of per-treatment with PDE5 inhibitor and β -AR stimulation during I/R on isolated ventricular cardiomyocytes survival	38
4.2.1	Average cell viability in percentage according to morphology	40
4.2.2	Average R/G fluorescence of JC-1 in percentage as an early apoptosis indicator.....	41
Chapter 5	SOLVING THE PROBLEMS.....	46

5.1	The experimental protocol	46
5.2	The method of analysis	46
5.3	The parameters measured	47
Chapter 6 HYPOTHESIS, AIMS AND OBJECTIVES		49
6.1	Hypothesis	49
6.2	Aims	49
6.3	Objectives	49
Chapter 7 MATERIALS AND METHODS		51
7.1	I/R, H/R and JC-1 staining	51
7.2	Data analysis	51
7.3	Statistics	52
Chapter 8 RESULTS		53
8.1	A comparison between ImageJ and CellProfiler analysis	53
8.1.1	Average R/G fluorescence of JC-1 in percentage as an early apoptosis indicator: ImageJ versus CellProfiler	53
8.2	A comparison between morphology and morphometry analysis	54
8.2.1	Average cell length and R/G fluorescence measured from cell shape outline (cell area) and straight line	55
8.2.2	Separating the viable rods and non-viable round cells according to length	57
8.2.3	Average cell viability: comparing morphology (rod shape) with morphometry (length ≥ 55 μm and $L/W \geq 1.5$) analysis	59
8.2.4	Average R/G fluorescence, cell length and L/W ratio of the viable population	60
8.3	The effect that different CBD concentrations exert during normoxia, ischemia and I/R on isolated ventricular cardiomyocytes survival	63
8.3.1	Average cell length in microns as indicator of contracture	64
8.3.2	Average cell viability in percentage: to compare morphology and length ≥ 55 μm	65
8.4	The effect of per-treatment with PDE5 inhibitor and β -AR stimulation during I/R on isolated ventricular cardiomyocytes survival	66
8.4.1	Average cell length in microns as indicator of contracture	66

8.4.2 Average cell viability in percentage: to compare morphology and length $\geq 55 \mu\text{m}$	67
DISCUSSION	68
CONCLUSION.....	76
RECOMMENDATIONS.....	77
REFERENCE LIST	78

LIST OF FIGURES

Figure 1.1 Pathology associated with acute myocardial ischemia and reperfusion	4
Figure 1.2 β -AR signaling during acute myocardial ischemia	8
Figure 1.3 The structure of CBD.....	10
Figure 1.4 PDE5 domain organization.....	15
Figure 1.5 The effect of high and low cGMP concentrations on PDE5, 2 and 3 activity	19
Figure 1.6 Cross-talk of other PDEs with PDE5.....	20
Figure 1.7 PDE2 domain organization.....	21
Figure 1.8 PDE2 localization and cAMP compartmentalization in cardiomyocytes	22
Figure 1.9 PDE3 domain organization.....	20
Figure 3.1 Protocol for ischemia-reperfusion	31
Figure 4.1 Fluorescence images of isolated cardiomyocytes treated with CBD	35
Figure 4.2 Cell viability for cardiomyocytes treated with different CBD concentrations	36
Figure 4.3 R/G fluorescence for cardiomyocytes treated with different CBD concentrations.....	37
Figure 4.4 Fluorescence images of cardiomyocytes pre-treated with PDE5 inhibitor and β -AR agonists ...	39
Figure 4.5 Cell viability for cardiomyocytes pre-treated with PDE5 inhibitor and β -AR agonists.....	40
Figure 4.6 R/G fluorescence for cardiomyocytes pre-treated with PDE5 inhibitor and β -AR agonists	41
Figure 5.1 Fluorescence image of a hypoxic population identifying the different degrees of cell injury	47
Figure 7.1 Protocol for ischemia-reperfusion and hypoxia-reperfusion	51
Figure 7.2 Analysing cells by drawing the cell shape outline or the length of the cell with a straight line..	52
Figure 8.1 R/G fluorescence: A comparison between ImageJ and CellProfiler analysis	53
Figure 8.2 R/G fluorescence: A comparison between cell shape outline and straight line measurement..	55
Figure 8.3 Cell length: A comparison between cell shape outline and straight line measurement.....	55
Figure 8.4 Separating the rod and the round cells according to length	57
Figure 8.5 Cell viability: Comparing morphology with morphometry analysis	59
Figure 8.6 R/G fluorescence: Comparing morphology with morphometry analysis	60
Figure 8.7 Cell length: Comparing morphology with morphometry analysis.....	61
Figure 8.8 LW : Comparing morphology with morphometry analysis	62
Figure 8.9 Cell length for cardiomyocytes treated with different CBD concentrations	64
Figure 8.10 Cell viability: A comparison between morphology and length $\geq 55 \mu\text{m}$	65
Figure 8.11 Cell length for cardiomyocytes pre-treated with PDE5 inhibitor and β -AR agonists	66
Figure 8.12 Cell viability: A comparison between morphology and length $\geq 55 \mu\text{m}$	67

LIST OF TABLES

Table 1.1 PDE5 inhibitors administrated during I/R to induce cardioprotection.....	18
Table 1.2 PDE3 inhibitors administrated during I/R or H/R to induce cardioprotection.	26

LIST OF ABBREVIATIONS

% :	percentage	eNOS :	Endothelial nitric oxide synthase
°C :	degree Celsius	ERK1/2 :	Extracellular signal-regulated kinase
2DG :	2-deoxy-D-3[H]glucose	g :	gram
2Na ⁺ -Ca ²⁺ :	Sodium-calcium	GC :	Guanylyl cyclase
3Na ⁺ -2K ⁺ :	Sodium-potassium	G _i :	Inhibitory G-protein
AAALAC :	Association for assessment and accreditation of laboratory animal care	GPCR :	G-protein coupled receptors
AC :	Adenylyl cyclase	GPR55 :	G protein-coupled receptor 55
AMI :	Acute myocardial infarction	G _s :	Stimulatory G-protein
ANOVA :	One-way analysis of variance	GSK3β :	Glycogen synthase kinase-3 beta
ANP :	Atrial natriuretic peptide	GTP :	Guanosine triphosphate
ATP :	Adenosine triphosphate	h :	hour/s
Bcl-2 :	B-cell lymphoma-2	H/R :	Hypoxia-reperfusion
BDM :	2,3-butanedione monoxime	H ⁺ :	Hydrogen
BSA:	Bovine serum albumin	HEPES :	4-(2-hydroxyethyl)-1-piperazineethanesulfonic acid
Ca ²⁺ :	Calcium	HIV :	Human immunodeficiency virus
cAMP :	Cyclic adenosine monophosphate	I/R :	Ischemia-reperfusion
CANP :	Calcium-activated neutral protease	ICa ²⁺ :	Intracellular calcium
CB :	Cannabinoid	ICER :	Inducible cAMP early repressor
CBD :	Cannabidiol	IL :	Inter-leukin
cGMP :	Cyclic guanosine monophosphate	iNOS :	Inducible nitric oxide synthase
CHD:	Coronary heart disease	IP3 :	Inositol-1,4,5-triphosphate
CN :	Cyclic nucleotide	JC-1 :	5,5',6,6'-tetrachloro-1,1',3,3'-tetraethylbenzimidazole-carbocyanide iodine
CO ₂ :	Carbon dioxide	JNK :	c-Jun N-terminal kinase
CREB :	cAMP response element binding protein	K ⁺ :	Potassium
EHNA :	<i>Erythro</i> -9-(2-hydroxyl-3-nonyl)adenine	K _{ATP} :	ATP-sensitive K ⁺ channel
		KCl :	Potassium chloride
		kg :	kilogram

L/E :	Laminin-Entactin	pGC :	Particulate guanylyl cyclase
L/W :	Length over width	PI3K :	Phosphatidylinositol 3-kinase
LDH :	Lactate dehydrogenase	PKA :	cAMP-dependent protein kinase
L-NAME :	N ^G -nitro-L-arginine methylester	PKB/Akt :	Serine/threonine-specific protein kinase
MEK :	Mitogen-activated protein kinase	PKC :	Calcium-activated serine-threonine kinase
MEK1/2 :	Mitogen-activated protein kinase p44/p42	PKG :	cGMP-dependent protein kinase
mg :	milligram	PLC :	Phospholipase C
MgSO ₄ :	Magnesium sulphate	R/G :	Red over green
min :	minute/s	RISK :	Reperfusion injury salvage kinase
mIU :	milli international unit	ROS :	Reactive oxygen species
ml :	millilitre	RTK :	Receptor tyrosine kinase
mM :	millimolar	SDT :	Sodium dithionite
mPTP :	Mitochondrial permeability transition pore	SERCA2 :	Sarcoplasmic Ca ²⁺ -ATPase
N ₂ :	Nitrogen	sGC:	Soluble guanylyl cyclase
Na ⁺ :	Sodium	STAT-3 :	Signal transducer and activator of transcription-3
Na ⁺ -H ⁺ :	Sodium-hydrogen	THC :	Delta-9-tetrahydrocannabinol
Na ₂ HPO ₄ :	Sodium hydrogen phosphate	TUNEL :	Terminal deoxynucleotidyl transferase-mediated nick end-labeling
NaCl :	Sodium chloride	U :	units
NaH ₂ PO ₄ :	Sodium dihydrogen phosphate	VSMC :	Vascular smooth muscle cells
NCD :	Non-communicable disease	WHO :	World Health Organization
NHR :	N-terminal hydrophobic membrane association regions	β :	beta
nM :	nanomolar	β-ARs :	Beta-adrenoreceptors
NO :	Nitric oxide	μg :	microgram
NOS :	Nitric oxide synthase	μl :	microlitre
NOS-NO :	Nitric oxide synthase-nitric oxide	μm :	micrometre
NPR1/NPRA/ANP _A :	Natriuretic peptide receptor-A	μM :	micromolar
O ₂ :	Oxygen		
PBS :	Phosphate-buffer-saline		
PDE :	Phosphodiesterase		

CHAPTER 1

Literature Review

1.1 Acute myocardial infarction

The World Health Organization (WHO) statistics indicate that, of the 56 million global deaths in 2012, non-communicable diseases contributed 68 % (Finegold et al., 2013). The leading non-communicable disease (NCD) is cardiovascular diseases, of which coronary heart disease (CHD) is most prevalent, contributing 17.5 million deaths. CHD is predicted to be close on the heels of human immunodeficiency virus (HIV) to become the leading cause of death and disability worldwide (Finegold et al., 2013).

CHD is prevalent amongst diabetic, hypertensive and heart failure patients. Alternative risk factors include genetic predisposition, smoking, unhealthy dietary habits, or sedentary lifestyle (Boersma et al., 2003). Vascular pathologies associated with these diseases and the risk factors mentioned can trigger ischemia, which leads to acute myocardial infarction (AMI) also known as a heart attack (Hausenloy & Yellon, 2013).

1.2 Pathology associated with acute myocardial ischemia (summarized in Figure 1.1)

Acute myocardial ischemia is prompted by a coronary occlusion, depriving the cardiomyocytes of oxygen, nutrients and energy (Reimer & Ideker, 1987), and is reflected by cardiomyocyte death. The deprivation of oxygen prevents oxidative phosphorylation in the mitochondria, leading to membrane depolarization, energy (adenosine triphosphate (ATP)) depletion and inhibition of cardiomyocyte contraction (Hausenloy & Yellon, 2013).

The heart attempts to compensate for the ATP loss by switching the cellular metabolism to anaerobic glycolysis. However, anaerobic glycolysis can only produce a very limited amount of ATP at a very slow rate, but with the addition of lactate accumulation, which contributes to the reduction of intracellular pH (to < 7.0) (Dennis et al., 1991; Hausenloy & Yellon, 2013). Anaerobic glycolysis and other ATP-dependent processes rapidly hydrolyse ATP, and thereby release hydrogen (H^+), which mainly contributes to acidosis (Dennis et al., 1991; Murphy & Steenbergen, 2008).

The intracellular protons generated during ischemia are removed by the sodium-hydrogen (Na^+-H^+) exchanger, which exchanges intracellular protons for Na^+ entry. Low ATP levels retard Na^+ removal by the ATP-dependent sodium-potassium ($3Na^+-2K^+$) ATPase, aggravating the accumulation of Na^+ in the cell in response to the effect of the Na^+-H^+ exchanger.

The cell, overloaded with Na^+ , activates the sodium-calcium ($2\text{Na}^+-\text{Ca}^{2+}$) ion exchanger in reverse mode (Avkiran & Marber, 2002). Under normal conditions the $2\text{Na}^+-\text{Ca}^{2+}$ ion exchanger extrudes Ca^{2+} from the cell by indirectly using the ATP of the Na^+ gradient set by the $3\text{Na}^+-2\text{K}^+$ ATPase. During ischemia, Na^+ overload reduces the inwardly directed Na^+ gradient, allowing Ca^{2+} to rise via $2\text{Na}^+-\text{Ca}^{2+}$ ion exchanger, in effect increasing Ca^{2+} levels within the cell (Imahashi et al., 2005).

Acidosis and alterations in the ion transport system, as a result from prolonged ischemia, can inhibit cardiomyocyte contraction and relaxation (Buja, 2005; Hausenloy & Yellon, 2013). Insufficient ATP supply prevents actin-myosin cross bridge dissociation and the restoration of resting cytosolic Ca^{2+} levels, which initiates contracture (Buja et al., 1988).

Ultimately, the various ischemic stress signals activate death pathways, apoptosis or necrosis. Cell death via necrosis is triggered by acute cellular injury, compared to programmed cell death via apoptosis. Apoptosis is triggered by the cell sensing stress within itself (*intrinsic pathway*) and receiving signals from adjacent cells (*extrinsic pathway*) (Buja, 2005).

1.3 Pathology associated with reperfusion (summarized in **Figure 1.1**)

Resupplying the heart with blood and thus oxygen (reperfusion) is critical and the common method used to preserve heart tissue viability. This increase in oxygen delivery can be rapid and forms reactive oxygen species (ROS) (Kilgore & Lucchesi, 1993) that conversely induce damage. The extent of damage depends on the duration of ischemia. If ischemia is prolonged, reperfusion leads to irreversible damage - reperfusion injury, first put forth in 1977 by Hearse.

Reperfusion is characterized by a rapid increase in intracellular free Ca^{2+} concentration (Kilgore & Lucchesi, 1993). The rise in Ca^{2+} is mainly due to a concentration gradient, which permits the cell to exchange Na^+ for Ca^{2+} via $\text{Na}^+-\text{Ca}^{2+}$ exchanger (Fehrer et al., 1980). If intracellular Ca^{2+} levels are above normal, cell death is activated (Murphy & Steenbergen, 2008).

Ca^{2+} influx initiates biochemical events, including enzyme activation and ultrastructural changes. Different groups of intracellular enzymes are activated: phospholipases, proteases and calpains. Phospholipases are mostly responsible for ATP depletion, by using ATP to hydrolyse fatty acids, preventing enough ATP to accumulate for the cardiomyocyte to survive (Becker & Ambrosio, 1987). Proteases, specifically calcium-activated neutral protease (CANP), mediate myofibrillar turnover and degrade various structural proteins, including cytoskeletal filaments, needed to maintain the rigid cardiomyocyte structure (Dayton et al., 1976). Calpain enzymes are involved in initiating cardiomyocyte death via activation of apoptosis and necrosis (Murphy & Steenbergen, 2008).

The ultrastructural changes include contracture bands development and the formation of large amorphous solidities within mitochondria (Kilgore & Lucchesi, 1993).

It is not just the Ca^{2+} levels that render the cardiomyocytes dead. During re-oxygenation there is a rapid ATP production recovery, which together with the Ca^{2+} overload reactivates the contractile machinery and leads to an uncontrolled Ca^{2+} -dependent contracture (Piper et al., 2003). Contracture is a condition of cardiomyocyte shortening, which renders the cardiomyocyte resistant to stretching. The low intracellular pH from ischemia is restored by the washout of lactate and the activation of the Na^+ - H^+ exchanger. The pH shift towards alkalinity causes continuation of cardiomyocyte contracture to a more severe degree – hypercontracture (Hausenloy & Yellon, 2013).

Oxidative stress, intracellular Ca^{2+} (ICa^{2+}) influx, phosphate overload, ATP depletion and the rapid shift in pH permits the opening of the mitochondrial permeability transition pore (mPTP). The mPTP is a non-selective channel of the inner mitochondrial membrane. This channel commonly remains closed during ischemia while the Ca^{2+} increase alone has no effect. When open, the mPTP results in mitochondrial membrane depolarization and oxidative phosphorylation uncoupling, leading to further ATP depletion and finally cell death (Hausenloy & Yellon, 2003).

Ischemic and reperfusion levels of Ca^{2+} , ATP, pH, the activation of necrosis and apoptosis, and changes in cell morphology and cell length, serve as indicative markers for protection versus damage signaling.

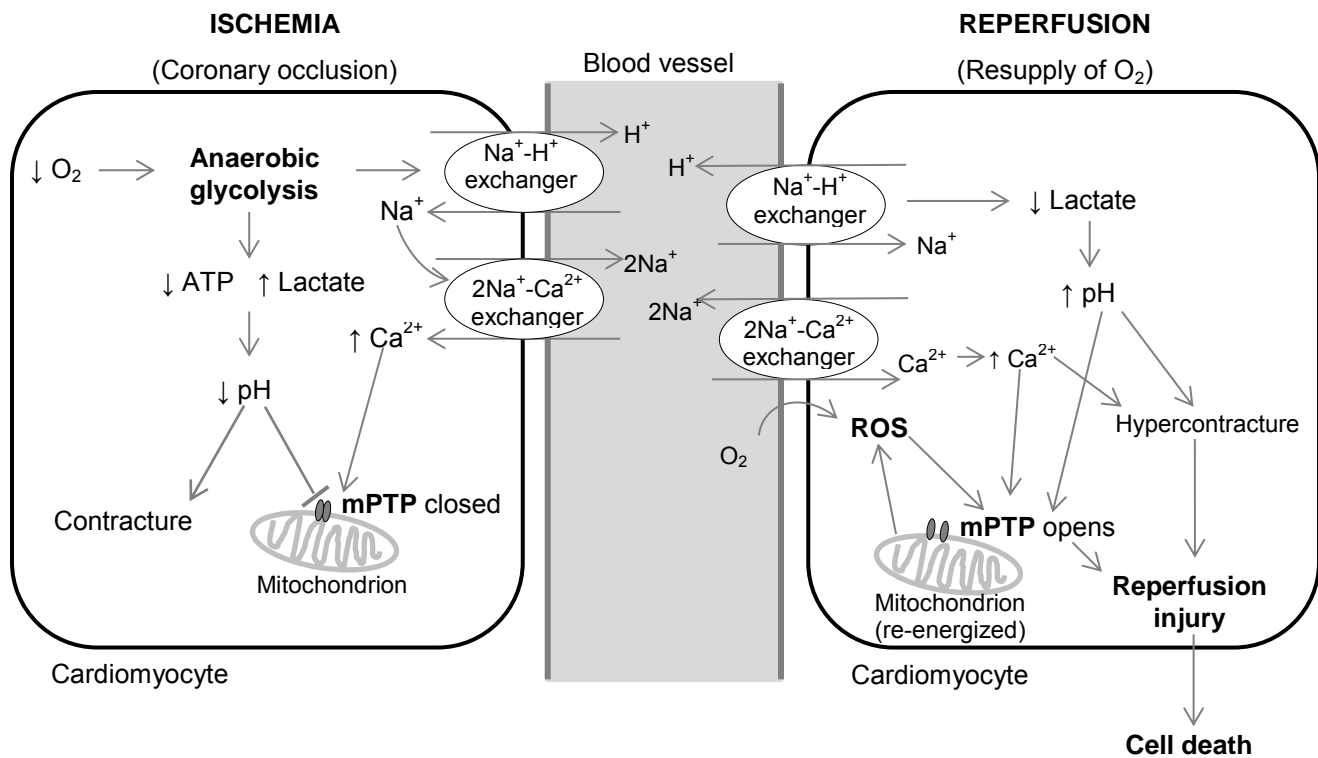


Figure 1.1 Pathology associated with acute myocardial ischemia and reperfusion. This figure is modified from (Hausenloy & Yellon, 2013). Acute myocardial ischemia is prompted by a coronary occlusion. The deprivation of oxygen prevents oxidative phosphorylation and the heart switches to anaerobic glycolysis, which causes lactate to accumulate and the intracellular pH to reduce. The low pH induces the Na^+-H^+ exchanger to extrude H^+ , resulting in intracellular Na^+ overload, which activates the $2Na^+-Ca^{2+}$ exchanger to function in reverse to extrude Na^+ for Ca^{2+} and consequently causes intracellular Ca^{2+} overload. The Low ATP levels retard Na^+ removal by the $3Na^+-2K^+$ ATPase, aggravating the accumulation of Na^+ in the cell in response to the effect of the Na^+-H^+ exchanger. The acidic pH condition during ischemia inhibits the opening of the mPTP and inhibits cardiomyocyte contracture. During reperfusion the increase in oxygen delivery can be rapid and forms ROS, which results in the opening of the mPTP. Reperfusion reactivates the Na^+-H^+ exchanger and leads to the washout of lactate, which rapidly restores the intracellular pH and ultimately stimulates the opening of the mPTP and activates hypercontracture. Reperfusion is characterized by a rapid increase in intracellular free Ca^{2+} concentration mainly due to a concentration gradient, which permits the cell to exchange Na^+ for Ca^{2+} via Na^+-Ca^{2+} exchanger. If intracellular Ca^{2+} levels are above normal the mPTP opens and hypercontracture is activated, which leads to reperfusion injury and finally cell death.

1.4 Conditioning as protective intervention

Conditioning is the process of giving a stimulus and then taking the stimulus away to stimulate cardioprotection. Cardiac conditioning can be done either before (pre), during (per), or after (post) ischemia (Bell & Yellon, 2012). Although protection from preconditioning seems to be most effective (Xin et al., 2010), the onset of ischemia can only be predicted in a few instances, for example in surgery, and therefore per- and post- conditioning is clinically more relevant.

It is possible to condition the heart directly, or via distal tissues (remote conditioning). Conditioning activates endogenous cytoprotective pathways, which stimulate protection against ischemia-reperfusion (I/R) injury in the heart and cardiomyocytes (Bell & Yellon, 2012).

Protection by conditioning mainly involves the activation of the reperfusion injury salvage kinase (RISK) pathway. RISK pathway activation signals via phosphatidylinositol 3-kinase (PI3K) and the mitogen-activated protein kinase p44/p42 (MEK1/2), which activates extracellular signal-regulated kinase (ERK1/2). Both these pathways exert a critical role in stimulating protection (Xin et al., 2010).

Alternatively, conditioning can activate the release of autacoids, such as adenosine, opioids, and bradykinin, which are chemical transmitter substances that act as local hormones (Downey & Cohen, 2006).

Autacoids are periodically released to handle several biological actions including modulating the activity of smooth muscles, platelets, glands, nerves and other tissues (Roy, 2007). Autacoids serve as agonists for beta-adrenoreceptors (β -ARs) coupling to inhibitory G-protein (G_i). Once activated, G_i activates calcium-activated serine-threonine kinase (PKC) and it is by this mechanism that protection is largely governed. The precise mechanism that leads to protection is still elusive (Downey & Cohen, 2006).

Conditioning, and the cardioprotective effect thereof, can be mimicked by drug treatment (Hausenloy & Yellon, 2011). Unlike conditioning, drug treatment involves giving a stimulus continuously, without removing the stimulus.

1.5 The isolated cardiomyocyte model

Cardiomyocytes account for approximately 60 % of the cells in the heart, and under normal conditions they allow continuous rhythmic contraction and relaxation for heart pump function (Maurice et al., 2003). Cardiomyocytes express a wide range of surface receptors, including G-protein coupled receptors (GPCRs) and receptor tyrosine kinases (RTKs). These cells can be isolated, cultured, and used for experimental purposes.

The isolated cardiomyocyte model gives great insight into single, or a cascade of, intracellular signaling candidates: for example visualizing Ca^{2+} flux, protein interactions, and cell mechanics (Louch et al., 2011). This is done in the absence of hormonal homeostasis and complex neural control (Kabaeva et al., 2008). The whole heart model does not allow for this attribute due to the influence of vasculature and other cells (Bell & Yellon, 2012).

Cultured cardiomyocytes can be used in various experimental settings: cell contractility assessment, cell viability, and cell-signaling studies.

There are two primary culture models - neonatal and adult cardiomyocytes. Neonatal cardiomyocytes, harvested from rats aged 1 - 3 days, are un-differentiated cells and thus provides a simpler experimental system. Compared to adult cardiomyocytes harvested from rats aged 7 - 8 weeks, neonatal cardiomyocytes are suitable candidates for non-viral gene transfer and have the advantage of being easily cultured and for longer time periods (Louch et al., 2011). Isolation of neonatal cardiomyocytes does not require the tedious procedure of aorta cannulation and perfusion, necessary to yield adult cardiomyocytes.

Yet, neonatal cells attach slower (24 h) to culturing adhesives than adult cardiomyocytes (1 - 4 h). Adult cardiomyocytes are mainly preferred because they are differentiated rod-shaped cells (Louch et al., 2011). Neonatal cells express genes differently and may not represent a good model for I/R, whereas the intracellular signaling in adult cardiomyocytes is more intricate and can serve as a better physiological comparison to human cardiomyocytes.

Some aspects of the adult cardiomyocytes isolation model remain a challenge, first to successfully isolate a high quality myocyte population with $\geq 80\%$ viability, and secondly the maintenance of these cells in culture without the loss of structure and function. Various factors influence the success of the isolation, including the weight and age of the rats, potency of enzymes used to digest the heart, effectiveness of products used and human error.

Immortalized cardiac cell lines, such as h9c2 cells, are commercially available. However, acutely isolated cardiomyocytes are physiologically more relevant to the living organism (Louch et al., 2011).

1.6 Signaling pathways that promote ischemic damage or protection

1.6.1 β -ARs signaling

β -ARs (β_1 , β_2 , and β_3) contribute significantly to the sympathetic nervous system control of heart function and enhancing cardiac performance to stress, exercise and injury (Lohse et al., 2003). β -ARs control heart function by mediating the physiological effects of catecholamines (Gao et al., 2014).

These receptors are expressed on the surface of cardiomyocytes, β 1-AR being the most abundant subtype accounting for \approx 80 % of β -AR (Communal et al., 1999) and the most active during ischemia. In the setting of acute myocardial ischemia, β 1-AR activation, from endogenous catecholamine released by sympathetic nervous stimulation, induces damage (Spear et al., 2007).

β -ARs, especially β 1 and β 2, regulate excitation-contraction coupling via stimulatory G-protein (G_s) coupling to adenylyl cyclase (AC) (Gao et al., 2014) (**Figure 1.2**). Activation thereof under acute myocardial ischemic conditions can induce apoptosis and necrosis. This is done by a mechanism dependent on the increase of cyclic adenosine monophosphate (cAMP) (described in section 1.7), which activates cAMP-dependent protein kinase (PKA) (Communal et al., 1999), finally increasing contraction and damage. Alternatively, β 2-AR can couple to pathways independent of cAMP and G_s , by signaling via G_i (Xiao et al., 1999) (**Figure 1.2**). β 2-AR coupling to G_i successfully attenuates acute myocardial ischemic cAMP/PKA activity, initiating cardioprotection (Communal et al., 1999).

A cultured isolated cardiomyocyte study by Communal and colleagues (1999) found that, β -AR stimulation with a non-selective agonist (norepinephrine) mediates two opposing effects on apoptosis, where activation of β 1-ARs stimulated apoptosis while activation of β 2-ARs inhibited apoptosis. They also found that β 2-AR stimulation inhibited β -AR-stimulated apoptosis, possibly via G_i . But, a decrease in β -AR-stimulated cAMP was not found, and they concluded that the G_i protection is possibly regulated by a cAMP-independent mechanism (Communal et al., 1999). It is possible that the change in cAMP, instead of the overall cAMP concentration, occurred in cAMP compartmentation, which they did not mention. They did not test for cyclic guanosine monophosphate (cGMP), and therefore it is also possible that the effects could have been via cGMP and cGMP-dependent protein kinase (PKG) signaling. The protective pathway activated from G_i coupling includes PI3K activation, activating its downstream target serine/threonine-specific protein kinase (PKB, also known as Akt) (Chesley et al., 2000; Gao et al., 2014).

β 3-AR is the rarest subtype, but expression can increase, divergent to β 1-AR and β 2-AR, with pathophysiological conditions such as heart failure and hypertrophy (Watts et al., 2013). High levels of catecholamines, for example released during acute myocardial ischemia, or the administration of a β 3-AR agonist, can stimulate β 3-AR. β 3-AR activation results in negative inotropic effect that opposes positive inotropic effects by β 1-AR and β 2-AR and promotes protection (**Figure 1.2**) (Isidori et al., 2015). This protection is mediated by G_i coupling to nitric oxide synthase-nitric oxide (NOS-NO), increasing cGMP levels, and activating PKG (Watts et al., 2013). This pathway might have been involved in the Communal paper (1999) described in the previous paragraph. PKG ultimately inhibits contraction and allows relaxation (Gauthier et al., 1998).

Despite the constant hyper-sympathetic activity from ischemia, the stimulated response is maintained by β_3 -AR lacking PKA phosphorylation sites (Watts et al., 2013). The protective signal from β_3 -AR can only be stopped once catecholamines release recedes. β_1 -AR and β_2 -AR have PKA phosphorylation sites that induce receptor desensitization: blunting receptor activation and the signal effect.

In isolated cardiomyocyte models β -AR agonists are used to activate β -ARs non-selectively (isoproterenol (Maurice et al., 2003; Yu et al., 2008)) to mimic damage (β_1 -AR: dobutamine (Chesley et al., 2000; Ufer & Germack, 2009)), and to promote protection (β_2 -AR: formoterol (Watson et al., 2013; Wills et al., 2012) and β_3 -AR: BRL-37433 (Gauthier et al., 1998; Niu et al., 2012)).

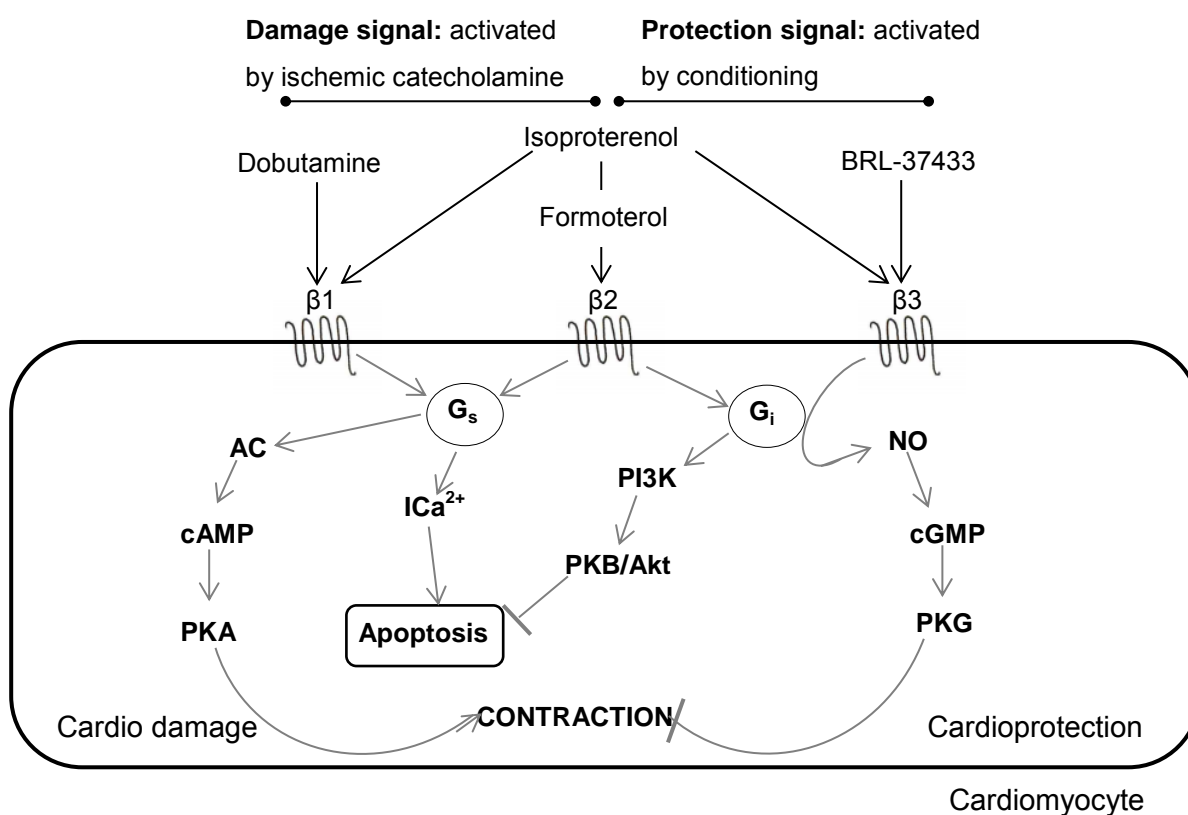


Figure 1.2 Proposed diagram whereby β -AR signaling governs damage versus protection during acute myocardial ischemia. During ischemia neuronal synapses are stimulated to release catecholamine, which stimulates β_1 -AR (agonist: dobutamine) coupling to G_s . G_s activates AC, increasing cAMP levels, which activates PKA and leads to contraction (damage). Alternatively, G_s initiates apoptosis by increasing the ICa^{2+} . β_2 -AR activation (by conditioning or agonist: formoterol) signals via G_s and/or G_i . G_i coupling activates PI3K, which activates PKB/Akt and inhibits apoptosis, promoting protection. β_3 -AR activation (by conditioning or agonist: BRL-37433) signals via G_i to increase nitric oxide (NO) levels, increasing cGMP and activates PKG. PKG activity blunts contraction and promotes ischemic cardioprotection. Isoproterenol is a non-selective agonist for β -ARs.

1.6.2 Cannabinoid signaling

Cannabinoid (CB) receptors, CB1 and CB2, cloned in 1990 and 1993 respectively (Howlett et al., 2002) form part of the GPCR family and are expressed in cardiomyocytes (Lamontagne et al., 2006; Walsh et al., 2010). Compared to CB1, CB2 is expressed in lower levels, but expression is up-regulated in response to conditions such as inflammation or tissue injury to promote protection (Steffens & Pacher, 2012). CB receptors control physiopathological functions in the cardiovascular system (Mendizabal & Adler-Graschinsky, 2007), but play a minor regulatory role under normal physiological conditions (Wagner et al., 1998).

Once activated, CB receptors mainly regulate heart rate and blood pressure (Hillard, 2000; Pacher et al., 2005; Wagner et al., 1998), where CB1 activation stimulates hypotension and bradycardia (Bonz et al., 2003; Gebremedhin et al., 1999; Wagner et al., 1998).

CB receptors are mainly characterized in other systems, not in cardiomyocytes. The activation of these receptors signal via the G_i pathway (Wagner et al., 1998). G_i inhibits AC, and thus cAMP production, which reduces PKA phosphorylation (Howlett et al., 2002), and it activates the mitogen-activated protein kinases (MEKs)-mediated cascade (Hillard, 2000; Wagner et al., 1998).

CB1 activation, in contrast to CB2, modulates ion channel functioning (Steffens & Pacher, 2012). CB1 signals through G_i to inhibit L-type Ca^{2+} channel currents and increase intracellular free Ca^{2+} (Gebremedhin et al., 1999). This is via G_i activating phospholipase C (PLC), which stimulates the release of inositol-1,4,5-triphosphate (IP3), finally initiating vasodilation in vascular smooth muscle cells (VSMC) (Howlett et al., 2002). The Ca^{2+} response mediated by CB2 is less pronounced (Steffens & Pacher, 2012). Similar to CB1, CB2 activation cause Ca^{2+} release from endoplasmic reticulum stores and L-type Ca^{2+} channel, but without channel inhibition (Zoratti et al., 2003).

Interestingly, in neuronal cells the activation of CB1 with the agonist CP55940 stimulate NO production, leading to G_i activation and enhanced neuronal nitric oxide synthase (NOS) activity, which produce cGMP (Carney et al., 2009). In cultured cardiomyocytes the activation of CB2 with delta-9-tetrahydrocannabinol (THC) induces NO production and leads to an increase in cGMP (Shmist et al., 2006). Thus, it seems that CB1 and CB2 are both capable of inducing NO production, which leads to an increase in cGMP.

In the absence of functional G_i coupling, Glass and Felder (1997) found that CB1 can activate G_s , which increases cAMP and PKA phosphorylation. CB1 is usually associated with inter-leukin (IL) -3, but when there is a double mutation in the amino-acid structure (Leucine-Alanine) of IL3, the helical domain makes into a single turn, and converts coupling of the receptor from G_i to G_s (Abadji et al., 1999).

Rhee and colleagues (1998) stated that the outcome of CB receptor stimulation is mainly determined by the AC isoforms expressed in the cell. Cells that express CB1 and CB2 receptors with co-expression of AC isoforms 1, 3, 5, 6, 8 or 9 inhibits cAMP accumulation, whereas AC isoforms 2, 4 or 7 stimulates cAMP accumulation (Rhee et al., 1998). The distribution of AC isoform in heart tissue was described in a review article (Hanoune & Defer, 2001), where isoforms 2, 3, 4, 7, 8 are distributed at low levels and 5, 6, 9 at high levels.

The activation of CB receptors with endogenous cannabinoids stimulates protection against myocardial ischemia and can preserve coronary endothelial function (Krylatov et al., 2001; Lasukova et al., 2008; Ugdyzhkova et al., 2001). Specific CB1 and CB2 blockers inhibit cardioprotection, indicating that the protective signal is receptor-mediated (Krylatov et al., 2001; Ugdyzhkova et al., 2001).

CB receptors can also respond to phyto (plant derived)- and synthetic cannabinoids (Walsh et al., 2010). The psychoactive THC and the non-psychoactive (-)-cannabidiol (CBD) are derived from the plant *Cannabis sativa* (Howlett et al., 2002; Lasukova et al., 2008) and serve as pharmacological active agents (Zoller et al., 2000). THC and CBD are the two most abundant compounds, out of the seventy active compounds, in *Cannabis sativa* (Walsh et al., 2010).

CBD, which structure is illustrated by **Figure 1.3**, is an agonist for CB1 and CB2 receptors – even at low concentrations: 1 μM – 10 μM (Thomas et al., 2007; Pertwee, 2008).

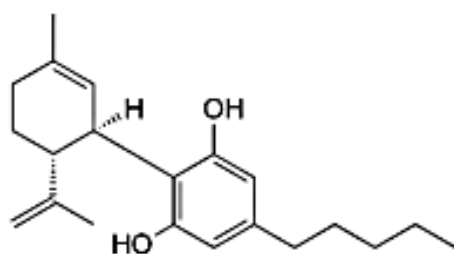


Figure 1.3 The structure of CBD (Mechoulam et al., 2007).

The precise pharmacological action of CBD is yet to be clarified. A review by Mechoulam and colleagues (2007) described the effects of CBD that mediate cardioprotection, including anti-necrotic, antioxidant, and anti-inflammatory. CBD has the ability to interfere with key pathological events during I/R, such as ion channel opening (Mamas & Terrar, 1998) and platelet activation (Formukong et al., 1989).

A study by Durst and colleagues (2007) tested the *in vivo* and *ex vivo* effects of CBD administration on I/R. *In vivo*, where rats received CBD 1 h before ischemia induction, and then again every 24 h for 7 days after ischemia, resulted in a decrease in infarct size, associated with reduced myocardial inflammation, and reduced IL-6 levels. *Ex vivo*, where rats received CBD 24 or 1 h before they were sacrificed, the isolated hearts showed no significant difference in the infarct size or left ventricular pressure development during I/R. They concluded that *in vivo*, but not *ex vivo*, CBD induces a significant cardioprotective effect against ischemia (Durst et al., 2007).

In 2010, Walsh and colleagues demonstrated that *in vivo* acute administration of CBD on rat hearts, either 10 min prior to 30 min of ischemia, or 10 min prior to 2 h of reperfusion, is cardioprotective by reducing both ventricular arrhythmias and infarct size. Thus, in whole hearts the acute CBD administration stimulates cardioprotection.

A doctoral thesis done by Hepburn (2014), firstly *in vivo*, investigated the receptors involved in the anti-arrhythmic effect of CBD in a coronary artery occlusion rat model. This is based on the ability of CBD to also activate the receptor G protein-coupled receptor 55 (GPR55) (Hepburn, 2014). CBD administration *in vivo* caused a hypotensive response, induced vasodepressor response, and reduced arrhythmias, which was potentiated when GPR55 was co-activated with the agonist AM251. This indicates the possible cross-talk between CB receptors and GPR55 to reduce the incidence of arrhythmias (Hepburn, 2014). Secondly, the *in vitro* experiments of the study determined if CBD alters ICa^{2+} in isolated cardiomyocytes, and found that CBD cannot modulate ICa^{2+} in cardiomyocytes.

In 2015 Feng and colleagues tested the therapeutic effects of CBD on I/R injury in rabbits, where 90 min coronary artery occlusion was induced, followed by 2 intravenous CBD doses before 24 h reperfusion. CBD reduced the infarct size and facilitated the restoration of left ventricular function.

Only these few studies have tested the role of CBD in the setting of I/R, where the whole heart was evaluated, but no work has been done on isolated cardiomyocytes. Although it seems that the *in vivo* anti-inflammatory response from CBD provides protection, we propose that another protective signal is involved. Given that CB receptors couple to G_i , we expect that CB activation will suppress cAMP levels and lead to an increase in cGMP, which initiates cardioprotection via PKG (see section 1.7). Other cannabinoids have been shown to stimulate cardioprotection *in vivo* and *in vitro*.

The activation of CB2 *in vivo*, with synthetic cannabinoid HU-210 (Krylatov et al., 2001) or the non-selective agonist WIN55212-2 (Di Filippo et al., 2004) before I/R, reduced the infarct size and ventricular arrhythmias.

In an *in vivo* mouse heart I/R study, CB2 was activated with the selective JWH-133 agonist 5 min before reperfusion (Montecucco et al., 2009). The results indicated a reduction in infarct size, which

was associated with a decrease in oxidative stress and neutrophil infiltration via activation of ERK1/2 and signal transducer and activator of transcription-3 (STAT-3). The researchers concluded that CB2 activation reduces the infarct size by a direct cardioprotective mechanism on cardiomyocytes and neutrophils (Montecucco et al., 2009).

An *in vitro* study (Shmist et al., 2006) tested the effect that pre-treatment with THC exerts on CB1 and CB2 in cultured neonatal cardiomyocytes, subjected to 60, 90 and 120 min hypoxia. They found that THC activating CB2, and not CB1, induces NO production and possibly “pre-trains” the cardiomyocytes to hypoxic conditions (Shmist et al., 2006).

It seems that the protection induced in myocardial ischemia from CB receptor activation is mainly mediated by CB2 activation, and not CB1 (Lamontagne et al., 2006).

Whole heart experiments prove that the administration of CBD can protect the heart from I/R damage (Durst et al., 2007; Hepburn, 2014; Mechoulam et al., 2007; Walsh et al., 2010), possibly by activating both CB1 and CB2 to modulate cyclic nucleotide (CN) levels via G_i coupling, or for CB1 via G_s . The lack of experiments that focus on the role of acute CBD administration in isolated cardiomyocytes in the setting of acute myocardial ischemia needs to be addressed. This study will evaluate the effect of CBD when administrated at the start of ischemia and continuously during I/R.

1.7 CN mediated signaling during I/R

CNs (cAMP and cGMP) are tightly regulated second messengers. They are critically involved in various intracellular processes (Dayton et al., 1976; Leineweber et al., 2006). Under normal conditions rhythmic contraction of the heart is maintained by cAMP and cGMP levels.

cAMP is synthesized from ATP by AC in response to G-protein activation by β -AR. cAMP production activates PKA and thereby enhance cardiac output through an integrated effect of increased contraction, relaxation and heart rate (Ishikawa & Homcy, 1997). Removal of the agonist from the β -AR rapidly reverses this effect, deactivates PKA and cAMP is degraded by phosphodiesterases (PDEs).

In pathophysiological conditions such as acute myocardial ischemia, catecholamine release and thus signaling is maintained, which in this case is released in response to the ischemic insult. β -AR signaling is therefore maintained, with the receptor desensitizing only after an elongated period. The resultant increase in cAMP during ischemia is detrimental, it leads to sustained and increased cardiac contraction, ATP depletion, tissue damage and cell death. Furthermore, Ishikawa and Homcy (1997) proposed that during ischemia, PKC regulates cardiac AC. The activity of PKC is sustained by the influx of Ca^{2+} during ischemia (described in section 1.2), and contributes to ischemic damage.

cGMP is the second messenger activated by NO and atrial natriuretic peptide (ANP), but unlike cAMP it is associated with cardioprotection (Dodge-Kafka et al., 2006). ANP couples natriuretic peptide receptor-A (NPR1/NPRA/ANP_A), which is a GPCR, to guanylyl cyclase (GC), and converts guanosine triphosphate (GTP) to cGMP. cGMP then stimulates PKG which initiates cardiomyocyte relaxation (Cawley et al., 2007).

cGMP elevation is associated with a negative inotropic effect that initiates protection against I/R injury and prevents apoptosis (Francis, 2010). PKG activated by cGMP lowers ICa^{2+} and thereby reduces contraction. Moreover, an elevation in cGMP can suppress β -AR damage signaling via PKG activity (Francis, 2010).

1.8 Compartmentation of cAMP and cGMP

cAMP and cGMP subcellular localization is critical in controlling the physiological effects, amplitude, and specificity of a signal. Specific localizations are known as compartments and serve as defined microenvironments (Fischmeister et al., 2006).

The assembled compartments comprise of unique cyclases, degradation enzymes (PDEs) and kinases that are attached to anchoring proteins (scaffolds), which bind to specific membrane molecules (Miller & Yan, 2010).

Anchoring proteins are therefore molecular configurations of micro-domains, which increase the efficacy and speed of signal transduction (Fischmeister et al., 2006). Recent CN studies revealed that compartmentation of certain signaling molecules independently regulate the signal for each physiological event (Omori & Kotera, 2007).

Compartments allow rapid and preferential modulation of cAMP and cGMP production (Fischmeister et al., 2006). Importantly, some cAMP compartments in the heart appear to be close to the sarcolemma, adjacent to β -ARs and under the control of specific regulating enzymes (Mongillo et al., 2006). Further action of cAMP localization is attributed to PKA pools, and their association with PKA-anchoring proteins (Dodge-Kafka et al., 2006).

Evidence for distinct cellular cGMP compartmentalization in the sub-sarcolemma and the cytosol are provided by several researchers (Castro et al., 2010; Maurice et al., 2003; McConnachie et al., 2006). The biological effects of both cGMP pools are mediated by PKG activity (Francis, 2010). Other compartmentation of CNs also occurs in other organelles and the nucleus (Dodge-Kafka et al., 2006; Fischmeister et al., 2006).

Fischmeister and colleagues (2006) proposed that cAMP and cGMP compartmentalized signal generation is controlled by a relationship between distinct synthesis sites and restricted cytoplasmic diffusion.

Intracellular CN levels are tightly regulated by their synthesis and degradation rate (Fischmeister et al., 2006). PDEs are the only enzymes that control CN levels by hydrolysis, and therefore PDEs largely control CN compartmentation (Miller & Yan, 2010), and can also serve as downstream effectors of cAMP and cGMP (Omori & Kotera, 2007).

1.9 Role of PDEs in regulating CN levels

PDE activity selectively catalyzes CN hydrolysis. PDEs directly target the 3', 5' cyclic phosphate bonds of cAMP and/or cGMP (Beavo, 1995; Bender & Beavo, 2006) to generate 5' AMP and 5' GMP (Francis et al., 2011).

PDEs enclose a highly conserved catalytic site, with approximately 270 amino acids, but differ significantly in other protein regions, specifically within the C- and N-terminal regions (Knight & Yan, 2013). They are subdivided into 11 distinct families, based on: primary amino acid sequence, complete domain structure, and catalytic and regulatory sites (Knight & Yan, 2013; Maurice et al., 2003). The subdivided families are classified as cAMP-specific (PDE4, 7 and 8), cGMP-specific (PDE5, 6 and 9) and dual-specific (PDE1, 2, 3, 10 and 11) (Francis et al., 2011).

The involvement of a specific PDE on cAMP and/or cGMP amplitude, duration, and location are regulated by numerous processes, including: phosphorylation, CN binding to the amino terminal allosteric regulatory site (GAF domains), expression level alterations, regulatory or anchoring protein interactions and reversible translocation between subcellular compartments (Francis et al., 2011). Worthy to note, is the statement made by Zaccolo (2006) "the compartmentalization of individual PDEs, rather than the total level of expression of the enzyme, appears to be of paramount importance in determining their effects on intracellular cAMP levels".

PDEs control cAMP and cGMP diffusion and can be targeted to specific subcellular compartments (Götz et al., 2014; Zaccolo et al., 2002). Specific PDE localization is thus important, for example PDE4 is found to play a crucial role in regulating cAMP levels generated by β -AR agonist stimulation (Mongillo et al., 2004). In contrast, PDE3 regulates cAMP levels in a functionally distinct pool associated with sarcoplasmic Ca^{2+} -ATPase (SERCA2), phospholamban, PKA inhibitory subunit 2, and protein phosphatase 2A (Knight & Yan, 2013).

In the heart, the activity of specific localized PDEs control cAMP and cGMP levels and localization in a cross-talk fashion, for example cGMP levels regulate the activity of PDE2 to hydrolyse cAMP.

As a result, the intracellular cGMP level influences the intracellular cAMP level (Zaccolo & Movsesian, 2007).

In the setting of acute myocardial ischemia the increase in cAMP can be detrimental. This damaging effect can be blunted, and protection stimulated, when cGMP levels increase (Yanaka et al., 2003).

Remember that specific PDEs are responsible for cAMP and/or cGMP levels. Therefore it is necessary to identify the key PDEs that are damaging or protective during ischemia, and whether their inhibition or activation elicits cardioprotection.

1.10 PDE5: cGMP specific enzymes

PDE5 is the first cGMP-PDE discovered and remains the best characterized (Senzaki et al., 2001; Vandewijngaert et al., 2013; Zhang et al., 2008). Three splice variants of PDE5 (A1 - A3) are identified in cardiomyocytes (Maurice et al., 2003).

PDE5 is specific for cGMP hydrolysis and contains GAF (amino terminal allosteric regulatory site) domains, refer to **Figure 1.4**. PKA activates and phosphorylates PDE5 (Beavo, 1995). Alternatively and more frequently, PDE5 is phosphorylated by PKG (Rao & Xi, 2009). The binding of cGMP to GAF A activates PDE5 and mediates PKG phosphorylation (Das et al., 2005), which increases PDE5 affinity for cGMP, and normalizes the levels of cGMP (Das et al., 2015).



Figure 1.4 PDE5 domain organization. This figure is modified from (Francis et al., 2011). A conserved catalytic domain is located in the COOH-terminal portion. One GAF domain provides for allosteric cGMP binding and the other GAF domain regulates catalytic site functions. Phosphorylation site is indicated by the encircled P.

1.10.1 The role and expression of PDE5 under normal physiological conditions

Under normal physiological conditions PDE5 is predominately expressed in VSMC, platelets, brain, lung, kidney, skeletal muscle and at low levels in the cardiomyocyte (Rao & Xi, 2009). PDE5 is localized relative to the z-band sarcomere structure and the sarcoplasmic reticulum (Rao & Xi, 2009; Senzaki et al., 2001).

NOS is suggested to be responsible for this localization. A study with endothelial NOS (eNOS) knockout mice and NOS inhibitor N^G-nitro-L-arginine methylester (L-NAME) chronically treated

wild-type cardiomyocytes, showed diffused PDE5 distribution (Takimoto et al., 2005). A similar diffused PDE5 distribution is found in failing hearts, where the localization of PDE5 with the z-band is altered (Senzaki et al., 2001).

PDE5 solely regulates NO-GC produced compartmentalized cGMP pools after β -AR stimulation (Götz et al., 2014; Senzaki et al., 2001). A cultured neonatal cardiomyocyte study by Isidori and colleagues (2015) examined the contribution of PDE5 to the isoproterenol stimulated contraction rate of all β -ARs. Their study showed that PDE5 inhibition increased cGMP levels and decreased the contraction rate from β -AR stimulation. Their study furthermore indicated that PDE5 inhibition counteracts β 2-AR signaling via a localized cascade of cGMP and PDE2, where PDE2 hydrolyses a subtype-specific cAMP pool. This supports the knowledge of β -AR signaling compartmentalization.

PDE5 activity influences cGMP physiological effects via PKG by maintaining vascular smooth muscle tone and directly affecting cardiomyocyte contractility (Maurice et al., 2003).

1.10.2 The role and expression of PDE5 in acute myocardial ischemia

PDE5 expression is found to increase in patients with ventricular hypertrophy and advanced left ventricle failure (Isidori et al., 2015; Johnson et al., 2012). Therefore, in the heart, PDE5 possibly exerts an adaptive role to an increase in stress (Vandenwijngaert et al., 2013). An increase in PDE5 expression thus serves as a molecular hallmark in hypertrophic hearts (Zhang et al., 2008).

Scientists developed the first selective PDE5 inhibitor (UK-92480) as part of a drug development program for antihypertension (Kumar et al., 2009). The drug was thought to augment intracellular cGMP levels to relax arteries and lower blood pressure, but the results were disappointing.

As yet, three selective PDE5 inhibitors are used to treat erectile dysfunction: vardenafil (Levitra™), tadalafil (Cialis™), and sildenafil (Viagra™) (Das et al., 2015; Kukreja et al., 2004; Senzaki et al., 2001). PDE5 inhibitors are approved to treat pulmonary arterial hypertension (Choi et al., 2009; Kumar et al., 2009; Senzaki et al., 2001; Sesti et al., 2007), congestive heart failure (Kass, 2012; Weeks et al., 2005), diabetes and cancer (Das et al., 2015).

Inhibition of PDE5 results in an elevated steady state of cGMP levels (Beavo, 1995; Cawley et al., 2007), which activates PKG. PKG opens the mitochondrial ATP-sensitive potassium (K_{ATP}) channels (Choi et al., 2009), stimulating protection in ischemic hearts by preventing ion gradient loss, allowing continued ATP production and Ca^{2+} transport out of the overloaded mitochondria (Rao & Xi, 2009; Takashi et al., 1999). Protection from I/R is also mediated by a PKG-dependent protein phosphorylation cascade, including ERK1/2 and glycogen synthase kinase-3 beta (GSK3 β)

phosphorylation (Das et al., 2008), which decreases ICa^{2+} and results in vasodilation (Kukreja et al., 2004).

There are significantly more studies based on PDE5 inhibition in I/R compared to PDE2 and PDE3. Most of these studies are described below and summarized in **Table 1.1**.

Novel investigations of myocardial preconditioning (Ockaili et al., 2002; Salloum et al., 2003) with sildenafil in rabbits and mice isolated perfused hearts identified that PDE5 inhibition can reduce the infarct size and results in cardioprotection. The rabbits were treated *in vivo* with sildenafil either acutely, 30 min before, or chronically, 24 h before, 30-min ischemia and 3-h reperfusion (30-min I/3-h R) (Ockaili et al., 2002). Sildenafil also significantly reduced blood pressure. For the mice experiment, sildenafil was administered *in vivo* 24 h before 20-min I/30-min R (Salloum et al., 2003). The cardioprotection stimulated from preconditioning with sildenafil was dependant on the induction of NOS, where inducible NOS (iNOS) appeared to be the primary isoform that mediates protection. NOS induction lead to the opening of the mitochondrial K_{ATP} channel.

The opening of the mitochondrial K_{ATP} channel was also identified as the possible end-effector of preconditioning with sildenafil in isolated rat hearts, where sildenafil was given 10 min before either 20-min global I/5-min R or 35-min regional I/30-min R (du Toit et al., 2005). This group, using radio-immunoassay kits, showed that sildenafil elevates myocardial cGMP levels and directly suppresses cAMP levels.

Salloum and colleagues (2006) confirmed that the opening of the mitochondrial K_{ATP} channel is crucial in perfused rabbit hearts. They found that preconditioning with vardenafil 30 min before 30-min I/3-h R induced protection from I/R injury. Even in infant rabbits (Bremer et al., 2005), *in vivo* treatment with sildenafil 30 min before 30-min I/3-h R also reduced the infarct size and preserved left ventricular cardiac output.

The same preconditioning effect was found by Das and colleagues (2002) in isolated perfused rat hearts, where *in vivo* administration of sildenafil 60 min before 30-min I/2-h R improved ventricular recovery, decreased infarct, and reduced the incidence of ventricular fibrillation.

The hypothesis behind these studies is that the vasodilatory effect of sildenafil, administered acutely or delayed, could possibly release endogenous preconditioning mediators, such as adenosine or bradykinin, from endothelial cells. These mediators potentially trigger a signaling cascade via kinase activity and results in NOS phosphorylation and NO release. NO can activate GC, which enhances cGMP levels and leads to kinase activation, such as PKG and PKC. Subsequently, PKG and PKC leads to the opening of the mitochondrial K_{ATP} channel and stimulates cardioprotection (Kukreja et al., 2004). Das and colleagues elaborated their results in 2009 and found that

preconditioning with sildenafil increases PKG-dependant ERK1/2 and GSK3 β phosphorylation significantly, where ERK phosphorylation is crucial for the induction of eNOS, iNOS, increasing B-cell lymphoma-2 (Bcl-2) and the resulting cardioprotective effect.

With regards to isolated cardiomyocytes, an *in vitro* study (Das et al., 2005) found that sildenafil (1 μ M or 10 μ M) given 1 h before 40-min simulated I/18-h R significantly reduced apoptosis and necrosis by enhancing the induction of iNOS and eNOS (to a smaller extent), increasing NO, which up-regulates Bcl-2. In 2006 the research group (Das et al., 2006) confirmed that the rise in PKG activity from sildenafil treatment plays a crucial role in protecting cardiomyocytes from necrosis and apoptosis by increasing PKB/Akt, ERK1/2, and c-Jun N-terminal kinase (JNK) phosphorylation, Bcl-2, iNOS, eNOS and decreasing the expression of the pro-apoptotic protein, Bax.

It seems that research based on pre- and post- I/R inhibition of PDE5 is limited, in fact, I could find only one article. The first research group that tested the inhibition of PDE5 at reperfusion was Salloum and colleagues (2007).

In rabbit hearts they found that the administration of sildenafil or vardenafil 5 min before reperfusion for 65 min with the protocol of 30-min I/3-h R decreased the infarct size in a similar mechanism as preconditioning, by opening the mitochondrial K_{ATP} channel.

Table 1.1 PDE5 inhibitors administrated at different time points during ischemia-reperfusion (I/R) to induce cardioprotection.

Drug	Animal model	Time point	Drug effect	Authors
Sildenafil	Perfused adult rabbit heart	Before I/R	Reduced infarct size	(Ockaili et al., 2002)
	Isolate rat heart		Improved ventricular recovery, decreased myocardial infarction and reduced incidence of ventricular fibrillation	(Das et al., 2002)
	Perfused mice hearts		Reduced infarct size	(Salloum et al., 2003)
	Perfused infant rabbit heart		Reduced infarct size and preserved left ventricular cardiac output	(Bremer et al., 2005)
	Isolated ventricular cardiomyocytes		Reduced apoptosis and necrosis	(Das et al., 2005)
	Isolated rat heart		Reduced infarct size	(du Toit et al., 2005)
Vardenafil	Perfused rabbit hearts	Onset R	Stimulated I/R protection	(Salloum et al., 2006)
Tadalafil	Isolated rat hearts		Reduced mean arterial pressure and infarct size	(Sesti et al., 2007)
Tadalafil	Isolated mouse hearts		Reduced apoptosis	(Ahmad et al., 2009)
Sildenafil	Isolated mouse hearts		Reduced infarct size	(Das et al., 2009)
Sildenafil/vardenafil	Perfused adult rabbit heart		Reduced infarct size	(Salloum et al., 2007)

PDE5 inhibition before I/R has frequently been proven to be protective (Ahmad et al., 2009; Bremer et al., 2005; Das et al., 2009; Das et al., 2002; du Toit et al., 2005; Kukreja et al., 2005; Ockaili et al., 2002; Salloum et al., 2006; Salloum et al., 2003; Sesti et al., 2007) and PDE5 inhibition at reperfusion (Salloum et al., 2007), by a similar mechanism as preconditioning, can stimulate cardioprotection. There is a major lack in research on the role of PDE5 in cultured isolated cardiomyocytes, and when PDE5 is inhibited at the onset of ischemia, at reperfusion or after I/R. This study aims to address this shortcoming.

However, PDEs do not function in isolation, and the activity or the inhibition of various PDEs might play an important role in mediating the cardioprotection stimulated by PDE5 inhibition. In the next section the PDEs that could be involved are identified and their specific role and expression under normal physiological conditions and in acute myocardial ischemia are explored.

1.11 Cardiomyocyte cAMP and cGMP cross-talk with PDE5

Isidori and colleagues (2015) found that PDE5 inhibition (with sildenafil) modulates the response of β -AR stimulation (isoproterenol) by influencing PDE2 activity, refer to **Figure 1.6**. After β -AR stimulation, PDE2 inhibition (with *erythro*-9-(2-hydroxyl-3-nonyl)adenine: EHNA) reversed the negative chronotropic effects of PDE5 inhibition. They proposed the following: the inhibition of PDE5 leads to an increase in cGMP levels. The high levels of cGMP activate PDE2 to hydrolyse cAMP, which were increased by β -AR stimulation.

A cross-talk between PDE5 and PDE3 contributes to the regulation of cGMP (Rao & Xi, 2009). In cardiomyocytes, cGMP influences Ca^{2+} levels via cAMP in a manner that is concentration dependent. Low cGMP concentrations inhibit PDE3 and increases Ca^{2+} levels (**Figure 1.5A**), while high cGMP concentrations activate PDE2 and decreases Ca^{2+} levels (**Figure 1.5B**) (Rao & Xi, 2009).

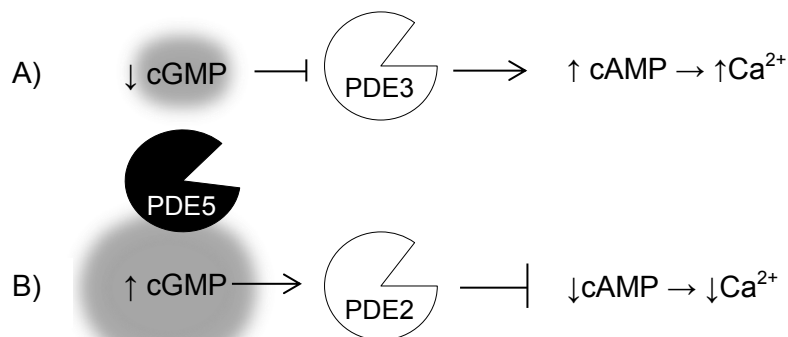


Figure 1.5 A) Low cGMP concentrations inhibit PDE3. PDE3 cannot hydrolyse cAMP and Ca^{2+} levels increase. PDE5 regulates cGMP levels B) High cGMP concentrations activate PDE2. PDE2 hydrolyses cAMP and Ca^{2+} levels decrease.

Taken together, refer to **Figure 1.6**, PDE2 and PDE3 mediate contrasting regulation (Bender & Beavo, 2006; Maurice et al., 2003). The cGMP-stimulated PDE2 and cGMP-inhibited PDE3 regulate cAMP signaling in the cardiomyocytes. cGMP-mediated PDE2 activation acts to limit the cAMP levels and Ca^{2+} current, stimulated by the cGMP-mediated effect on PDE3 (Maurice et al., 2003). Under conditions where cGMP levels are low and PDE2 and PDE3 are inhibited, it seems that PDE3 plays a more prominent role in regulating cAMP (Bender & Beavo, 2006). Compared to the effect of PDE2 inhibition, PDE3 inhibitors (for example milrinone) alone have a greater effect on platelet aggregation.

Wen and colleagues (2004) proposed that soluble GC (sGC) and particulate GC (pGC) both regulate cGMP/PDE/cAMP signaling (refer to **Figure 1.6**). sGC and pGC are possibly related to functional cGMP compartments attributable to localized accumulation in cGMP (Wen et al., 2004). Therefore, the roles of PDE2 and PDE3 are related to the two phase effect of cGMP on cardiac Ca^{2+} current.

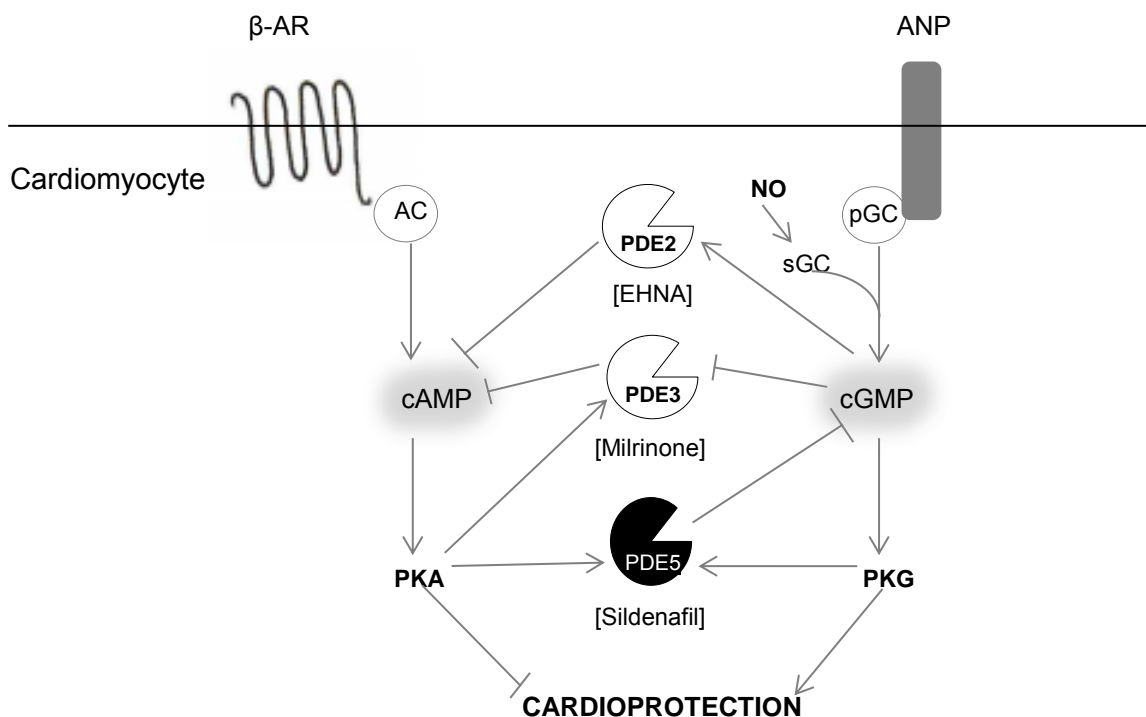


Figure 1.6 Schematic summary of PDE5 cross-talk with PDE2 and PDE3 in cardiomyocytes, adapted from (Rao & Xi, 2009). β -AR stimulation increases cAMP via AC, activating PKA, which leads to cardio damage. ANP stimulation increases cGMP via pGC. cGMP is also increased by NO via sGC. cGMP activates PKG, which leads to cardioprotection. PKA activates and phosphorylates both PDE3 and 5. PDE5 can also be activated and phosphorylated by PKG. An increase in cGMP activates PDE2 (inhibitor: EHNA) to hydrolyse cAMP. Low levels of cGMP furthermore inhibits PDE3 (inhibitor: milrinone) leading to an increase in cAMP. Active PDE5 (inhibitor: sildenafil) hydrolyses cGMP. PDEs, and their inhibition, tightly regulate cAMP and/or cAMP levels.

1.12 PDE2: cGMP stimulated to hydrolyse cAMP and cGMP

PDE2 (splice variants: A1, A2 and A3) is a dual-specific PDE and hydrolyses both cAMP ($K_m = 30 \mu\text{M}$) and cGMP ($K_m = 10 \mu\text{M}$) (Fischmeister et al., 1995; Zaccolo et al., 2006). However, only cGMP binding to any one of the two GAF domains (refer to **Figure 1.7**), via allosteric modification, can activate PDE2 (Bender & Beavo, 2006; Maurice et al., 2003).



Figure 1.7 PDE2 domain organization. This figure is modified from (Francis et al., 2011). A conserved catalytic domain is located in the COOH-terminal portion. One GAF domain provides for allosteric cGMP binding and the other GAF domain regulates catalytic site functions.

The binding of cGMP lowers the affinity of PDE2 for cAMP by 30-fold (Knight & Yan, 2013), activates PDE2 activity to hydrolyse cAMP (Zaccolo & Movsesian, 2007), which is quantitatively more important than the competitive inhibition of cAMP hydrolysis. cAMP hydrolysis can be inhibited when cGMP concentrations are high ($> 50 \mu\text{M}$) (Zaccolo & Movsesian, 2007) and results in PDE2 hydrolyzing cGMP (Mokni et al., 2010; Vandecasteele et al., 2001), where PDE2 is mainly associated with pGC produced cGMP pools (Knight & Yan, 2013).

Interestingly, in adult cardiomyocytes, only β_3 -AR coupled NOS-NO derived cGMP can bind to the GAF domains. cGMP derived from ANP receptor without concomitant β -AR stimulation cannot bind the GAF domains. This is contradictory to what is found in neonatal cardiomyocytes, where cGMP from both pathways can activate PDE2 (Lee & Kass, 2012). This indicates the development of complex compartmentalized signaling in adult cardiomyocytes.

1.12.1 The role and expression of PDE2 under normal physiological conditions

Under basal conditions PDE2 expression, refer to **Figure 1.8**, is found in the isolated cardiomyocyte (Francis et al., 2011). PDE2 is encoded by a single gene that is alternatively spliced to produce three isoforms: A1 – A3. PDE2A2 and PDE2A3 show clear distinct membrane localization, indicating anchoring to compartments. Distribution is found to be at the sarcolemma, sarcoplasmic reticulum membrane (Zaccolo et al., 2006), and the z-line (Takimoto, 2012). Both isomers are functionally coupled to a pool of AC activated by β -AR stimulation where they primarily regulate cAMP originating

from this compartment. PDE2A1, attributable to the absence of a unique N-terminal amino acid sequence, is soluble and found in the cytoplasm (Bender & Beavo, 2006). Once activated, PDE2 reduces L-type Ca^{2+} currents and blunts contraction (Knight & Yan, 2013; Maurice et al., 2003).

PDE2 represents only 1 % of total PDE activity for cAMP at basal (Mongillo et al., 2006). Despite the marginal PDE2 activity, (Zaccolo et al., 2006) showed that PDE2 inhibition, in combination with β -AR-agonists, greatly elevates cAMP levels. This proves the important role of PDE2 in controlling the cAMP response to catecholamines.

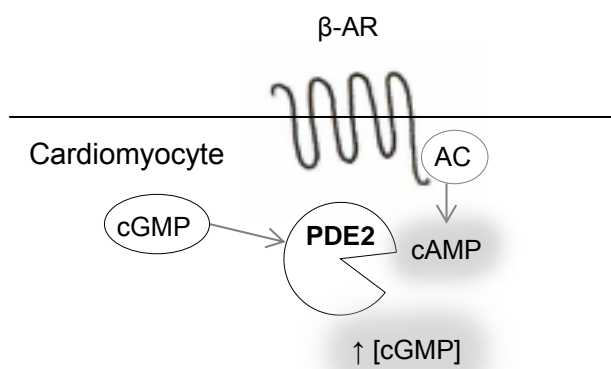


Figure 1.8 Schematic representation of PDE2 localization and cAMP compartmentalization in cardiomyocytes. PDE2A2 and PDE2A3 are functionally coupled to AC pools activated by specific GPCR β -AR stimulation. cGMP activates PDE2 activity to hydrolyse cAMP, and at high concentrations cGMP, localized in specific compartments.

Normoxic cardiomyocyte studies show that cGMP, through activating PDE2, opposes cAMP by reducing cAMP levels and directly affects cardiac function (Fischmeister et al., 1995; Vandecasteele et al., 2001).

1.12.2 The role and expression of PDE2 in acute myocardial ischemia

Nothing is known about the role of PDE2 in the setting of I/R. Studies with Angiotensin-II-induced hypertrophy in rat whole hearts (Mokni et al., 2010) and ventricles subjected to pressure overload (Yanaka et al., 2003) provide evidence that PDE2's activity to hydrolyse cAMP increases in heart diseases. The potent PDE2 inhibitor, EHNA (Abi-Gerges et al., 2000; Maurice et al., 2003; Mokni et al., 2010; Vandecasteele et al., 2001) is however frequently used in studies to block cAMP hydrolysis.

As explained in section 1.2, detrimental levels of cAMP cause damage during ischemia. The prediction can be made that, if the activity of PDE2 is increased during acute myocardial ischemia, by inhibiting

cGMP-specific PDEs to increase cGMP levels, the levels of cAMP will decrease and cardioprotection can be stimulated.

1.13 PDE3: cGMP-inhibited cAMP-hydrolysing enzymes

PDE3 (subfamilies: A and B) regulates both cAMP- and cGMP-mediated intracellular signaling (Isidori et al., 2015; Wechsler et al., 2002). The binding affinity for cAMP ($K_m < 0.4 \mu\text{M}$) and cGMP ($K_m < 0.3 \mu\text{M}$) is equally high (Bender & Beavo, 2006), and hydrolysis of both is done in a mutually competitive fashion (Wechsler et al., 2002).

The C-terminal catalytic domain of PDE3, refer to **Figure 1.9**, contributes to catalytic activity and inhibitor selectivity by expressing a unique 44 amino acid sequence (Maurice et al., 2003). The catalytic rate for cAMP is 10-fold higher compared to cGMP. The slower hydrolysis of cGMP allows cAMP to be spared which is how cGMP inhibits PDE3 hydrolysis of cAMP (Zaccolo & Movsesian, 2007).

PDE3 also contains N-terminal hydrophobic membrane association regions, named NHR1 and NHR2, refer to **Figure 1.9**. These regions control PDE3 localization and thereby influence PDE3 activity (Zaccolo & Movsesian, 2007). PKA or PKB/Akt phosphorylation activates PDE3 at consensus sites of phosphorylation for each kinase located between NHR2 and the catalytic domain (Maurice et al., 2003).

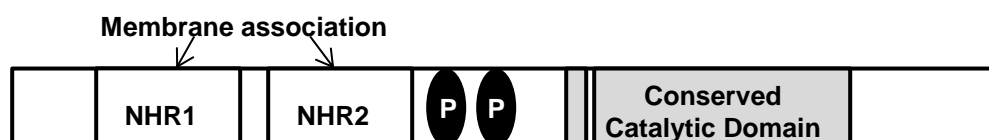


Figure 1.9 PDE3 domain organization. This figure is modified from (Francis et al., 2011). A conserved catalytic domain is located in the COOH-terminal portion. Phosphorylation sites are indicated by the encircled P. A unique complement of NHR1 and NHR2 contribute to activity regulation.

1.13.1 The role and expression of PDE3 under normal physiological conditions

The PDE3 isoforms, A and B, are structurally similar, but differences can be found in the catalytic domain, where they have different 44-amino acid sequences, and in the N-terminal, where they have different regions (Wechsler et al., 2002). Although the isoforms have similar pharmacological and kinetic properties there is a distinction in the expression profiles. *PDE3A* expression is more abundant

than *PDE3B*, and primarily found in cardio and vascular myocytes (Maurice et al., 2003). *PDE3A* is localized in cytosolic and microsomal compartments, in close proximity to selective cAMP pools, associated with SERCA2, phospholamban, PKA inhibitory subunit 2, and protein phosphatase 2A (Knight & Yan, 2013). These pools can be regulated by direct PDE3 regulation (Wechsler et al., 2002). *PDE3B* expression is found in pancreatic cells, hepatocytes, and adipocytes (Rao & Xi, 2009; Wechsler et al., 2002).

In cardiomyocytes, at basal level, the cAMP-hydrolysing activity of PDE3 is abundant (Francis et al., 2011; Johnson et al., 2012; Maurice et al., 2003). Together, PDE3 and PDE4 are mainly responsible to control ICa^{2+} for contraction and relaxation (Johnson et al., 2012).

PDE3 activity controls ICa^{2+} levels in a PKA-dependent manner (Kirstein et al., 1995) through L-type Ca^{2+} channels and SERCA2 (Wechsler et al., 2002). ICa^{2+} release is induced via a NO-cGMP pathway in the following manner. Low levels of NO stimulates sGC to produce cGMP, which inhibits PDE3, increasing the cAMP levels and thereby stimulates an increase in ICa^{2+} (Vandecasteele et al., 2001).

cGMP produced by pGC when stimulated by natriuretic peptides also inhibits PDE3 (Götz et al., 2014). Interestingly, a perfused beating rabbit atrial study (Wen et al., 2004) indicated that cGMP production from sGC or pGC has different effects on cAMP levels, suggesting compartmentalization of cGMP/PDE3/cAMP signaling. The different effects have not yet been clarified. Nonetheless, these cGMP pools are responsible for the “cross-talk” between cAMP and cGMP (Götz et al., 2014).

β 1- and β 2-AR cAMP-mediated signaling is regulated by PDE3 (Fischmeister et al., 2006). Yet it is suggested that PDE3 is mainly associated with β 2-ARs. PDE3 blunts the response of β 2-AR, activated by catecholamine release, to increase cAMP levels (Christ et al., 2009). Nikoleav and colleagues (2006) proposed that cAMP stimulated by β 1-AR generates a cAMP gradient, which propagates throughout the cell, whereas β 2-AR cAMP signaling remains locally restricted in compartments.

1.13.2 The role and expression of PDE3 in acute myocardial ischemia

The chronic inhibition of PDE3 in heart failure is vastly studied, but limited publications have focused on the role PDE3 inhibition exerts during acute myocardial ischemia. Nevertheless, what is known of cardioprotection exerted by PDE3 inhibitors is described below.

In cardiomyocytes the inhibition of PDE3 elevates cAMP levels and the L-type Ca^{2+} currents (Wechsler et al., 2002), resulting in positive inotropic (contraction) and vasodilatory (relaxation) effects (Miller & Yan, 2010; Rao & Xi, 2009). Milrinone, a selective inhibitor of PDE3, is commonly used to

treat congestive heart failure due to the positive inotropic effects (Francis et al., 2011; Miller & Yan, 2010; Zaccolo & Movsesian, 2007). It is a major concern that mortality is found to increase with chronic milrinone treatment, mainly attributable to arrhythmias and sudden death (Miller & Yan, 2010).

Chronic PDE3 inhibition promotes apoptosis (Zaccolo et al., 2005) potentially via increased localized cAMP that sustains the induction of inducible cAMP early repressor (ICER) transcription (Tomita et al., 2003). ICER mediates apoptosis partially through the cAMP response element binding protein (CREB)-mediated transcription inhibition and Bcl-2 downregulation (Ding et al., 2005; Shin et al., 2014; Tomita et al., 2003). In contrast, PDE3 overexpression prevents cardiomyocyte death (Shin et al., 2014).

Some studies regarding the role of PDE3 inhibition (with milrinone or amrinone) on ischemic and hypoxic hearts will now be described and are summarized in **Table 1.2**.

In 1992, Löwe and Jacobsohn found that in a perfused rabbit heart, where milrinone was continuously administered in a perfusion medium during 5 min hypoxia and 15 min reperfusion (5-min H/15-min R), improved contractile recovery, but the mechanism involved was not described.

Experiments that followed by other researchers (Sanada et al., 2001; Shibata et al., 2013) identified the role of PDE3 in the cAMP/PKA/p38 MEK-dependent pathway that stimulates cardio damage. PDE3 inhibition with milrinone, 30 min before 90 min I/6 h R, increases cAMP, which activates PKA to elicit protection (Sanada et al., 2001). The same result was found when PDE3 was inhibited 20 min directly after 12-min I/90-min R or 20-min after I/R for 70 min (Shibata et al., 2013). Sanada and colleagues (2001) also found that PDE3 plays a role in the PKC-independent pathway, however the precise mechanism involved is still elusive.

PDE3 inhibition after acute ischemia has an inotropic effect (Zucchi et al., 1990) also when amrinone was given 20 min before 30-min I/30-min R (Rechtman et al., 2000). The inotropic effect identifies the role PDE3 inhibition exerts to increase Ca^{2+} levels, which correlates with the cAMP/PKA/p38 MEK-dependent pathway.

In a rat heart model, Huang and colleagues (2011) found that Milrinone, in combination with a β 1-AR blocker, administered for 10 min from the last 5 min of ischemia until the initial 5 min of reperfusion, robustly reduced left ventricular myocardial infarct size via PKA and subsequent PKB/Akt activation. This indicates that active PDE3 plays a role in activating apoptosis, which they confirmed in rat isolated cardiomyocyte cultures that underwent 2-h H/1-h R.

Table 1.2 PDE3 inhibitors administrated at different time points during ischemia-reperfusion (I/R) or hypoxia-reperfusion (H/R) to induce cardioprotection.

Drug	Animal model	I/R or H/R	Drug administration	Drug effect	Authors
Milrinone	Perfused rabbit heart	H/R	During H/R	Improved contractile recovery	(Löwe & Jacobsohn, 1992)
	Canine heart	I/R	Before I/R	Reduced infarct size	(Sanada et al., 2001)
	Swine heart	I/R	Onset of R or 20 min after R	Onset of R: Attenuated myocardial stunning	(Shibata et al., 2013)
Amrinone	Isolated rat heart	I/R	After I/R	Improved contractile recovery	(Zucchi et al., 1990)
	Perfused rabbit heart	I/R	Before I/R	Reduced infarct size and reduced incidences of ventricular fibrillation	(Saltman et al., 2000)
	Isolated rat heart	I/R	Before I/R	Reduced I/R injury	(Rechtman et al., 2000)
Milrinone + Esmolol (β 1 blocker)	Isolated rat heart	I/R	Late I/ early R	Reduced left ventricular myocardial infarct size	(Huang et al., 2011)
	Cultured cardiomyocytes	H/R	During H	Reduced myocyte death rates	

Studies to determine the role of acute PDE3 inhibition in the setting of acute myocardial ischemia is still lacking, in isolated cardiomyocytes even more so than in heart model experiments. As acute PDE3 inhibition does not activate apoptosis, and the experiments described above prove PDE3 inhibition initiates cardioprotection, the prediction can be made that PDE3 inhibition during acute myocardial ischemia in isolated cardiomyocytes will stimulate protection. Possibly, this protection is induced by the activation of the cAMP/PKA/p38 MEK-dependent pathway to increase ICa^{2+} .

It is, however, very interesting that the increase in cAMP from PDE3 inhibition leads to protection, as increased cAMP levels are usually associated with contraction and damage (section 1.2).

CHAPTER 2

Hypothesis, Aims, Objectives and Value of Research

In summary, acute myocardial I/R induces injury in cardiomyocytes that can be blunted, and protection can be stimulated, with the application of different treatments. The increase in cAMP during ischemia can be detrimental, whereas an increase in cGMP stimulates cardioprotection. PDEs control these cAMP/cGMP levels (Fischmeister et al., 2006).

The inhibition of PDE5 is cardioprotective (Ockaili et al., 2002; Das et al., 2015) and leads to an increase in cGMP, which can possibly suppress the damaging effect of the increase in cAMP from β -AR activation. We therefore speculate that the compartmentalization of cAMP/cGMP plays a critical role in governing protection versus damage signaling during I/R.

CBD has already been shown to protect the isolated whole heart (Durst et al., 2007; Feng et al., 2015; Walsh et al., 2010) and might therefore also protect isolated heart cells. CBD possibly protect heart cells against I/R injury by activating CB receptors that couple to G_i and thereby increase cGMP (Carney et al., 2009). This CBD-mediated protection might be controlled by specific PDEs, possibly PDE5.

2.1 Hypothesis

We hypothesize that acute myocardial I/R injury can be blunted, and protection stimulated with the PDE5 inhibitor, and that CBD-mediated protection is dependent on the inhibition of PDE5.

2.2 Aims

The main aim of this study was to determine the role of PDE5 in regulating cardioprotection versus damage.

The second aim was to determine if CBD protects cardiomyocytes against I/R injury and whether the protection is dependent on the inhibition of PDE5.

2.3 Objectives

1. To evaluate whether CBD at 0.001 μ M, 1 μ M, or 100 μ M can protect adult rat cardiomyocytes from I/R damage, specifically contracture/hypercontracture and apoptosis.

2. a) To determine if the inhibition of PDE5 during ischemia protect cardiomyocytes against I/R damage.
 - b) To determine if the inhibition of PDE5 during ischemia protect cardiomyocytes against enhanced I/R damage, driven by general β -ARs stimulation with isoproterenol, or β 1-AR stimulation with dobutamine.
 - c) To determine if, when β 2-AR stimulation with formoterol protects cardiomyocytes against I/R damage, PDE5 inhibition further enhance protection.
3. To evaluate if protection elicited by CBD depends on PDE5 inhibition.
 4. To investigate whether greater protection can be elicited by CBD in combination with the PDE5 inhibitor.

The objectives for Part 1 of this study could not be met and new objectives in Part 2 of this study focused on evaluating where the problem was.

2.4 Value research contributes to society

Heart attacks are the cause of too many deaths globally. The treatments currently available are found to be mostly protective when given as preconditioning, which is clinically not relevant, as normally a heart attack cannot be predicted. There is a need to identify novel treatments that can intervene during ischemia or during reperfusion. This project will contribute by identifying alternative treatments that stimulate protection, evaluating CBD with and without the PDE5 inhibitor. CBD is non-psychoactive, does not exert any harmful effects, and can easily be extracted from the plant *Cannabis sativa*.

CHAPTER 3

Materials and Methods

3.1 Animals

Adult male Wistar rats (260 - 290 g) were bred and housed in an internationally accredited AAALAC (association for assessment and accreditation of laboratory animal care) from the Faculty of Medicine and Health Sciences, Stellenbosch University. The animals had free access to standard lab food and water, and were maintained on a 12 h day/night cycle.

3.2 Ethical approval

Ethical approval was granted for the project by the Animal Ethics committee of the University of Stellenbosch (Faculty of Health Sciences) with project number SU-ACUM13-00018. The project conformed to the conditions stated in the "Revised South African National Standard for the care and use of Animals for Scientific purposes" (South African Bureau of Standards, SANS 10386, 2008).

3.3 Reagents

All reagents were obtained from Sigma-Aldrich, unless specified as other. Where necessary, the chemicals were stored at -4 °C and -20 °C.

3.4 Coating culture surface with Laminin-Entactin adhesive

96-well clear bottom tissue culture plates were used for all experiments. Laminin-Entactin (L/E, obtained from Lilly) was diluted to 100 µg/ml in PBS (6 mM KCl, 1 mM Na₂HPO₄, 0.2 mM, NaH₂PO₄.H₂O, 1.4 mM MgSO₄.7H₂O, 128 mM NaCl, 1.2 mM Ca²⁺, and 10 mM Hepes). 5 µl L/E was pipetted in the centre of each well and incubated overnight at 5 % CO₂ and 37 °C. The next day the L/E was removed, the wells washed (x 2) with 100 µl PBS and air dried in the laminar flow cabinet.

3.5 Isolation of adult rat ventricular cardiomyocytes

The Langendorff perfusion system was assembled in a laminar flow cabinet and thoroughly rinsed with sterile ethanol and left to dry. The ventricular cardiomyocytes were isolated using a modified

enzymatic technique (Fischer et al., 1991). All isolation buffers were continuously gassed with 5 % CO₂ and 95 % O₂ and contained 1 % penicillin/streptomycin (BD Biosciences).

In brief each rat was anesthetized with 60 mg sodium pentobarbital (Bayer), the heart removed and retrograde perfused (37 °C) with buffer A (Ca²⁺ free PBS with 11 mM D-glucose, 2 mM pyruvate and, 3 mIU/ml insulin (Humulin R by Lilly)) for 5 min. Enzymatic digestion was commenced by perfusion with buffer B (buffer A containing 0.5 % fatty acid free bovine serum albumin (BSA, obtained from Roche), 18 mM 2,3-butanedione monoxim (BDM), 1.8 mg/ml collagenase II (240 U/mg Worthington), and 0.2 mg/ml protease type IV (≥ 3.5 U/mg). Ca²⁺ was increased with 0.1 mM increments at 10 and 20 min thereafter. The digested ventricular tissue was cut off, placed in a petri dish and gently shook in buffer D (5 ml buffer B and 10 ml buffer C) with tweezers to facilitate cell dissociation. The cells were filtered through a 200 µm mesh and pelleted by 1 min centrifugation at 60 g. The cell pellet was re-suspended in buffer C (buffer A containing 0.5 % BSA, 0.5 % BSA fatty acid free, and 9 mM BDM) and the Ca²⁺ sequentially increased to 0.6, 0.9, and finally 1.2 mM.

150 µl cell suspension was removed and cells counted under the light microscope to determine percentage cell viability. The cells were diluted in a modified M199 culture buffer (40 % M199 supplemented with 10 mM HEPES, 5 mM creatine, 5 mM carnitine, 5 mM taurine mixed with 60 % buffer C containing 1.2 mM Ca²⁺ but not BDM) with 10 µM blebbistatin. The cells were counted under the light microscope using a hemocytometer. For normoxic conditions a final concentration of 2500 cells/100 µl/well was used, while 5000 cells/100 µl/well were used for ischemic experiments. Under ischemic conditions more cells wash off of the plate compared to the normoxic conditions, and to compensate for the loss of cells more cells are plated for ischemia experiments. The isolated cardiomyocytes were then seeded in the 96-well clear bottom L/E coated plates and cultured overnight in the incubator at 5 % CO₂ and 37 °C.

3.6 I/R and JC-1 staining

Cardiomyocytes were washed (x 3) for 30 min with modified M199 culture buffer (without blebbistatin), followed by simulated ischemia. 2-deoxy-D-3[H]glucose (2DG), which inhibits glycolysis, and sodium dithionite (SDT), an oxygen scavenger that generates superoxide radicals, were the chemical drugs used to simulate ischemia. Simulated ischemia was induced for 20 min by ischemic wash (40 % M199 with 1 % penicillin/streptomycin, and 60 % PBS containing 1.2 mM Ca²⁺ (without HEPES), pH = 6.4) with 3 mM 2DG and 10 mM SDT (**Figure 3.1**). Ischemia was followed by 60 min reperfusion with modified M199 culture buffer (without blebbistatin), which included 15 min incubation with 15 µM JC-1 stain, two washes and 30 min stain development, before images were captured (**Figure 3.1**). Normoxic cells received the same number of buffer changes as I/R, followed by JC-1 staining. JC-1

(5,5',6,6'-tetrachloro-1,1',3,3'-tetraethylbenzimidazole-carbocyanide iodine) stains the cytosol green, while only viable mitochondria with an active membrane potential difference will stain red. Therefore, a fluorescence ratio of red over green (R/G) indicates mitochondrial function, and thus cellular viability. Each experimental condition was repeated on cardiomyocytes harvested from 4 – 8 different rats, to yield $n = 4 - 8$. For each treatment group per heart there was at least 3 images, repeats, with 40 – 50 cardiomyocytes per image.

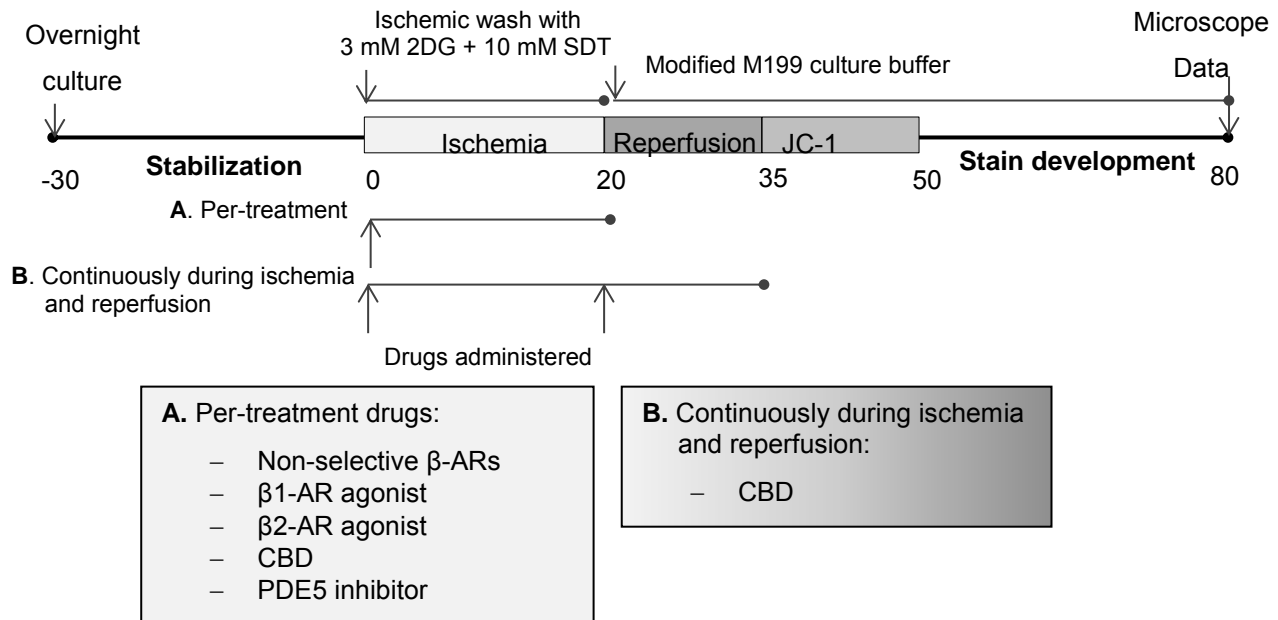


Figure 3.1 Protocol for 20 min simulated ischemia (3 mM 2DG and 10 mM SDT) followed by 60 min reperfusion, which included 15 min JC-1 stain.

3.7 Drug concentrations

- Non-selective β -ARs: 100 nM isoproterenol
- β 1-AR: 10 μ M dobutamine
- β 2-AR: 10 μ M formoterol (donated by Dr R. Salie (Tocris))
- CBD: 0.001 μ M, 1 μ M, and 100 μ M
- PDE5 inhibitor: 10 μ M Sildenafil

3.8 Data collection and analysis

The Nikon fluorescence microscope was used to capture images following JC-1 staining. A dual band excitation filter was used, which allowed red and green fluorescence emission detection. The NIS-element Basic Research imaging software (Nikon) was used to capture images at a 100 x magnification.

ImageJ (Schneider et al., 2012) freeware was used for image analysis to determine cell viability and R/G fluorescence. The “freehand tool” was selected and used to manually draw the shape outlines of the cells, the fluorescence ratio of the cell measured. Viability according to morphology was done by visually counting the total number of rod shaped viable cells, versus round shaped non-viable cells. The entire cell population within an image was analysed, excluding cells that overlapped and were partly outside the image.

3.9 Statistics

Data are presented as mean \pm SEM. GraphPad Prism[®] 6 was used for graph plotting and analysis done with one-way analysis of variance (ANOVA) multiple comparison and Bonferonni *post hoc* test. $p \leq 0.05$ was considered to be statistically significant.

CHAPTER 4

Results

The results of this study were obtained by evaluating the following endpoints:

1. Cell viability according to morphology
2. R/G fluorescence intensity of JC-1 to measure mitochondrial function.

Both parameters can be used to determine the degree of damage or survival of cardiomyocytes (Geisbuhler et al., 2002; Stapleton & Allshire, 1998). The average cell viability is commonly measured according to morphology. An increase in the amount of rod shaped cells would indicate protection, and can be presented as the percentage viable cells in the total population. The R/G fluorescence ratio was determined and given as percentage of untreated normoxic cardiomyocytes. A high percentage would mean that red fluorescence intensity was high and green fluorescence intensity was low, indicating a viable population where mitochondrial function is high. A low percentage, where green fluorescence intensity was high and red fluorescence intensity was low, would indicate a population that consists mainly of cardiomyocytes with low mitochondrial function, and can be considered non-viable or destined for apoptosis.

4.1 The effect that different CBD concentrations exert during normoxia, ischemia and I/R on isolated ventricular cardiomyocytes survival

Objective 1:

To evaluate whether CBD at 0.001 μM , 1 μM , or 100 μM can protect adult rat cardiomyocytes from I/R damage, specifically contracture/hypercontracture and apoptosis.

CBD concentrations, 0.001 μM , 1 μM , or 100 μM , were administered during normoxia to determine cytotoxicity. Representative fluorescence images for cell viability and R/G fluorescence can be seen in **Figure 4.1**, where normoxia without CBD (A) is given, and then normoxia with 0.001 μM (B), 1 μM (C) and 100 μM (D) CBD.

Ischemia was induced for 20 min and reperfusion for 60 min, and is represented by (E). It was then determined if CBD could protect the isolated cardiomyocytes against I/R injury. The CBD concentrations were administered either during ischemia only, as can be seen in **Figure 4.1** for 0.001 μM (F), 1 μM (G), or 100 μM (H) CBD, or throughout ischemia and reperfusion, as can be seen for 0.001 μM (I), 1 μM (J), or 100 μM (K) CBD. Four hearts ($n = 4$), with two repeats per heart for each treatment group were analysed, except for I/R without CBD, which had 4 repeats per heart. The isolations yielded an average cell viability of 84 %.

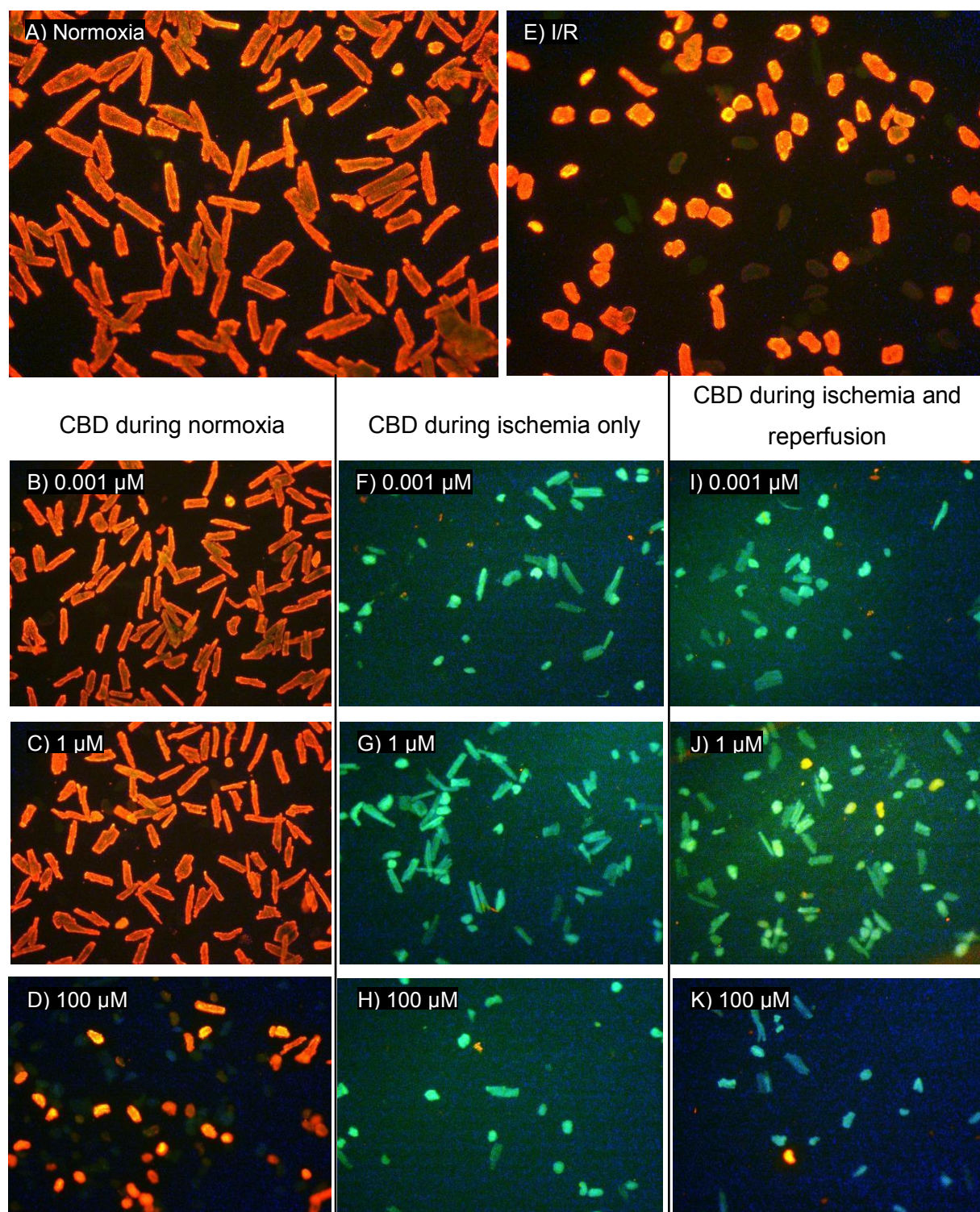


Figure 4.1 Representative fluorescence images of isolated ventricular cardiomyocytes treated with different CBD concentrations during normoxia, ischemia and I/R. Normoxic control without CBD treatment is represented by (A). CBD was then administered during normoxia, 0.001 μM (B), 1 μM (C), and 100 μM (D), to determine cytotoxicity. Control I/R without CBD treatment is represented by (E). CBD was tested during ischemia, 0.001 μM (F), 1 μM (G), and 100 μM (H), and during I/R, 0.001 μM (I), 1 μM (J), and 100 μM (K), to determine if protection could be stimulated.

4.1.1 Average cell viability in percentage according to morphology

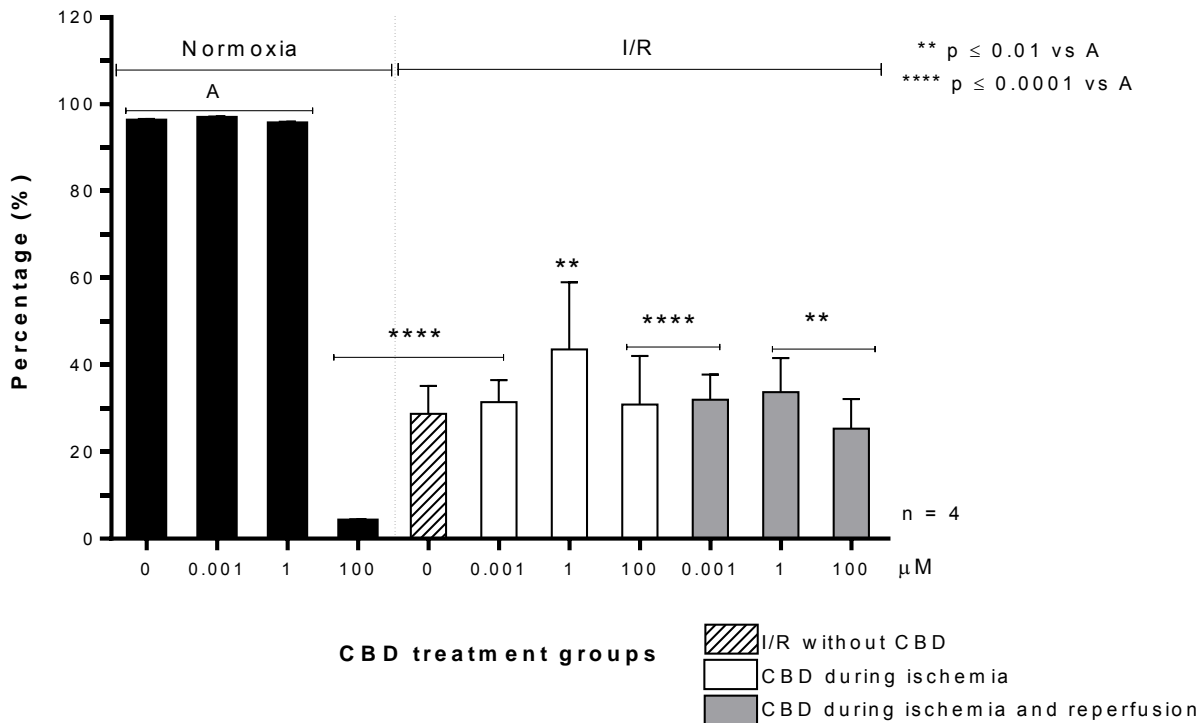


Figure 4.2 The effect of 0.001 μM, 1 μM, and 100 μM CBD on average cell viability during normoxia only, during ischemia only, or throughout ischemia and reperfusion. Data are presented as mean ± SEM, n = 4.

Cell viability according to morphology can be seen in **Figure 4.2**. Cell viability during normoxia without CBD treatment had a high percentage, 95.00 ± 0.64 %. This was also seen for the normoxic group with 0.001 μM CBD (96.00 ± 0.53 %) and 1 μM CBD (95.00 ± 0.66 %). The administration of 100 μM CBD was cytotoxic and significantly ($p \leq 0.0001$) reduced the cell viability from 95.00 ± 0.64 % to 3.89 ± 0.58 %. Cell viability was also greatly ($p \leq 0.0001$) reduced by I/R without CBD treatment to 28.72 ± 6.41 %. A similar trend was seen for all I/R groups that received CBD compared to the normoxic groups, A. None of the CBD concentrations could stimulate protection when compared to I/R without CBD treatment.

4.1.2 Average R/G fluorescence of JC-1 in percentage as an early apoptosis indicator

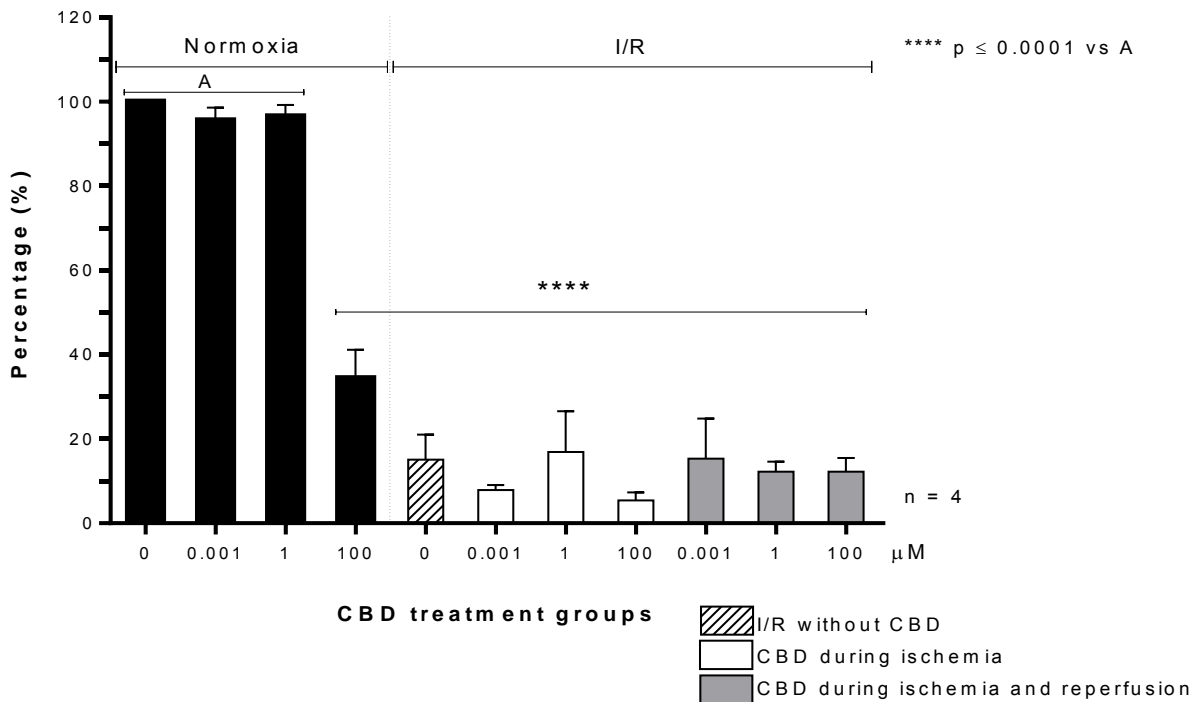


Figure 4.3 The effect of 0.001 μM, 1 μM, and 100 μM CBD on average R/G fluorescence of JC-1 during normoxia only, during ischemia only, or throughout ischemia and reperfusion. Data are presented as mean ± SEM, n = 4.

Figure 4.3 shows the average R/G fluorescence of JC-1 in percentage as an early apoptosis indicator. The normoxic group without CBD treatment was defined as 100 % R/G fluorescence, and the other groups calculated as a percentage thereof. The R/G percentages for normoxia with 0.001 μM CBD (95.56 ± 2.99 %) and 1 μM CBD (96.55 ± 2.63 %) were equally high. 100 μM CBD significantly ($p \leq 0.0001$) reduced the R/G fluorescence percentage from 100 % to 34.45 ± 6.69 %, which confirmed cytotoxicity and apoptosis activation. The R/G fluorescence percentage for all I/R treatment groups was significantly ($p \leq 0.0001$) reduced compared to the normoxic groups, A. None of the CBD treatments could oppose the loss of R/G fluorescence percentage to prevent apoptosis.

4.2 The effect of per-treatment with PDE5 inhibitor and β -AR stimulation during I/R on isolated ventricular cardiomyocytes survival

Objective 2:

- a) To determine if the inhibition of PDE5 during ischemia protect cardiomyocytes against I/R damage.
- b) To determine if the inhibition of PDE5 during ischemia protect cardiomyocytes against enhanced I/R damage, driven by general β -ARs stimulation with isoproterenol, or β 1-AR stimulation with dobutamine.
- c) To determine if, when β 2-AR stimulation with formoterol protects cardiomyocytes against I/R damage, PDE5 inhibition further enhance protection.

PDE5 was inhibited with 10 μ M sildenafil during 20 min ischemia only, to determine if PDE5 activity during ischemia is harmful and thereby contributes to I/R injury. In order to investigate the relationship between PDE5 and β -AR signaling, PDE5 inhibition during ischemia was also applied together with selective β -AR stimulation during I/R. β -ARs were stimulated by the non-selective β -AR agonist, isoproterenol (100 nM), the selective β 1-AR agonist, dobutamine (10 μ M) and the β 2-AR agonist, formoterol (10 μ M), respectively. The concentrations of drugs were obtained from the literature and from tests previously done in our laboratory, and representative images for cell viability and R/G fluorescence are shown in **Figure 4.4**. An n = 8 for all treatment groups were analysed, except for the non-selective β -AR (isoproterenol) groups, which had an n = 4. For each treatment group two repeats per heart were analysed. The isolations yielded an average cell viability of 82 %.

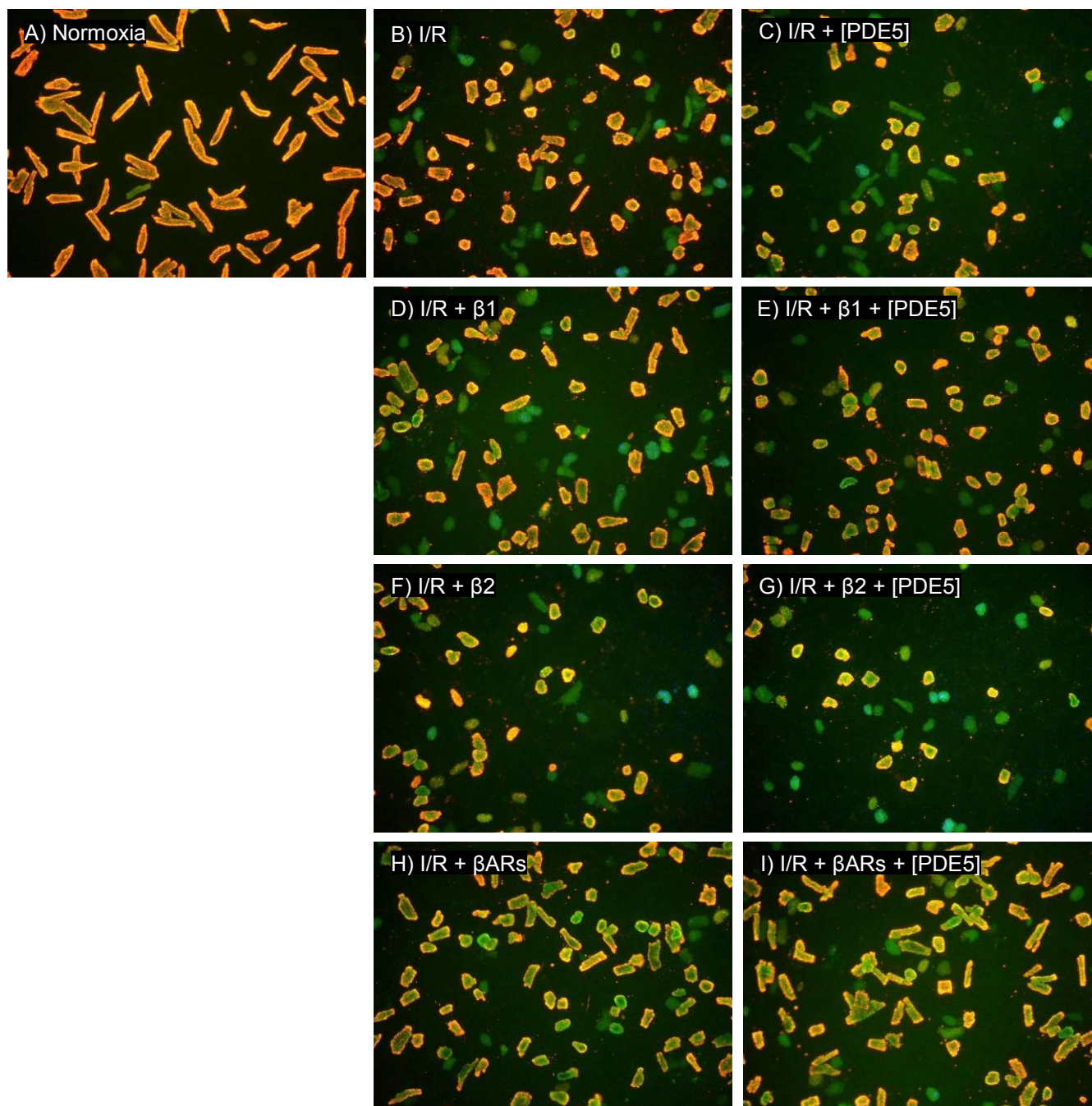


Figure 4.4 Representative fluorescence images of isolated ventricular cardiomyocytes per-treated with PDE5 inhibitor (sildenafil), β_1 -agonist (dobutamine), β_2 -agonist (formoterol), and a general β ARs-agonist (isoproterenol). Ischemia was induced for 20 min, followed by 60 min reperfusion, which included JC-1 staining. Normoxic control (A) cells, I/R control (B), I/R with PDE5 inhibitor (C), I/R with β_1 -agonist (D), I/R with β_1 -agonist and PDE5 inhibitor (E), I/R with β_2 -agonist (F), I/R with β_2 -agonist and PDE5 inhibitor (G), I/R with β ARs-agonist (H), and I/R with β ARs-agonist and PDE5 inhibitor (I).

4.2.1 Average cell viability in percentage according to morphology

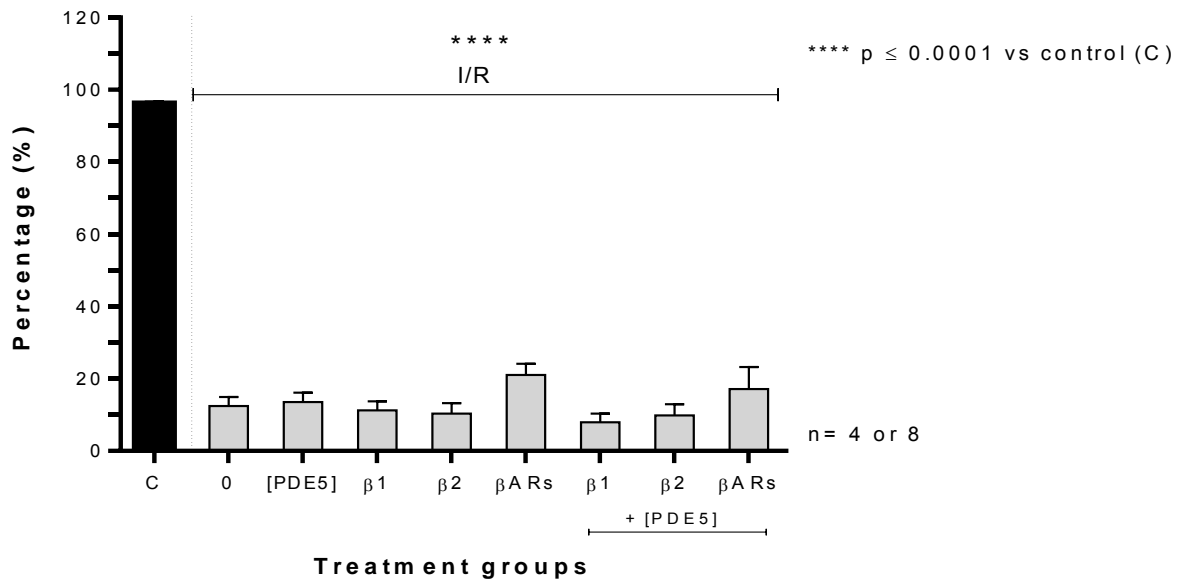


Figure 4.5 The effect of per-treatment with PDE5 inhibitor (sildenafil) and β -AR stimulation during I/R on average cell viability. Data are presented as mean \pm SEM, β -ARs (isoproterenol) groups had an n = 4 and all other groups had n = 8.

Cell viability according to morphology can be seen in **Figure 4.5**. Cell viability was significantly ($p \leq 0.0001$) reduced from normoxic control (C), 96.13 ± 0.64 %, to I/R without treatments (0), 12.45 ± 2.55 %, as was similar for all I/R treatment groups. No significant difference between the different I/R per-treatment groups were found. None of these per-treatments protected the isolated ventricular cardiomyocytes against I/R injury, or enhanced damage.

4.2.2 Average R/G fluorescence of JC-1 in percentage as an early apoptosis indicator

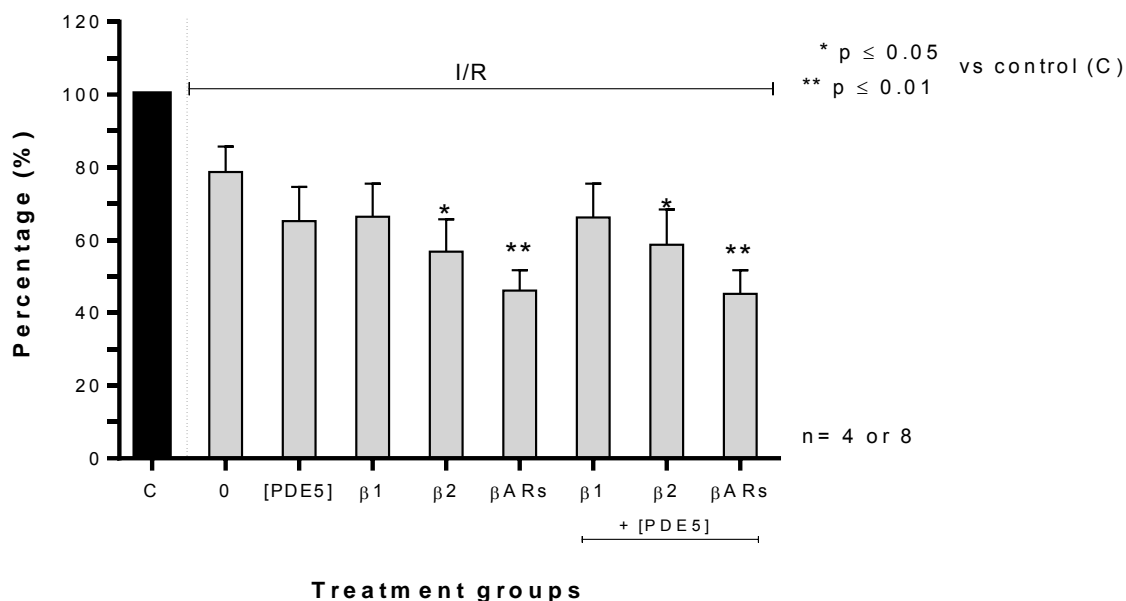


Figure 4.6 The effect of per-treatment with PDE5 inhibitor (sildenafil) and β -AR stimulation during I/R on average R/G fluorescence of JC-1. Data are presented as mean \pm SEM, β -ARs (isoproterenol) groups had an n = 4 and all other groups had n = 8.

Figure 4.6 shows the average R/G fluorescence of JC-1 in percentage as an early apoptosis indicator. I/R without per-treatment (0) did not indicate apoptosis activation. The average R/G fluorescence in percentage for normoxic control (C), 100 %, was significantly ($p \leq 0.01$) reduced by I/R with β -ARs stimulation, 46.18 ± 5.58 %, and I/R with β -ARs and PDE5 inhibition (β -ARs + [PDE5]), 45.26 ± 6.46 %. This significant reduction ($p \leq 0.05$) was also seen with $\beta 2$ stimulation during I/R, 56.82 ± 8.97 %, and I/R with $\beta 2$ stimulation and PDE5 inhibition ($\beta 2$ + [PDE5]), 58.74 ± 9.73 %, compared to the normoxic control (C), 100 %. There was no significant difference between any I/R per-treatment groups compared to I/R without treatment.

DISCUSSION

This study aimed to determine whether the function of PDE5 can regulate cardioprotection or damage. This study also aimed to evaluate whether CBD can protect cultured adult cardiomyocytes against I/R damage. Additionally the role of PDE5 in protection by CBD was also planned to be tested.

CBD, during ischemia only and continuously during I/R, and per-treatment with PDE5 could not protect the isolated ventricular cardiomyocytes from I/R injury. This was evident in both endpoints, cell viability (**Figure 4.2** and **Figure 4.5**) and R/G fluorescence (**Figure 4.3** and **Figure 4.6**), evaluated.

CBD did not protect isolated ventricular cardiomyocytes against I/R injury

This was the first study that determined the effect of different CBD concentrations on isolated ventricular cardiomyocytes when administered throughout ischemia, or from the start of ischemia and for 15 min at the start of 60 min reperfusion. Cardioprotection could not be stimulated with 0.001 μM or 1 μM CBD, while 100 μM was found to be cytotoxic, as indicated by the decreased cell viability (**Figure 4.2**) and R/G fluorescence (**Figure 4.3**).

The activation of CB receptors with cannabinoids was found to stimulate protection against myocardial ischemia and can preserve coronary endothelial function (Krylatov et al., 2001; Lasukova et al., 2008; Ugdyzhkova et al., 2001). CBD can activate both CB1 and CB2 receptors, at concentration between 1 μM – 10 μM , and is known to have therapeutic potential (Pertwee, 2008; Thomas et al., 2007), possibly by modulating CN levels via G_i coupling, or for CB1 via G_s . It was expected that 1 μM CBD should be adequate to activate the CB receptors to stimulate cardioprotection against I/R, via increasing cGMP or reducing cAMP levels.

The limited research done, only 3 *in vivo* studies, on CBD in the setting of I/R has provided some evidence of the potential of CBD as cardioprotective agent, described below.

Durst and colleagues (2007) found that the hearts from rats that received CBD (5 mg/kg) 1 h before ischemia induction, and then again every 24 h for 7 days after ischemia, had a decreased infarct size, associated with reduced myocardial inflammation, and reduced IL-6 levels.

Walsh and colleagues (2010) found that in rat hearts, where CBD was administered, either 10 min prior to 30 min of ischemia (10 or 50 $\mu\text{g}/\text{kg}$), or 10 min prior to 2 h of reperfusion (50 $\mu\text{g}/\text{kg}$), was cardioprotective by reducing both ventricular arrhythmias and infarct size.

Feng and colleagues (2015) experimented on rabbit hearts, where a 90 min coronary artery occlusion was followed by 2 intravenous doses (100 mg/kg) of CBD before 24 h reperfusion, and they found CBD reduced the infarct size and restored the left ventricular functioning.

It is possible that a higher concentration CBD, above 1 μM , but below 100 μM to avoid cytotoxicity, would be more sufficient to stimulate CB receptors to induce protection in the isolated cardiomyocytes. Alternatively, the administration of CBD might be more dependent on the involvement of the immune system. Therefore whole heart studies, or isolated cardiomyocyte studies with the co-culturing of other cells, including endothelial and immune cells to mimic the immune response in a whole heart, might provide a better understanding of the mechanism by which CBD possibly induces protection.

Per-treatment with PDE5 inhibition did not protect the isolated ventricular cardiomyocytes against I/R injury

PDE5 activity is specific for cGMP hydrolysis, and the inhibition thereof stimulates protection in various disorders, including erectile dysfunction, heart failure, pulmonary hypertension, and diabetes (Das et al., 2015; Senzaki et al., 2001).

More importantly, both *in vivo* (Das et al., 2002; Ockaili et al., 2002; Salloum et al., 2003; Salloum et al., 2006) *in vitro* (Das et al., 2005; Das et al., 2006) studies provide evidence of PDE5 inhibitor as protective agent against I/R injury. However, the main focus of these studies was to inhibit PDE5 activity only prior to ischemia, and not at the onset of ischemia, which was the novel aim of this study.

We did not find any cardioprotection when PDE5 was inhibited at the start of ischemia, but other researchers could induce cardioprotection when PDE5 was inhibited prior to ischemia. There are many more articles, but some are explained below.

Das and colleagues (2005) in a cultured isolated cardiomyocyte study found that, the inhibition of PDE5 with 1 μM or 10 μM Sildenafil 1 h prior to 40-min I/1 or 18-h R significantly reduced apoptosis and necrosis, with an $n = 3$. They simulated ischemia with 10 mM 2DG, pH set at 6.2, and N_2 gas balanced with 1 - 2 % O_2 and 5 % CO_2 . They determined cell viability by visually counting the cells as identified by necrosis, trypan blue staining and lactate dehydrogenase (LDH) release, and apoptosis, JC-1 staining and terminal deoxynucleotidyl transferase-mediated nick end-labeling (TUNEL) assay.

In 2008 Das and colleagues followed a similar protocol and found that PDE5 inhibition with 1 μM or 10 μM Sildenafil 1 h prior to 20-min I/30-min R significantly reduced apoptosis and necrosis, with an $n = 4$. They again determined cell viability by only visually counting the cells as identified by necrosis using trypan blue staining, and by apoptosis using the TUNEL assay. For both these experiments, the

isolated cardiomyocytes were cultured for only 1 h, compared to the overnight culture protocol used in this study.

It is interesting to note that Das and colleagues did not fix the trypan blue stain. Trypan blue was supplemented into the cardiomyocyte plate, and left to develop for ~ 5 min. The stained cells were then counted under the microscope and cell viability as a percentage of the total population was evaluated. Not fixing the stain could allow for the stain to leak out of the cells, which makes identifying the stained necrotic cells difficult. This is only the case with adult cardiomyocytes, because of their size and irregular shape, and not when trypan blue is used to stain other, smaller, cells. Trypan blue stain was also previously tried in our laboratory, but the stain could not be successfully fixed, and when the fixing buffer was removed the stain leaked out of the cells.

Only one study found that PDE5 inhibition induced cardioprotection when inhibited at the start of reperfusion. Salloum and colleagues (2007) inhibited PDE5 at the start of 3 h reperfusion for 65 min, after 30 min ischemia, in rabbit hearts. They found that cardioprotection could be stimulated, by a similar mechanism as preconditioning with mitochondrial K_{ATP} channel opening, and that the infarct size was reduced.

In this study the inhibition of PDE5 with 10 μ M sildenafil as per-treatment could not stimulate the expected cardioprotection against I/R injury. The involvement of specific β_1 , β_2 , and non-specific β -ARs with PDE5 inhibition was evaluated, but could also not be identified. None of the β -AR agonists had an effect, which is strange, since β_1 -AR activation leads to cardio damage (Spear et al., 2007) and β_2 -AR activation was found to stimulate cardioprotection (Communal et al., 1999).

There is a possibility that the drug treatment did not work, and a positive control would have been beneficial for this study. Unfortunately, there were not enough funds available to purchase the cGMP antibody kit, which is very expensive. Furthermore, when this study originated, research was also being done on the inhibition of PDE3 and PDE4 using the same I/R protocol. PDE4 inhibition (with 10 μ M Rolipram) could not stimulate cardioprotection, and PDE3 inhibition (with 10 μ M Milrinone) stimulated minor cardioprotection, but not significantly. Both PDE3 and PDE4 inhibitors were tested with a cAMP assay and the assay proved that the inhibitors could alter cAMP levels.

The 10 μ M sildenafil used in this study is similar to the concentration found in the literature and it was expected that PDE5 activity would be blunted to induce cardioprotection. Both β_1 -AR stimulation with dobutamine, to induce damage, and β_2 -AR stimulation with formoterol, to stimulate protection, did not have the desired outcomes. It was also expected that the administration of CBD would result in cardioprotection. Subsequently, it is possible that this study had a problem, potentially with the method of analysis or with the way the experiments were conducted. The next part of the study focused on determining where the problem was.

PART 2

CHAPTER 5

Solving the Problems

No cardioprotection could be elicited with PDE5 inhibition, CBD treatment, or β 2-AR (formoterol) stimulation, yet all these treatments are known to be cardioprotective. Additionally I/R damage could also not be enhanced by β 1-AR (dobutamine) stimulation or general β -AR (isoproterenol) stimulation, yet these stimuli are known to enhance I/R damage. Thus, none of the drugs used in this study could alter I/R damage, which clearly indicates an error in this study. Areas to consider where errors might have occurred include the experimental protocol, the method of analysis, or the parameters measured, which were addressed in this part of the study.

5.1 The experimental protocol

It is possible, but less likely, that there was a problem with the experimental protocol. Average cell viability after I/R, for the CBD experiment (**Figure 4.2**), was reduced from 95.95 ± 1.27 % to 28.72 ± 18.13 %, and for the PDE5 experiment (**Figure 4.5**), from 96.13 ± 1.80 % to 12.45 ± 2.55 %. The average R/G fluorescence for the CBD experiment (**Figure 4.3**) was also significantly reduced from 100 % to 15.07 ± 16.85 %.

Nonetheless, previous experiments in our laboratory found that, with the same ischemic buffer combination, formoterol could induce cardioprotection. Furthermore, the 10 mM SDT used in this study to induce acute ischemia correlates with the range found in literature, 0.5 – 10 mM (Chanoit et al., 2008; Ruiz-Meana et al., 2011; Wei et al., 2007; Yeung et al., 2007). Although, the ischemic buffer with 10 mM SDT was applied for only 10 min (Yeung et al., 2007), while it was applied for 20 min in our study. Therefore, the 20 min ischemic period might have been too long. The concentration of 3 mM 2DG is lower compared to the range found in literature, 10 – 20 mM (Cao et al., 2005; Hu et al., 2008), and it is not expected that the 3 mM 2DG would induce harsh injury.

5.2 The method of analysis

It is possible that the error was with the program used for analysis, Image J (Schneider et al., 2012), and another image analysis program could provide different results, which was tested in this part of the study.

5.3 The parameters measured

The standard method used to evaluate viability or injury of isolated cardiomyocytes is according to morphology, and was used to determine cell viability for **Figure 4.2** and **Figure 4.5**. Morphology analysis classifies rod shaped cells as viable and round shaped cells as non-viable, and is generally used to define injury in terms of cell viability percentage.

It is with rod and round classification where the error possibly was. The same cell could be classified as either rod or round by different researchers, depending on the researcher's personal interpretation. In an injured cell population the cells cannot always clearly be distinguished as rod or round shaped as can be seen below in **Figure 5.1** with C and D. With I/R, explained in section 1.2, the dynamics of cardiomyocytes are effected through a cascade of molecular, biochemical, and morphological changes (Buja, 2005). The healthy rod shaped cells become shortened and box shaped, and with further injury or reperfusion they become round, hypercontracted, and cellular function is lost (**Figure 5.1**) (Abdallah et al., 2006; Boston et al., 1998; Bowers et al., 1992).

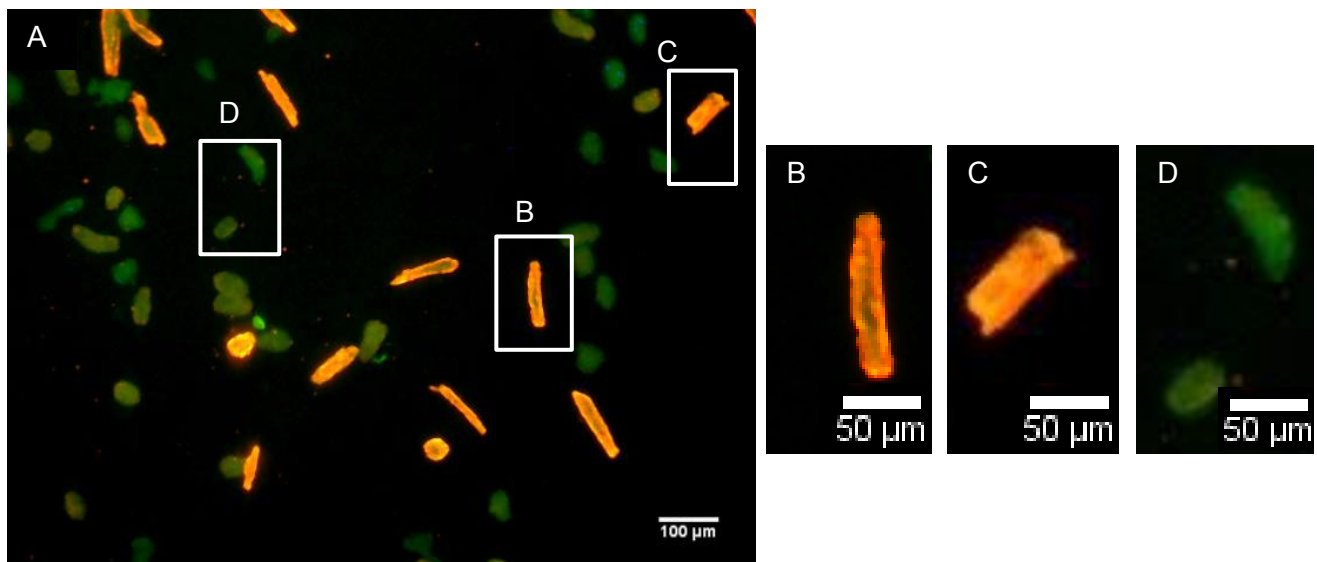


Figure 5.1 A) Fluorescence image of an injured hypoxic population. With I/R, viable rod shaped cells (B) become box shaped (C), and with further injury or reperfusion they can become round, hypercontracted, (D) and lose cellular function.

It is important to remove the human aspect when analysing the images to produce clear and consistent results. Therefore, a gold standard or criteria is necessary whereby analysis should be done.

Although, less popular, morphometry analysis can be used to separate the viable rods from non-viable round cells, also to evaluate cell viability percentage. Morphometry analysis is based on measuring the length and width of cells and is expressed as a ratio (L/W). Geisbuhler and colleagues (2002) used L/W to characterize adult rat cardiomyocytes, with $L/W > 8$ as viable cells, cells with an L/W of 1.5 – 8 as in contracture but still viable, and cells with $L/W < 1.5$ as hypercontracted round cells that were non-viable. Another research group, Boston and colleagues (1998) also used L/W to separate the rod and round cells, but here they used adult rabbit cardiomyocytes which are bigger than rat cardiomyocytes, and considered $L/W < 3$ as hypercontracted cells. L/W can measure the degree of contracture/hypercontracture for a cardiomyocyte population, which cannot be done with morphology analysis.

It is noteworthy that cardiomyocyte length is often measured in single cardiomyocyte experiments to evaluate contracture (Louch et al., 2011; Webster et al., 2012), but has not yet been used to separate rod and round cells. It is possible that length can report similar information about the injured cardiomyocyte population as L/W, and will take half of the manual analysis time.

CHAPTER 6

Hypothesis, Aims and Objectives

6.1 Hypothesis

We hypothesize that the experimental error was not with the analysis program, but with the parameters measured, where morphology analysis provides unreliable results, and morphometry analysis provides impartial results.

6.2 Aims

The first aim of Part 2 of this study was to compare the results from ImageJ analysis with the results from another image analysis program.

The second, but main aim, was to compare morphology analysis with morphometry analysis to determine if morphology is biased. For this aim it was important to quantify length of hypercontracted cardiomyocytes, see objective 3 below. Quantifying length will enable its use as morphometry measurement, to measure the average contraction of the population, and to sort the rod from the round cells.

6.3 Objectives

1. To evaluate if ImageJ analysis and another image analysis program (CellProfiler) provide similar results.
2. To determine whether similar values of R/G fluorescence and cell length can be calculated from the cell area selected by cell shape outline, compared to a straight line selection along the cell length.
3. To determine the average length of round hypercontracted cells, in order to sort non-viable from viable cardiomyocytes based on cell length.
4. a) To compare the average cell viability determined by morphology and morphometry measurements
to establish whether morphology provides biased results.
b) To evaluate the average R/G fluorescence, cell length and L/W ratio of the viable population selected by morphology and morphometry, to characterize the viable population.
5. To re-evaluate the CBD and PDE5 inhibition data from Part 1 using morphometry analysis.

To achieve objectives 1 – 4 I/R and H/R will be induced to compare the results between three different conditions: normoxia, I/R and H/R.

CHAPTER 7

Materials and Methods

The same protocols provided in Chapter 3 for isolating and culturing cardiomyocytes and for data collection were followed.

7.1 I/R, H/R and JC-1 staining

Cardiomyocytes were washed (x 3) for 30 min with modified M199 culture buffer (without blebbistatin), followed by ischemia or hypoxia. Ischemia was induced for 60 min by ischemic wash (refer to section 3.6) with 5 mM 2DG and 5 mM SDT (**Figure 7.1**). Hypoxia was induced for 60 min by ischemic wash with 10 mM 2DG and 100 % N₂ gas (**Figure 7.1**). Ischemia and hypoxia were followed by 60 min reperfusion with modified M199 culture buffer (without blebbistatin), which included 15 min incubation with 15 μM JC-1 stain, two washes and 30 min stain development, before images were captured. Normoxic cells received the same number of buffer changes as I/R or H/R, followed by JC-1 staining.

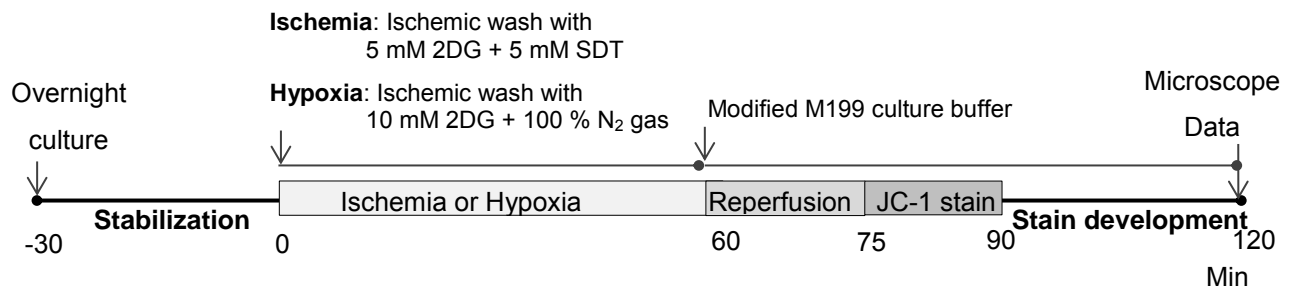


Figure 7.1 Protocol for 60 min simulated ischemia (5 mM 2DG and 5 mM SDT) or hypoxia (10 mM 2DG and 100 % N₂ gas), followed by 60 min reperfusion, which included 15 min JC-1 stain.

7.2 Data analysis

ImageJ (Schneider et al., 2012) and CellProfiler (Kamentsky et al., 2011) freeware were used for image analysis to compare the two analysis programs. ImageJ was used for image analysis for ischemia and hypoxia experiments. The “freehand tool” was selected and used to manually draw the shape outlines (A on **Figure 7.2**) of the cells, the fluorescence and the length of the cells measured. Cell length was measured by measurement of a straight line drawn along the cell length (A on **Figure 7.2**), and by feret measurement. Feret is a measure of the distance of the two furthest points of

a cell and is determined by ImageJ, which automatically draws a virtual rectangle around the selected shape outline (A on **Figure 7.2**). Straight line was also used for L/W measurement, by drawing a straight line across the length and width of the cell (C on **Figure 7.2**).

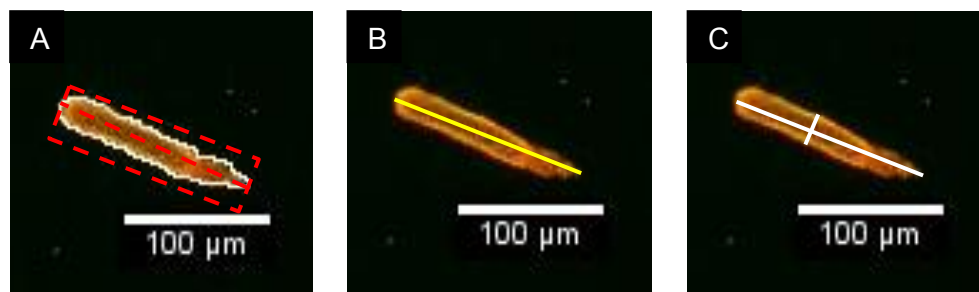


Figure 7.2 A) Shape outline is drawn, indicated by the white outline, and ImageJ evaluates cell length with the feret measurement, indicated by the red rectangle B) Straight line is drawn, indicated by the yellow line, to measure cell length C) Straight line is drawn, indicated by the white line, to measure cell length and width.

7.3 Statistics

Data are presented as mean \pm SEM. GraphPad Prism[®] 6 was used for graph plotting and analysis done with one-way analysis of variance (ANOVA) multiple comparison and Bonferonni *post hoc* test. $p \leq 0.05$ was considered to be statistically significant.

Due to the complexity of the comparisons, differences between groups were indicated with different letters of the alphabet, for example A versus B. If groups were similar and no difference exist, then they would either have at least one letter that is the same, for example A versus A, or A versus AB.

CHAPTER 8

Results

8.1 A comparison between ImageJ and CellProfiler analysis

Data from 20-min I/60-min R (**Figure 4.6**) for ImageJ (n = 8) were compared with re-evaluated data from CellProfiler (n = 4). The isolations had an average cell viability of 82 %.

Objective 1:

To evaluate if ImageJ analysis and another image analysis program (CellProfiler) provide similar results.

8.1.1 Average R/G fluorescence of JC-1 in percentage as an early apoptosis indicator: ImageJ versus CellProfiler

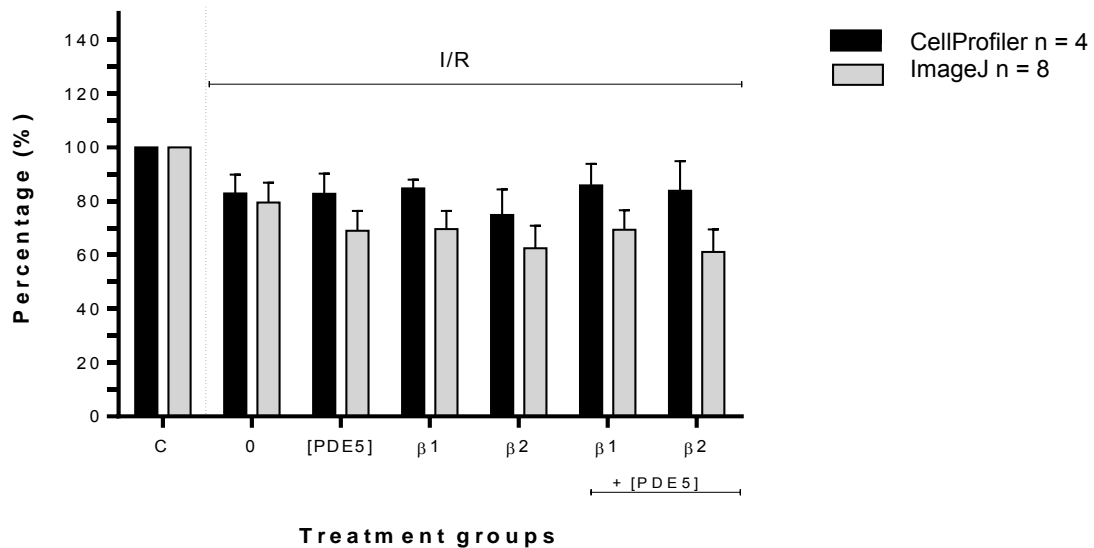


Figure 8.1 A comparison between CellProfiler and ImageJ analysis: the effect of per-treatment with PDE5 inhibitor, $\beta 1$, and $\beta 2$ stimulation during I/R on average R/G fluorescence. Data are presented as mean \pm SEM, n = 4 for CellProfiler; n = 8 for ImageJ.

Figure 8.1 shows that there was no significant difference between CellProfiler and ImageJ analysis for all of the per-treatment groups. The two analysis programs provided similar results, and therefore the original results from ImageJ were accurate.

8.2 A comparison between morphology and morphometry analysis

Data from normoxic, 1-h I/60-min R and 1-h H/60-min R were compared for 8 hearts (n = 8), with two repeats per heart. The isolations yielded an average cell viability of 75 %.

Objective 2:

To determine whether similar values of R/G fluorescence and cell length can be calculated from the cell area selected by cell shape outline, compared to a straight line selection along the cell length.

The cell shape outline is drawn to measure the R/G fluorescence for the total cell area. It is not clear if drawing a straight line can provide similar results as drawing the outline of the cell. Cell shape outline was used to measure the R/G fluorescence for the CBD (**Figure 4.3**) and PDE5 (**Figure 4.6**) experiments. The straight line measurement is used to measure the length of a cell. The shape outline can also be used to measure the length of a cell, given as the feret measurement (refer to **Figure 7.2 A and B**). Drawing the cell shape outline is a time consuming process, whereas drawing a straight line would be much simpler. Thus if the straight line can evaluate R/G fluorescence accurately, it would reduce the time analysis takes.

8.2.1 Average cell length and R/G fluorescence measured from cell shape outline (cell area) and straight line

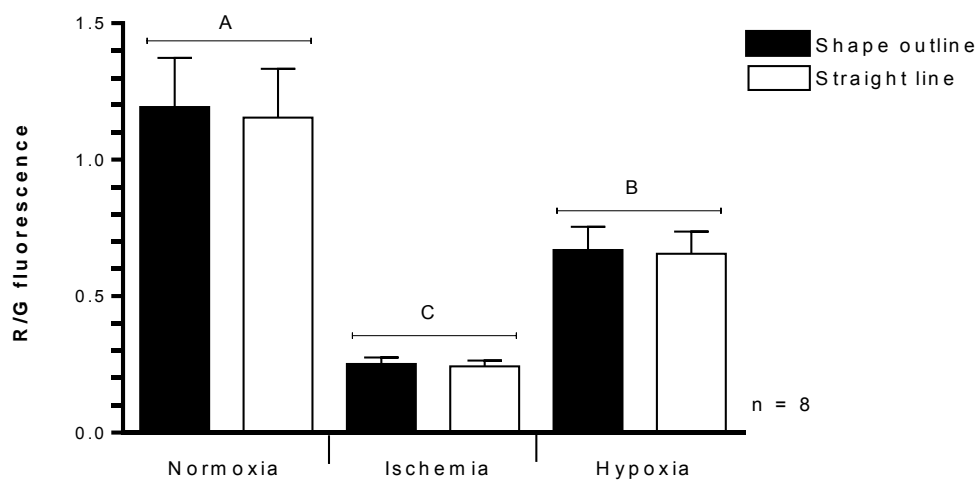


Figure 8.2 The average R/G fluorescence for normoxia, ischemia and hypoxia as identified by cell shape outline (cell area) and straight line. Data are presented as mean ± SEM, n = 8.

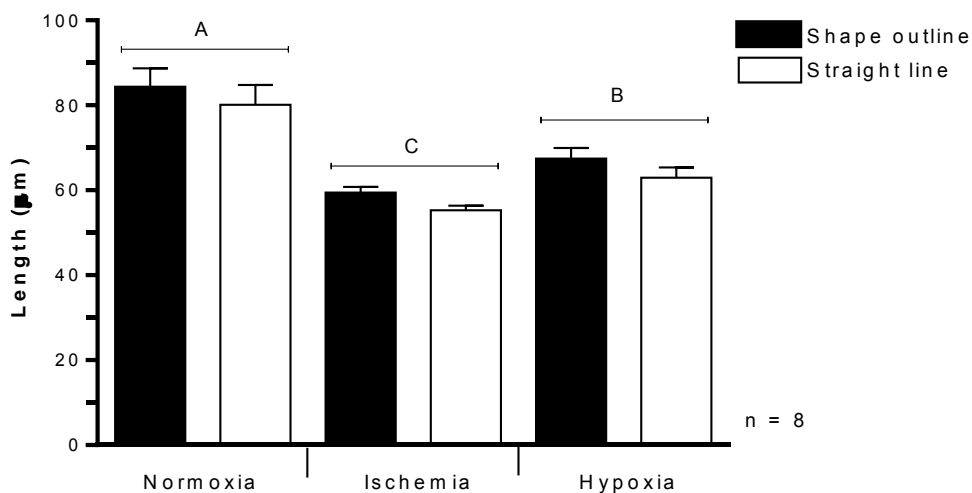


Figure 8.3 The average cell length for normoxia, ischemia and hypoxia as identified by cell shape outline (cell area) and straight line. Data are presented as mean ± SEM, n = 8.

Average R/G fluorescence, refer to **Figure 8.2**, by cell shape for normoxia, A: 1.19 ± 0.17 , was significantly higher than ischemia, C: 0.25 ± 0.02 ($p \leq 0.0001$), and hypoxia, B: 0.66 ± 0.08 ($p \leq 0.05$). The same trend was seen with straight line measurement, where R/G fluorescence for ischemia, C: 0.24 ± 0.02 ($p \leq 0.0001$), and hypoxia, B: 0.65 ± 0.08 ($p \leq 0.05$), were significantly lower than

normoxia, A: 1.15 ± 0.17 . No significant difference was found between cell shape outline and straight line.

Average cell length, refer to **Figure 8.3**, according to cell shape for ischemia, A: $59.43 \pm 1.39 \mu\text{m}$ ($p \leq 0.0001$), and hypoxia, B: $67.43 \pm 2.52 \mu\text{m}$ ($p \leq 0.01$), were significantly reduced compared to normoxia, $84.37 \pm 4.37 \mu\text{m}$. Cell length as quantified by straight line provided similar results, where the averages for ischemia, A: $55.28 \pm 1.06 \mu\text{m}$ ($p \leq 0.0001$), and hypoxia, B: $62.93 \pm 2.41 \mu\text{m}$ ($p \leq 0.01$), were significantly shorter than normoxia, $80.14 \pm 4.67 \mu\text{m}$. No significant difference was found between cell shape outline and straight line.

The results from average R/G fluorescence, **Figure 8.2**, and average cell length, **Figure 8.3**, indicate that drawing a straight line across the cardiomyocytes is as sufficient and accurate as cell outline, but is less time consuming.

Straight line measurement was used to achieve Objective 3, 4 and 5.

Objective 3:

To determine the average length of round hypercontracted cells, in order to sort non-viable from viable cardiomyocytes based on cell length.

Length has never been used to evaluate cell viability in a total cell population, and had to be characterized. For the normoxic population, morphology selection was used to sort the rod and the round cells from each other. The average cell length for the entire rod shaped cells and the entire round shaped cells were calculated.

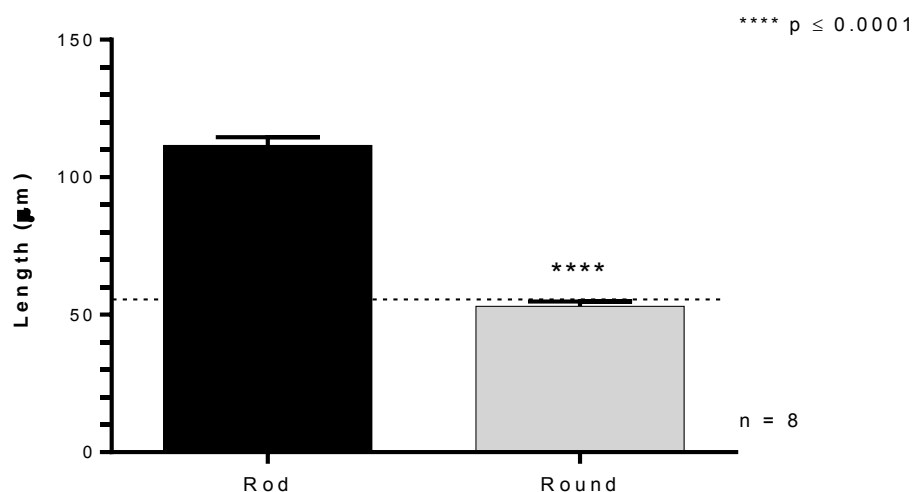
8.2.2 Separating the viable rods and non-viable round cells according to length

Figure 8.4 Average length of rod and round cells during normoxia. Data are presented as mean \pm SEM, $n = 8$.

Figure 8.4 shows the average cell length for rod and round shaped cells in a normoxic population. The average cell length for the round cells were significantly ($p \leq 0.0001$) shorter than the rod cells. The round cells were consistently below 55 μm , and thus cells above 55 μm can be considered viable, although in an injured population these viable cells will exhibit different degrees of contracture.

Length $\geq 55 \mu\text{m}$ was selected as morphometry measurement to identify viable cardiomyocytes in Objective 4.

Objective 4:

- a) To compare the average cell viability determined by morphology and morphometry measurements, to establish whether morphology provides biased results.
- b) To evaluate the average R/G fluorescence, cell length and L/W ratio of the viable population selected by morphology and morphometry, to characterize the viable population.

To determine if morphology selection provides biased results, the viable population, as selected by morphology (rod shape) and as selected by morphometry (length $\geq 55 \mu\text{m}$ and L/W ≥ 1.5), was compared. Average cell viability as identified by morphology and morphometry was evaluated first. The selected viable population was then assessed according to R/G fluorescence, cell length and L/W ratio to identify any differences between morphology and morphometry. It is possible that PDE5 inhibition and CBD administration did stimulate cardioprotection, but morphology (rod shape) selection simply could not detect it. Length $\geq 55 \mu\text{m}$ has never been used as morphometry measurement to evaluate a total cell population, and it is unclear if it can provide similar results to L/W ≥ 1.5 . Length $\geq 55 \mu\text{m}$ and L/W ≥ 1.5 might also differ in sensitivity, which needs to be determined.

8.2.3 Average cell viability: comparing morphology (rod shape) with morphometry (length $\geq 55 \mu\text{m}$ and $L/W \geq 1.5$) analysis

Cell viability is a very informative parameter and can immediately provide information on the quality of the cells, either before, during, or after an experiment. However, it is not known whether viability determined by cell shape selection of viable cells provide similar results as morphometric selection.

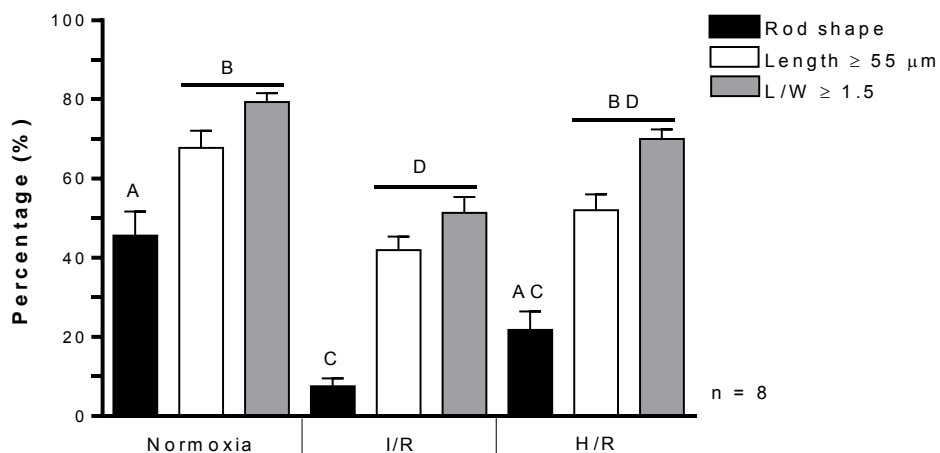


Figure 8.5 Average cell viability of adult cardiomyocytes after normoxia, I/R and H/R. The viable cells were selected by rod shape, length $\geq 55 \mu\text{m}$ and $L/W \geq 1.5$. The different letters indicate significant differences between treatment groups, and differences between the different methods of analysis within the same treatment. Data are presented as mean \pm SEM, $n = 8$.

Average cell viability, as can be seen in **Figure 8.5**, for rod shape was significantly ($p \leq 0.0001$) higher for normoxia, A: $45.62 \pm 6.11 \%$, than for I/R, C: $7.57 \pm 1.95 \%$. The viability of cells with a length $\geq 55 \mu\text{m}$ and $L/W \geq 1.5$ were significantly ($p \leq 0.001$) higher for normoxia, B: $67.78 \pm 4.37 \%$ and $79.35 \pm 2.26 \%$, compared to I/R, D: $41.95 \pm 3.41 \%$ and $51.41 \pm 3.93 \%$, respectively. Rod shape, length $\geq 55 \mu\text{m}$, and $L/W \geq 1.5$ showed no significant difference between H/R and normoxia. No differences were found between normoxia and H/R for any of the selection methods.

Rod shape, length $\geq 55 \mu\text{m}$ and $L/W \geq 1.5$ were compared within normoxia, I/R, and H/R. For normoxia, cell viability was significantly lower for rod shape, A: $45.62 \pm 6.11 \%$, compared to length $\geq 55 \mu\text{m}$, B: $67.78 \pm 4.37 \%$ ($p \leq 0.01$), and $L/W \geq 1.5$, B: $79.35 \pm 2.26 \%$ ($p \leq 0.001$). The same was found for I/R and H/R, where rod shape (I/R: C, $7.57 \pm 1.95 \%$, and H/R: AC, $21.78 \pm 4.70 \%$) was significantly lower than length $\geq 55 \mu\text{m}$ (I/R: D, $41.95 \pm 3.41 \%$, and H/R: BD, $52.08 \pm 3.94 \%$; both $p \leq 0.001$) and $L/W \geq 1.5$ (I/R: D, $51.41 \pm 3.93 \%$, and H/R: BD $70.03 \pm 2.38 \%$; both $p \leq 0.0001$).

For all conditions was cell viability for rod shape significantly lower than for length $\geq 55 \mu\text{m}$ and $L/W \geq 1.5$. These results indicate that morphology selection provided different results compared to morphometry selection, and therefore morphology might be biased. No differences were seen between the two morphometric methods, indicating that length $\geq 55 \mu\text{m}$ and $L/W \geq 1.5$ are equally reliable when assessing cell viability.

8.2.4 Average R/G fluorescence, cell length and L/W ratio of the viable population

It was important to characterize the viable population as selected by morphology and morphometry in order to determine whether there are any differences between these selected populations. Therefore the average R/G fluorescence, cell length and L/W ratio was determined for the cardiomyocytes selected by morphology and morphometry.

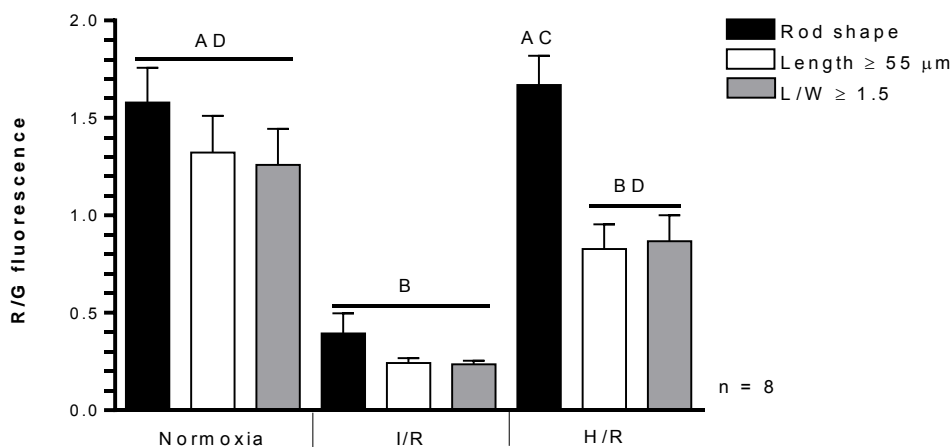


Figure 8.6 Average R/G fluorescence of adult cardiomyocytes after normoxia, I/R and H/R. The viable cells were selected by rod shape, length $\geq 55 \mu\text{m}$ and $L/W \geq 1.5$. The different letters indicate significant differences between treatment groups, and differences between the different methods of analysis within the same treatment. Data are presented as mean \pm SEM, $n = 8$.

Figure 8.6 show that the average R/G fluorescence for rod shape was significantly ($p \leq 0.0001$) reduced after I/R, B: 0.39 ± 0.10 , compared to normoxia, AD: 1.58 ± 0.17 . Similarly, the R/G fluorescence of cells with a length $\geq 55 \mu\text{m}$ and $L/W \geq 1.5$ were significantly reduced after I/R, B: 0.24 ± 0.02 ($p \leq 0.0001$) and 0.25 ± 0.01 ($p \leq 0.001$), compared to normoxia, AD: 1.32 ± 0.18 and 1.30 ± 0.21 , respectively. There were no significant differences found between normoxia and H/R.

The comparison between rod shape, length $\geq 55 \mu\text{m}$ and $L/W \geq 1.5$ per treatment condition, showed no difference for normoxia and I/R. However with H/R, the R/G fluorescence for rod shape, AC: 1.67 ± 0.15 , was significantly ($p \leq 0.01$) higher than both length $\geq 55 \mu\text{m}$, BD: 0.82 ± 0.13 , and $L/W \geq 1.5$, BD: 0.89 ± 0.15 .

For length $\geq 55 \mu\text{m}$ and $L/W \geq 1.5$, no significant difference could be detected between these two methods for normoxia, I/R and H/R, indicating that both morphometry measurements provide similar data. Yet, rod shape did not follow a similar trend in all the conditions, which suggests that morphology selection is not consistent and could provide misleading results under certain conditions.

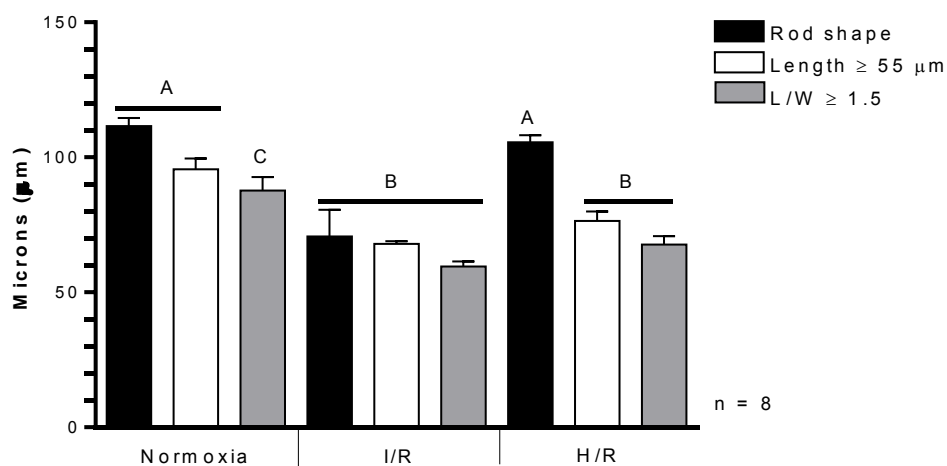


Figure 8.7 Average cell length of adult cardiomyocytes after normoxia, I/R and H/R. The viable cells were selected by rod shape, length $\geq 55 \mu\text{m}$ and $L/W \geq 1.5$. The different letters indicate significant differences between treatment groups, and differences between the different methods of analysis within the same treatment. Data are presented as mean \pm SEM, $n = 8$.

Average cell length, as can be seen in **Figure 8.7**, for rod shape was significantly ($p \leq 0.0001$) reduced after I/R, B: $70.67 \pm 9.87 \mu\text{m}$, compared to normoxia, A: $111.50 \pm 3.04 \mu\text{m}$. Cell length for cells with length $\geq 55 \mu\text{m}$ and $L/W \geq 1.5$ was significantly reduced after I/R, B: $67.95 \pm 1.05 \mu\text{m}$ and $59.61 \pm 1.77 \mu\text{m}$ (both $p \leq 0.001$), and H/R, B: $76.44 \pm 3.54 \mu\text{m}$ and $67.73 \pm 3.14 \mu\text{m}$ (both $p \leq 0.05$), compared to normoxia, A: $95.55 \pm 3.99 \mu\text{m}$ and $87.66 \pm 5.00 \mu\text{m}$, respectively. Rod shape, length $\geq 55 \mu\text{m}$ and $L/W \geq 1.5$ per condition were compared. For normoxia, rod shape, A: $111.50 \pm 3.05 \mu\text{m}$, had a significantly ($p \leq 0.01$) higher cell length than L/W , C: $87.66 \pm 5.00 \mu\text{m}$. No differences were found for I/R, but for H/R a significantly lower length was found for both length $\geq 55 \mu\text{m}$, B: 76.44

$\pm 3.54 \mu\text{m}$ ($p \leq 0.001$), and $L/W \geq 1.5$, B: $67.73 \pm 3.14 \mu\text{m}$ ($p \leq 0.0001$), compared to rod shape, A: $105.60 \pm 2.60 \mu\text{m}$.

Rod shape selection indicated a significant reduction in cell length after I/R compared to normoxia, but not for H/R. However, when length $\geq 55 \mu\text{m}$ and $L/W \geq 1.5$ as selections were used, a significant reduction in cell length was found for I/R and H/R versus normoxia. Thus length $\geq 55 \mu\text{m}$ and $L/W \geq 1.5$ accounted for differences between normoxia and H/R, which rod shape selection could not detect.

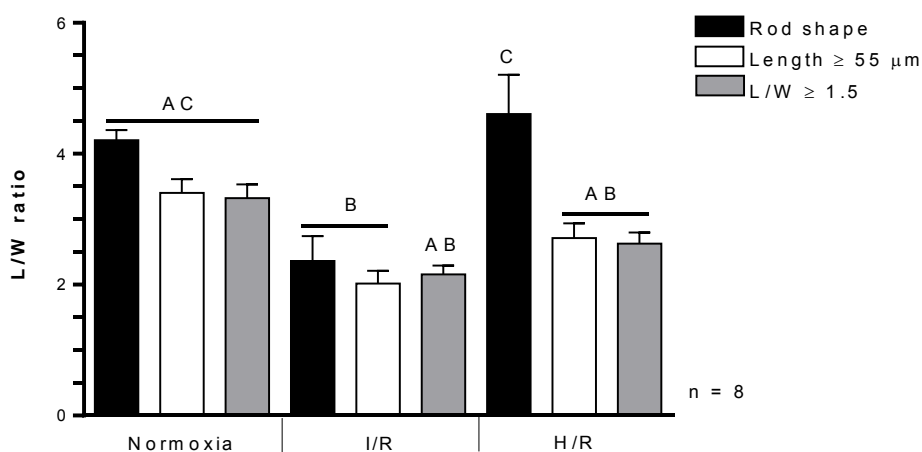


Figure 8.8 Average L/W ratio of adult cardiomyocytes after normoxia, I/R and H/R. The viable cells were selected by rod shape, length $\geq 55 \mu\text{m}$ and $L/W \geq 1.5$. The different letters indicate significant differences between treatment groups, and differences between the different methods of analysis within the same treatment. Data are presented as mean \pm SEM, $n = 8$.

Figure 8.8 show that Rod shape selection indicated that L/W was significantly ($p \leq 0.001$) reduced with I/R, B: 2.36 ± 0.38 , compared to normoxia, AC: 4.21 ± 0.15 . For cells with length $\geq 55 \mu\text{m}$, L/W was significantly ($p \leq 0.01$) higher for normoxia, AC: 3.40 ± 0.20 , compared to I/R, B: 2.32 ± 0.38 . L/W for cells defined by $L/W \geq 1.5$ showed no significant difference when I/R and H/R were compared to normoxia. When the three selections were compared per condition, the only differences were found for H/R, where rod shape, C: 4.61 ± 0.60 , had a significant higher L/W ratio than length $\geq 55 \mu\text{m}$, AB: 2.71 ± 0.22 ($p \leq 0.001$), and $L/W \geq 1.5$, AB: 2.63 ± 0.17 ($p \leq 0.0001$).

The length $\geq 55 \mu\text{m}$ selection accounted for a differences between normoxia and I/R, which could not be detected by $L/W \geq 1.5$ selection, and thus length $\geq 55 \mu\text{m}$ can be considered a more sensitive measurement. The fact that there is such a big difference between morphology and morphometry data

with H/R for R/G fluorescence and cell length indicated that rod shape selection is unreliable. Morphometry analysis is objective and is not influenced by the personal interpretation of the researcher.

8.3 The effect that different CBD concentrations exert during normoxia, ischemia and I/R on isolated ventricular cardiomyocytes survival

Objective 5:

Re-evaluate the CBD and PDE5 inhibition data from Part 1 using morphometry analysis.

Given that rod shape selection of viable cells seems to be inconsistent and thus unreliable, it is very possible that the cell viability data analysed by morphology in Part 1 (**Figure 4.2** and **4.5**) of this study are incorrect. Therefore the images collected for CBD treatments during normoxia, ischemia, and I/R, and for PDE5 inhibition as per-treatment were re-evaluated using morphometry, more specifically cell length. The reason for using length instead of L/W is because it takes less time and appeared to be more sensitive in finding differences than L/W (**Figure 8.8**). The average cell length was measured because it can report whether contracture/hypercontracture injury was induced (**Figure 8.9** and **Figure 8.11**). The cell viability data were also re-evaluated (**Figure 8.10** and **Figure 8.12**) with length $\geq 55 \mu\text{m}$ and compared to the original morphology result (**Figure 4.2** and **Figure 4.5**), which possibly provided untruthful results.

8.3.1 Average cell length in microns as indicator of contracture

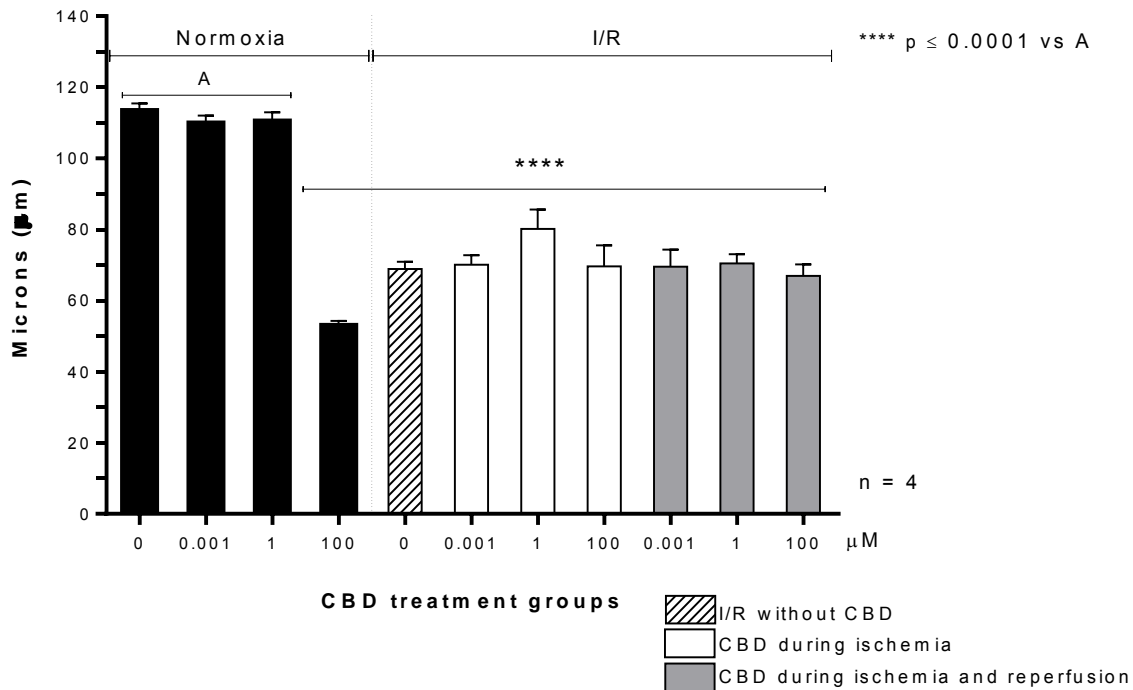


Figure 8.9 The effect of 0.001 CBD, 1 CBD, and 100 µM CBD on average cell length during normoxia and I/R. CBD was administered during ischemia only or continuously during I/R. Data are presented as mean ± SEM, n = 4.

Figure 8.9 show average cell length in microns as indicator of contracture. The average cell length for normoxia without CBD treatment was $113.30 \pm 2.18 \mu\text{m}$. Similar averages were found for the normoxic group with 0.001 µM CBD ($109.80 \pm 2.25 \mu\text{m}$) and 1 µM CBD ($110.40 \pm 2.59 \mu\text{m}$). 100 µM CBD during normoxia was cytotoxic as seen by the significantly ($p \leq 0.0001$) reduced cell length of $52.88 \pm 1.38 \mu\text{m}$ compared to the normoxic groups, A. The same significant ($p \leq 0.0001$) reduction in cell length was seen for all I/R treatment groups compared to the normoxic groups, A. None of the CBD treatment groups could prevent contracture.

8.3.2 Average cell viability in percentage: to compare morphology and length $\geq 55 \mu\text{m}$

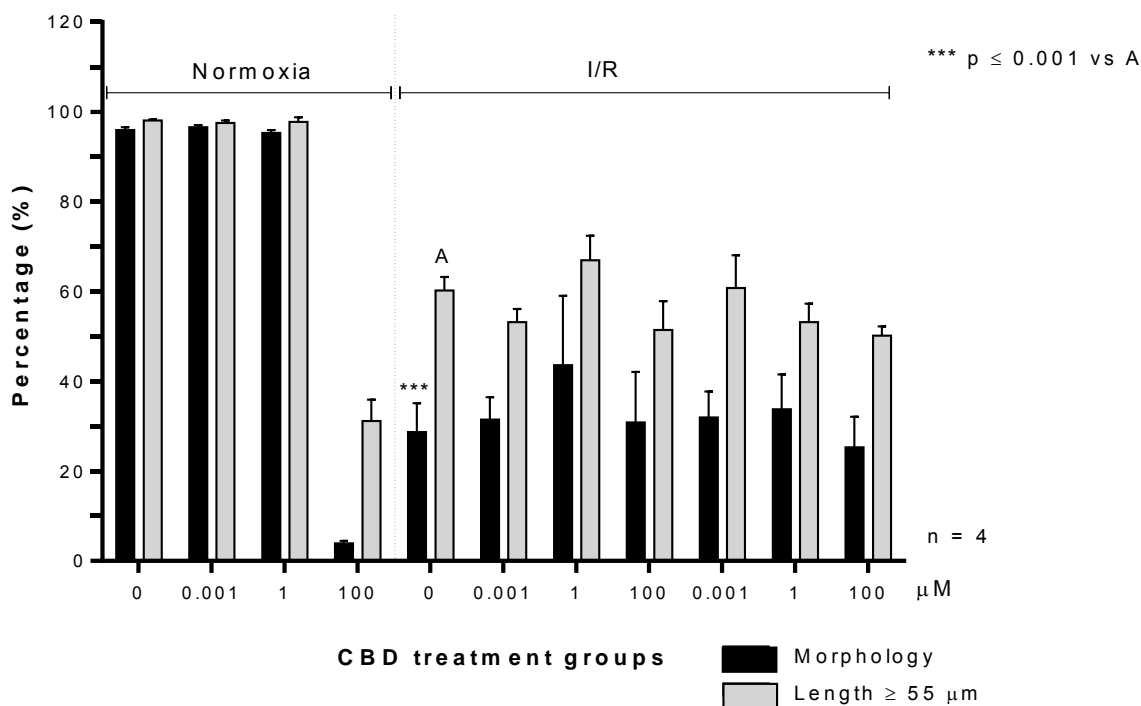


Figure 8.10 A comparison between morphology and length $\geq 55 \mu\text{m}$: the effect of 0.001 CBD, 1 CBD, and 100 μM CBD on average cell viability during normoxia and I/R. CBD was administered either during ischemia only or continuously during I/R. Data are presented as mean \pm SEM, $n = 4$.

Average cell viability, as can be seen on **Figure 8.10**, for I/R without CBD treatment (0) was significantly ($p \leq 0.001$) lower according to morphology, $28.72 \pm 6.41 \%$, than length $\geq 55 \mu\text{m}$, A: $60.24 \pm 2.98 \%$. Cell viability was not significantly increased by length $\geq 55 \mu\text{m}$ for any other CBD treatment group. No significant difference between all I/R CBD treatment groups compared to I/R without CBD (0) could be found for length $\geq 55 \mu\text{m}$ selection.

Length $\geq 55 \mu\text{m}$ did not provide more information about the CBD treatment groups than morphology, and none of the CBD treatment groups stimulated protection against I/R injury.

However, the error bars for length $\geq 55 \mu\text{m}$ was smaller compared to the error bars for morphology. This indicated that the selections made by length $\geq 55 \mu\text{m}$ were closer in values, the repeats were more similar, than the repeats selected by morphology.

8.4 The effect of per-treatment with PDE5 inhibitor and β -AR stimulation during I/R on isolated ventricular cardiomyocytes survival

8.4.1 Average cell length in microns as indicator of contracture

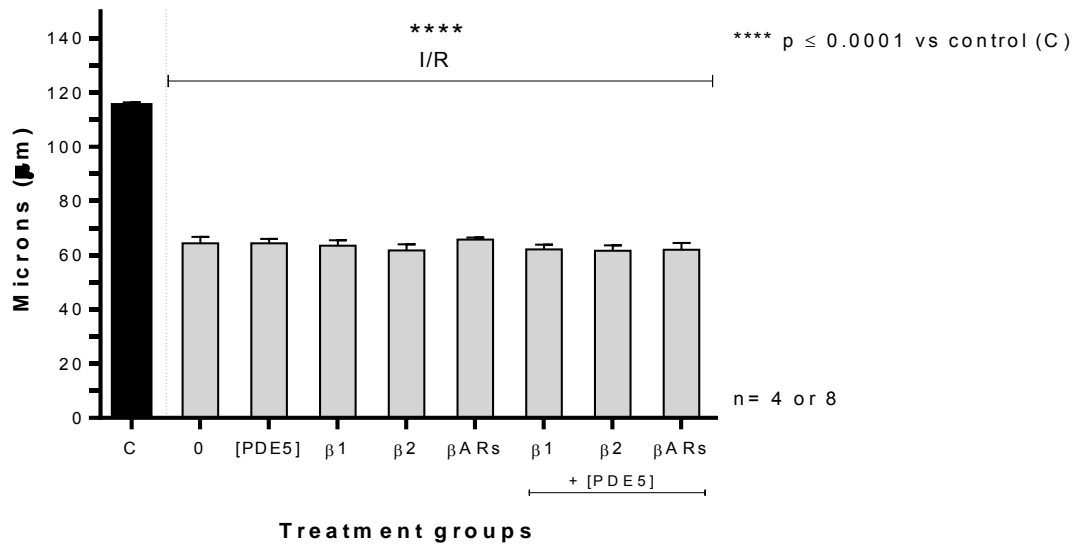


Figure 8.11 The effect of per-treatment with PDE5 inhibitor and β -AR stimulation during I/R on average cell length. Data are presented as mean \pm SEM, β -ARs groups (isoproterenol) had an $n = 4$ and all other groups had $n = 8$.

The average cell length in microns as indicator of contracture can be seen in **Figure 8.11**. There was a significant difference ($p \leq 0.0001$) between the normoxic control (C) and I/R without per-treatment (0), where cell length was decreased from $115.10 \pm 1.39 \mu\text{m}$ to $64.44 \pm 2.37 \mu\text{m}$. This was also found for all I/R per-treatment groups, with no significant difference between them.

None of these per-treatments stimulated protection against I/R injury.

8.4.2 Average cell viability in percentage: to compare morphology and length $\geq 55 \mu\text{m}$

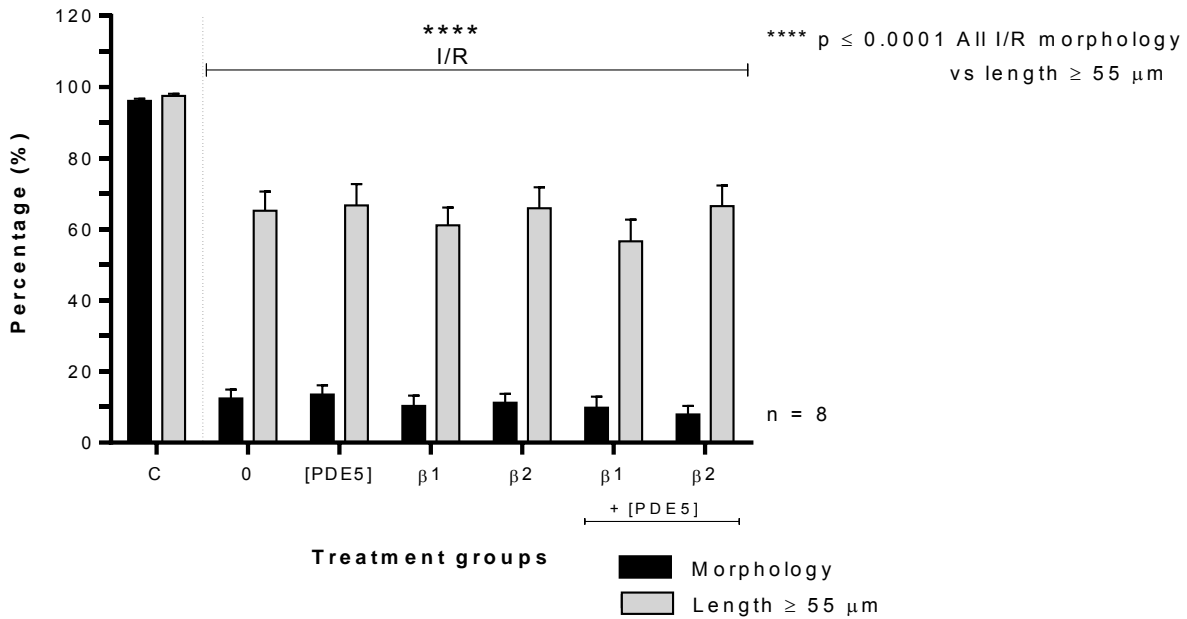


Figure 8.12 A comparison between morphology and length $\geq 55 \mu\text{m}$: the effect of per-treatment with PDE5 inhibitor, $\beta 1$, and $\beta 2$ stimulation during I/R on cell viability. Data are presented as mean \pm SEM, n = 8.

Figure 8.12 show the average cell viability in percentage: to compare morphology and length $\geq 55 \mu\text{m}$. Length $\geq 55 \mu\text{m}$ selection significantly ($p \leq 0.0001$) increased average cell viability for all I/R treatment groups compared to morphology. However, no significant difference between any I/R treatment group compared to I/R without treatment (0) could be found when length $\geq 55 \mu\text{m}$ was used as measurement. Although the average cell viability for all I/R treatment groups were increased by length $\geq 55 \mu\text{m}$ selection, it could not provide more information than morphometry. Per-treatment with PDE5 inhibitor did not protect the isolated ventricular cardiomyocytes against I/R injury.

Re-evaluating the cell viability data with length $\geq 55 \mu\text{m}$ as selection for the CBD treatment and PDE5 inhibition experiments did not provide more information than morphology selection, and none of these treatments could induce cardioprotection.

DISCUSSION

Part 2 of this study focused on finding a reason why no protection could be elicited with PDE5 inhibition and CBD treatment in cultured adult cardiomyocytes, evaluating if the error was with the image analysis program or with the parameters measured.

There is a possibility that the error was with the experimental protocol previous experiments in our laboratory found that, with the same ischemic buffer combination, formoterol could induce cardioprotection. The 3 mM 2DG and 10 mM SDT also correlates with the concentration ranges found in the literature (Hu et al., 2008; Ruiz-Meana et al., 2011; Yeung et al., 2007). Accordingly, it was first determined if the error was with the analysis program and thereafter with the parameters measured.

PDE5 inhibition and the administration of CBD did not induce cardioprotection in this study. No research has been done on PDE5 inhibition as per-treatment or on the effects of CBD on cultured isolated cardiomyocytes. The novelty of this study made comparing the results found to the results in the literature impossible, where cardioprotection with PDE5 inhibition was induced by treatment prior to ischemia (Ahmad et al., 2009; Bremer et al., 2005; Das et al., 2002; Das et al., 2009; du Toit et al., 2005; Kukreja et al., 2005; Ockaili et al., 2002; Salloum et al., 2003; Salloum et al., 2006; Sesti et al., 2007). The literature provides evidence that β 1-AR stimulation increases I/R damage (Spear et al., 2007) and β 2-AR stimulation induces protection (Communal et al., 1999), but this was also not found in this study.

ImageJ is a reliable open-source analysis program

The first aim of Part 2 of this study was to determine if the original R/G fluorescence results from ImageJ analysis (**Figure 4.6**) were reliable. The results from ImageJ (Schneider et al., 2012) analysis were compared to the results from CellProfiler (Kamentsky et al., 2011) (**Figure 8.1**). Both programs are open-source freeware and can easily be downloaded from the internet. There was no significant difference between the results from the two programs. The R/G fluorescence results from ImageJ analysis are thus trustworthy.

Morphology analysis is biased, whereas morphometry analysis is reliable

The parameters, cell viability and R/G fluorescence intensity, were evaluated in Chapter 4 to determine the degree of damage or survival of cardiomyocytes.

For cell viability assessments (**Figure 4.2** and **Figure 4.5**) morphology analysis was used, where cells were identified as either rod or round, and was presented as the percentage viable cells in the total population. But there is a discrepancy when morphology analysis was used, for the reason that in an injured population it is difficult to separate rod and round shaped cells (**Figure 7.2**). This could mean that different researchers would classify the same cell either as rod, or as round, depending on personal justification, indicating that morphology measurement could be biased (**Figure 8.5 – 8.8**).

Straight line measurement is as accurate as cell shape outline to measure the R/G fluorescence of a cardiomyocyte population

R/G fluorescence intensity per cell area was measured by drawing the shape outline and the average R/G fluorescence for the cardiomyocyte population (**Figure 4.3** and **Figure 4.6**) was then determined. Drawing the shape outline for the total cell population per image is a time consuming process. Straight line measurement can be used to measure the length of a single cell, and when straight line was used for analysis it also seemed to accurately measure the R/G fluorescence of the cell. However, the use of cell length as a measurement of R/G fluorescence for a total population has never been quantified. Therefore average R/G fluorescence (**Figure 8.2**) and cell length (**Figure 8.3**) for the normoxic, ischemic and hypoxic populations, were measured by the straight line measurement and the shape outline measurement to determine if both measurements provided similar results.

There was no significant difference between the cell shape outline measurement and the straight line measurement. Straight line measurement can be used to not only evaluate the cell length and R/G fluorescence of a single cardiomyocyte, but could evaluate the total cardiomyocyte population. Straight line measurement is thus a quicker, more effective, measurement than shape outline.

Length could be quantified to be used as morphometry measurement

The straight line measurement is versatile and could measure average R/G fluorescence and contracture/hypercontracture for an injured population, but could not identify the percentage of contracted cells in the population. Therefore, Part 2 of this study aimed to enable the use of length as a morphometry measurement, by sorting the rod and the round shaped cells according to length. Morphology analysis was used to separate the rod from the round shaped cells and the average cell length for the rods and the rounds was determined.

Figure 8.4 found that rod shaped cells were consistently above 55 μm , whereas round shaped cells were consistently below 55 μm . It is important to note that the viable cells, above 55 μm , will exhibit varying degrees of contracture in an injured population. Length $\geq 55 \mu\text{m}$ was selected as morphometry

measurement to identify viable cells in a cardiomyocyte population, which could then be presented as percentage cell viability.

Both length $\geq 55 \mu\text{m}$ and $L/W \geq 1.5$, previously used by Geisbuhler and colleagues (2002) to characterize viable adult cardiomyocytes, can thus measure the degree of contracture/hypercontracture for a cardiomyocyte population, which cannot be done with morphology analysis.

Morphology analysis is biased, morphometry analysis is reliable

The second aim of Part 2 of this study was to determine if morphology analysis, with rod shaped selection, produced biased results compared to morphometry analysis, with the selections length $\geq 55 \mu\text{m}$ and $L/W \geq 1.5$.

Average cell viability, as identified by morphology and morphometry, for the normoxic, ischemic and hypoxic populations was evaluated first (**Figure 8.5**). For all three experimental conditions, the cell viability according to morphology selection was significantly lower compared to when morphometry selection was used. This indicates that when morphology selection was used, fewer cells were selected and the researcher was stricter with the quality of cells selected, whereas both morphometry selections were more lenient and included more cells. Length $\geq 55 \mu\text{m}$ and $L/W \geq 1.5$ provided similar results.

The quality of the cells selected, presented by the average cell viability, was evaluated with regards to R/G fluorescence, cell length and L/W ratio.

The R/G fluorescence intensity (**Figure 8.6**) for the cells selected by morphology was similar for normoxia and hypoxia, whereas with morphometry selection the R/G fluorescence for the normoxic population was significantly higher than for hypoxia. This means that the few cells selected by morphology for each of the three experimental conditions, derived from the cell viability (**Figure 8.5**), had a similar R/G fluorescence intensity. Morphometry accounted for differences between normoxia and hypoxia, unlike morphology.

Average cell length (**Figure 8.7**) for the hypoxic population found that the cells selected by morphology were significantly longer in length than the cells selected by morphometry. Again, with morphology selection, no significant difference in cell length was found when normoxia was compared to hypoxia, but a significant difference was found when the morphometry selections were used.

Interestingly, for the average L/W (**Figure 8.8**), the selection length $\geq 55 \mu\text{m}$ identified a significant reduction in average L/W for ischemia compared to normoxia, which was not found when the selection

$L/W \geq 1.5$ was used. The conclusion can be made that length $\geq 55 \mu\text{m}$ is more sensitive than $L/W \geq 1.5$.

For average R/G fluorescence (**Figure 8.6**) and cell length (**Figure 8.7**), the morphometry selections accounted for significant differences between normoxia and hypoxia that morphology selection could not detect. Morphometry selection is thus more sensitive and reliable than selection with morphology and could account for differences between experimental conditions. Morphology was repetitively proven to be biased, by selecting only a few cells (**Figure 8.5**) that have a high R/G fluorescence (**Figure 8.6**) and do not show any contracture/hypercontracture injury (**Figure 8.7** and **8.8**). Length $\geq 55 \mu\text{m}$ was found to be a more sensitive measurement than $L/W \geq 1.5$.

The administration of CBD and PDE5 inhibition could not protect the isolated cardiomyocytes against I/R damage

The average cell length for the CBD (**Figure 8.9**) and PDE5 (**Figure 8.11**) experiments were evaluated, but cardioprotection was not found. The morphometry selection Length $\geq 55 \mu\text{m}$ was then used to re-evaluate the cell viability images for the CBD and PDE5 inhibition experiments. The results were compared to the original cell viability results where morphology selection was used (**Figure 8.10** and **Figure 8.12**). Length $\geq 55 \mu\text{m}$ selection increased the overall cell viability for all of the ischemic groups, but no significant difference between ischemia and any of the treatment groups was found. Cardioprotection was not induced. The only possible explanation was that the error of the study was with the experimental protocol, where the ischemia induced was too harsh.

Ischemia induced irreversible damage, whereas hypoxia induced unsatisfactory damage

Remember that the control simulated ischemia achieved a great level of cardio damage with regards to all endpoints evaluated. Specifically for cell viability after I/R, Das and colleagues (2005) reported a viability of 60 %, and (2008) 58 %, where PDE5 inhibition could induce protection, compared to the 12 % cell viability achieved after I/R in **Figure 4.5**. The 12 % average cell viability indicated that the cardiomyocytes underwent harsh injury, to such an extent that PDE5 inhibition could not prevent the damage. Cell viability after ischemia was also decreased for the CBD experiments (**Figure 4.2**), from 96 % to 29 %, which indicated that the cardiomyocytes were again possibly harmed beyond the ability of CBD to induce cardioprotection.

A low average cell viability after I/R was also found for the morphology selection (**Figure 8.5**), cell viability decreased from 46 % to 8 %. The morphometry measurements increased the average cell

viability after I/R significantly compared to the 8 % measured by morphology, where length $\geq 55 \mu\text{m}$ measured 42 % and $L/W \geq 1.5$, 51 %.

The same trend was found for **Figure 8.10** and **Figure 8.12**, where length $\geq 55 \mu\text{m}$ compared to morphology increased cell viability with 50 % and 80 %, respectively. The average cell viability after I/R measured by length $\geq 55 \mu\text{m}$ of 60 % (**Figure 8.10**) and 65 % (**Figure 8.12**) were equal to and higher than 60 %, which are similar to that reported by Das and colleagues in 2005 and 2008, but the cardiomyocytes could still not be protected. 54 % of the cells selected by length $\geq 55 \mu\text{m}$ were 55 - 70 μm . Thus, although length $\geq 55 \mu\text{m}$ could significantly increase the average cell viability compared to morphology, the injury induced by ischemia was too harsh and the cells were greatly injured.

The ischemic buffer in Part 1 of this study contained 10 mM SDT and 3 mM 2DG applied for 20 min. SDT, $\text{Na}_2\text{S}_2\text{O}_4$, is an oxygen scavenger and generates superoxide radicals, a reactive oxygen species, that causes much greater damage than 2DG, including acidosis, metabolic inhibition and anoxia (Ho et al., 2002; Wei et al., 2007). Many studies have used SDT, but in lower concentrations or for a shorter period. Examples of these studies are provided below.

Ischemia with 10 mM SDT and 10 mM 2DG was induced for short periods of 5-min I/10-min R (Cao et al., 2005) and 9 or 10-min R (Bian et al., 2005). Trypan blue stain was used for both studies to evaluate cell viability by counting the unstained cells as a percentage of the total population. Both studies also evaluated cell morphology, where only rod shaped cells ($L/W > 3:1$) were included in the results. Interestingly, according to the average cell viability figure of Cao and colleagues (2005), the cell viability for the normoxic controls was low at 55 % and decreased to ± 26 % after I/R, which also indicates that the cardiomyocytes were greatly injured. They did not provide the precise statistical values.

Lower concentrations of SDT were used in other simulated ischemia experiments.

Wei and colleagues (2007) used a model to evaluate myocardial stunning, where they did not want I/R to induce contracture/hypercontracture. Here simulated ischemia was for 8 min, with 2 mM SDT with 10 mM 2DG, pH set at 6.4, followed by 30 min reperfusion (Wei et al., 2007). Trypan blue stain was used to evaluate cell viability by counting the unstained cells as a percentage of the total population. The researchers found that there was no significant difference between the cell viability for the normoxic controls and after I/R, both achieved ± 70 %.

One study used 2.5 mM SDT, with 20 mM 2DG and 20 mM sodium lactate (used to mimic the accumulation of local lactate), pH = 6.5, for 35-min I/10-min R (Hu et al., 2008). Another study used

only 0.75 mM SDT, with 10 mM DG and 20 mM lactate for 15 min ischemia, followed by 30 min reperfusion (Yu et al., 2008).

The aim of this study was to induce acute ischemia, but the 10 mM SDT induced severe cardiomyocyte injury. The SDT concentration should be much lower, rather between 1 - 3 mM, to prevent damaging the cardiomyocytes to the extent that was found in this study.

Contrary to the harsh injury induced by ischemia, the injury induced by hypoxia was too weak for all of the parameters measured (**Figure 8.5 – 8.8**). Specifically again for cell viability, the morphology selection (**Figure 8.5**) found that hypoxia decreased viability from 46 % to 22 %, where I/R decreased the viability to 8 %. With morphometry measurements the cell viability percentage after H/R was higher, with 52 % for length $\geq 55 \mu\text{m}$, and 70 % for L/W ≥ 1.5 , compared to the cell viability measured after I/R, 42 % and 51 % respectively. Hypoxia did not induce satisfactory injury compared to the normoxic population, only a few cardiomyocytes were damaged and the population seemed to be thriving and happy. There is a problem with the ischemia being too harsh, and the hypoxia not inducing enough injury.

Unfortunately, there are other occurring problems, rarely mentioned in the literature, which affects the experimental outcome.

Problems that could affect the experimental outcome

Variances between the rats

Individual differences between rats, which can include stress levels, diet and overall health, affects the quality of the heart and the cardiomyocytes isolated. The heart of a rat that exhibited stress and restlessness before being sacrificed frequently was of a poorer quality than the heart of a calm rat. The isolated heart would beat furiously and in most cases the heart had infarcted tissue, or would stop beating, before being cannulated and had to be discarded.

Even if the isolated heart did not show any signs of stress and the isolation protocol was accurately followed, the ventricular cardiomyocyte pellet, at the sedimentation step, would suddenly appear white, indicating a mass of dead cells. Individual rat heart differences can also be seen during the enzyme digestion step, where not one heart takes the same amount of time to digest.

A critical factor is the weight of the rat. Rats above ~ 260 g are ideal for isolations, because the size of the heart and aorta ensures easy dissection and cannulation. The total amount of cardiomyocytes isolated from a bigger rat is much higher than from a smaller and younger rat. Differences between rats that were included in this study were not an issue.

Reliability of isolation

Producing consistent and reliable isolations are very important. Small human errors during the isolation protocol have a great impact on the quality of the isolated cardiomyocytes, which cannot always be identified with the eye. These errors can include: not working sterile, cutting the aorta to short when dissecting, dropping the isolated heart before it is cannulated, not gassing the isolation buffers continuously, forgetting a buffer component, and not accurately following the time period per isolation step as stipulated by the protocol.

Inconsistencies between enzyme batches

The collagenase, used for digestion, when ordered is delivered in different batch numbers, with batch variance. It is important to test the new enzyme batch to determine the efficacy and digestion duration. Not testing the collagenase can result in the hearts not digesting properly and the hearts go to waste. A poor digested heart also reflects in poor quality cardiomyocytes with low average cell viability after isolation and experiments. Yet, high cell viability was achieved 6 years prior when new enzyme batches were tested, and it is unlikely that there would be a problem with new batches. Consequently, we did not test new collagenase batches, although we should have just to confirm the efficacy of the enzyme. Some of the hearts used in this study did not digest completely, but high cell viability was still achieved with the cells that could dissociate.

Quality of cells

The quality of the isolated cardiomyocytes is determined directly after isolation by evaluating cell viability. Cell viability should be above 70 % to yield cardiomyocytes of a high quality, and below 65 % is not accepted. However, after the perfusion system went through an acid and water wash, the cell viability is usually very low, and only after 4 or 5 hearts are isolated can a high quality be achieved again. Cell viability for this study was between 75 – 88 %, which is satisfactory, compared to the 70 % (2005) and 85 % (2008) achieved by Das and colleagues.

Cell viability determined after isolation, after culturing and during I/R

The quality of the cardiomyocytes is determined directly after isolation by evaluating cell viability. The cardiomyocytes are then plated and cultured overnight in the incubator. It is critical that the quality of the cardiomyocytes is confirmed under the light microscope the next day before conducting experiments. The cardiomyocytes should also be evaluated under the light microscope during an experiment, to determine if the period of I/R or H/R was effective. More importantly, cells could wash off during an experiment, and evaluating the plate under the microscope throughout the experiment can determine when the cells started to wash off. The cultured cardiomyocytes are extremely

susceptible to infections, which emphasizes the importance of working sterile. Infected cardiomyocytes cannot be used for experiments. Occasionally in our laboratory plates with infected cardiomyocytes, after a successful isolation the previous day, had to be thrown away.

Sensitivity of adhesive

The L/E, stored at -20 °C, is temperature sensitive and dilution thereof must be done on ice to avoid gel formation. If the L/E is not diluted accurately the cardiomyocytes will not adhere, resulting in cardiomyocytes simply washing away during the experiment.

Time of day experiments are done

The time of day the experiments are conducted could affect the quality of the experimental results, where experiments later in the day might result in weaker cells, since the cells are still cultured in the same buffer from the previous day. To be consistent, it is important that for a set of experiments each experimental day starts at the same time. If experiments will be done later in the day, it might be beneficial to, in the morning, remove the buffer the cells were cultured in overnight and to overlay with fresh culturing buffer. The experiments in this study were not always conducted at the same time of day and might have had an impact on the results.

The effect of pH change

The pH of the culturing buffer is set at 7.4 and has a pink alkali colour. Frequently, after overnight incubation, when the culturing buffer was removed, the buffer had a yellow colour, which indicates an acidic solution. The plates are incubated overnight with 5 % CO₂, and it is possible that the CO₂ reacts with the buffer to decrease the pH. Culturing the cardiomyocytes too long in this acidic buffer could induce injury, where the normoxic cells appeared to have undergone I/R.

Delay between buffer preparation with treatments and administration thereof

The normoxic wash can be made fresh at the beginning of each experimental week. The ischemic/hypoxic buffer, with the supplemented drug treatments, should be made fresh directly before ischemia/hypoxia is induced. It is a problem when various different treatments are used in the same experiment, which elongates the buffer preparation time. It is not possible to prepare all of the treatment buffers at the same time, but it is important to determine which treatments take preference and to prepare them last. Preparing the treatment buffers too early in advance can influence drug efficacy and produce misleading experimental results.

CONCLUSION

This study found that 100 μM CBD is cytotoxic, whereas 0.001 μM and 1 μM CBD are tolerated by isolated adult rat cardiomyocytes. Cell viability according to morphology found that per-treatment with PDE5 inhibitor, or the administration of different CBD concentrations, during ischemia only or continuously during ischemia and reperfusion, did not stimulate cardioprotection.

Length as a morphometry measurement was quantified, where length $\geq 55 \mu\text{m}$ indicates viable cells in a cardiomyocyte population. Morphology selection was proven to be biased and unreliable when compared to the morphometry selections, length $\geq 55 \mu\text{m}$ and $L/W \geq 1.5$. With morphometry measurements the human aspect is removed and the results are consistent and reliable. Length $\geq 55 \mu\text{m}$ was found to be a more sensitive selection than $L/W \geq 1.5$ and can be used to evaluate a total cardiomyocyte population.

The average cell length for the CBD and PDE5 inhibition experiments were evaluated, but cardioprotection was not found. Re-evaluating the average cell viability for CBD and PDE5 inhibition with length $\geq 55 \mu\text{m}$ could also not detect any cardioprotection.

The ischemia induced, for 20 min with 10 mM SDT and for 60 min with 5 mM SDT, was too harsh and the cardiomyocytes were injured beyond the ability of the treatments to stimulate protection. In contrast, the injury induced by hypoxia compared to the normoxic population was not harsh enough and did not induce satisfactory damage.

RECOMMENDATIONS

Simulated ischemia should be induced with a SDT concentration below 10 mM, possibly between 1 - 3 mM, which needs to be optimized. Hypoxia also needs to be optimized. The experiments should be repeated with the new optimized SDT concentration and with the optimized hypoxia. A more extensive titration of CBD concentrations between 1 μ M and 100 μ M should be done to determine the optimum concentration that can induce cardioprotection.

Straight line measurement can be used to measure both the R/G fluorescence and length of a cell to evaluate a total cardiomyocyte population. Morphometry analysis, with length ≥ 55 μ m as measurement, should be used to analyse an injured cardiomyocyte population, and morphology analysis should be avoided.

REFERENCE LIST

- Abadji, V., Lucas-Lenard, J.M., Chin, C., & Kendall, D.A. 1999. Involvement of the carboxyl terminus of the third intracellular loop of the cannabinoid CB1 receptor in constitutive activation of G_s. *Journal of Neurochemistry*, 72:2032-2038.
- Abdallah, Y., Gkatzoflia, A., Gligorievski, D., Kasseckert, S., Euler, G., et al. 2006. Insulin protects cardiomyocytes against reoxygenation-induced hypercontracture by a survival pathway targeting SR Ca²⁺ storage. *Cardiovascular Research*, 70(2):346–353.
- Abi-Gerges, N., Ji, G.J., Lu, Z.J., Fischmeister, R., Hescheler, J., et al. 2000. Functional expression and regulation of the hyperpolarization activated non-selective cation current in embryonic stem cell-derived cardiomyocytes. *Journal of Physiology*, 523(2):377–389.
- Ahmad, N., Wang, Y., Ali, A.K., & Ashraf, M. 2009. Long-acting phosphodiesterase-5 inhibitor, tadalafil, induces sustained cardioprotection against lethal ischemic injury. *American Journal of Physiology Heart and Circulatory Physiology*, 297(1):H387–H391.
- Avkiran, M., & Marber, M.S. 2002. Na⁺/H⁺ exchange inhibitors for cardioprotective therapy: progress, problems and prospects. *Journal of the American College of Cardiology*, 39(5):747–753.
- Beavo, J.A. 1995. Cyclic nucleotide phosphodiesterases: functional implications of multiple isoforms. *Physiological Reviews*, 75(4):725–749.
- Becker, L.C., & Ambrosio, G. 1987. Myocardial consequences of reperfusion. *Progress in Cardiovascular Diseases*, 30(1):23–44.
- Bell, R.M., & Yellon, D.M. 2012. Conditioning the whole heart - not just the cardiomyocyte. *Journal of Molecular and Cellular Cardiology*, 53(1):24–32.
- Bender, A.T., & Beavo, J.A. 2006. Cyclic nucleotide phosphodiesterases: molecular regulation to clinical use. *Pharmacological Reviews*, 58(3):488–520.
- Bian, J., Yong, Q.C., Pan, T., Feng, Z., Ali, M.Y., et al. 2005. Role of hydrogen sulphide in the cardioprotection caused by ischemic preconditioning in the rat heart and cardiac myocytes. *American Society for Pharmacology and Experimental Therapeutics*, 1–39.
- Boersma, E., Mercado, N., Poldermans, D., Gardien, M., Vos, J., et al. 2003. Acute myocardial infarction. *Lancet*, 361:847–858.
- Bonz, A., Laser, M., Küllmer, S., Kniesch, S., Babin-Ebell, J., et al. 2003. Cannabinoids acting on CB1 receptors decrease contractile performance in human atrial muscle. *Journal of Cardiovascular Pharmacology*, 41(4):657–664.
- Boston, D., Koyama, T., Rodriguez-Larrain, J., Zou, A., Su, J., et al. 1998. Effects of angiotensin II on intracellular calcium and contracture in metabolically inhibited cardiomyocytes. *Journal of Pharmacology and Experimental Therapeutics*, 285:716–723.

- Bowers, K.C., Allshire, A.P., & Cobbold, P.H. 1992. Bioluminescent measurement in single cardiomyocytes of sudden cytosolic ATP depletion coincident with rigor. *Journal of Molecular and Cellular Cardiology*, 24:213–218.
- Bremer, Y.A., Salloum, F., Ockaili, R., Chou, E., Moskowitz, W.B., et al. 2005. Sildenafil citrate (viagra) induces cardioprotective effects after ischemia/reperfusion injury in infant rabbits. *Pediatric Research*, 57(1):22–27.
- Buja, L.M., Hagler, H.K., & Willerson, J.T. 1988. Altered calcium homeostasis in the pathogenesis of myocardial ischemic and hypoxic injury. *Cell Calcium*, 9:205–217.
- Buja, L.M. 2005. Myocardial ischemia and reperfusion injury. *Cardiovascular Pathology*, 14(4):170–175.
- Cao, C., Chen, M., & Wong, T. 2005. The K_{Ca} channel as a trigger for the cardioprotection induced by kappa-opioid receptor stimulation – its relationship with protein kinase C. *British Journal of Pharmacology*, 145:984–991.
- Carney, S.T., Lloyd, M.L., MacKinnon, S.E., Newton, D.C., Jones, J.D., et al. 2009. Cannabinoid regulation of nitric oxide synthase I (nNOS) in neuronal cells. *Journal of Neuroimmune Pharmacology*, 4:338–349.
- Castro, L.R.V., Schittl, J., & Fischmeister, R. 2010. Feedback control through cGMP-dependent protein kinase contributes to differential regulation and compartmentation of cGMP in rat cardiac myocytes. *Circulation Research*, 107:1232–1240.
- Cawley, S.M., Sawyer, C.L., Brunelle, K.F., van der Vliet, A., & Dostmann, W.R. 2007. Nitric oxide-evoked transient kinetics of cyclic GMP in vascular smooth muscle cells. *Cellular Signalling*, 19:1023–1033.
- Chanoit, G., Lee, S., Xi, J., Zhu, M., McIntosh, R.A., et al. 2008. Exogenous zinc protects cardiac cells from reperfusion injury by targeting mitochondrial permeability transition pore through inactivation of glycogen synthase kinase-3 β . *American Journal of Physiology Heart and Circulatory Physiology*, 295(3):H1227–H1233.
- Chesley, A., Lundberg, M.S., Asai, T., Xiao, R., Ohtani, S., et al. 2000. The β_2 -adrenergic receptor delivers an antiapoptotic signal to cardiac myocytes through G_i -dependent coupling to phosphatidylinositol 3'-kinase. *Circulation Research*, 87:1172–1179.
- Choi, D.E., Jeong, J.Y., Lim, B.J., Chung, S., Chang, Y.K., et al. 2009. Pretreatment of sildenafil attenuates ischemia-reperfusion renal injury in rats. *American Journal of Physiology Renal Physiology*, 297:F362–F370.
- Christ, T., Galindo-Tovar, A., Thoms, M., Ravens, U., & Kaumann, A.J. 2009. Inotropy and L-type Ca^{2+} current, activated by β_1 - and β_2 -adrenoceptors, are differently controlled by phosphodiesterases 3 and 4 in rat heart. *British Journal of Pharmacology*, 156(1):62–83.

- Communal, C., Singh, K., Sawyer, D.B., & Colucci, W.S. 1999. Opposing effects of β 1- and β 2-adrenergic receptors on cardiac myocyte apoptosis: role of a pertussis toxin – sensitive G protein. *Circulation*, 100:2211–2212.
- Das, A., Durrant, D., Salloum, F.N., Xi, L., & Kukreja, R.C. 2015. PDE5 inhibitors as therapeutics for heart disease, diabetes and cancer. *Pharmacology and Therapeutics*, 147:12–21.
- Das, A., Maulik, N., Das, D.K., Kadowitz, P.J., & Bivalacqua, T.J. 2002. Cardioprotection with sildenafil, a selective inhibitor of cyclic 3',5'-monophosphate-specific phosphodiesterase 5. *Drugs under Experimental and Clinical Research*, 28(6):213–219.
- Das, A., Salloum, F.N., Xi, L., Rao, Y.J., & Kukreja, R.C. 2009. ERK phosphorylation mediates sildenafil-induced myocardial protection against ischemia-reperfusion injury in mice. *American Journal of Physiology Heart and Circulatory Physiology*, 296(5):H1236–H1243.
- Das, A., Smolenski, A., Lohmann, S.M., & Kukreja, R.C. 2006. Cyclic GMP-dependent protein kinase α attenuates necrosis and apoptosis following ischemia/reoxygenation in adult cardiomyocyte. *Journal of Biological Chemistry*, 281(50):38644–38652.
- Das, A., Xi, L., & Kukreja, R.C. 2005. Phosphodiesterase-5 inhibitor sildenafil preconditions adult cardiac myocytes against necrosis and apoptosis: essential role of nitric oxide signaling. *Journal of Biological Chemistry*, 280(13):12944–12955.
- Das, A., Xi, L., & Kukreja, R.C. 2008. Protein kinase G-dependent cardioprotective mechanism of phosphodiesterase-5 inhibition involves phosphorylation of ERK and GSK3 β . *Journal of Biological Chemistry*, 283(43):29572–29585.
- Dayton, W.R., Reville, W.J., Goll, D.E., & Stromer, M.H. 1976. A Ca^{2+} -activated protease possibly involved in myofibrillar protein turnover. Partial characterization of the purified enzyme. *Biochemistry*, 15(10):2159–2167.
- Dennis, S.C., Gevers, W., & Opie, L.H. 1991. Protons in ischemia: where do they come from; where do they go to? *Journal of Molecular and Cellular Cardiology*, 23:1077–1086.
- Di Filippo, C., Rossi, F., Ross, S., & D'Amico, M., 2004. Cannabinoid CB2 receptor activation reduces mouse myocardial ischemia-reperfusion injury: involvement of cytokine/chemokines and PMN. *Journal of Leukocyte Biology*, 75(3):453–459.
- Ding, B., Abe, J.I., Wei, H., Huang, Q., Walsh, R.A., et al. 2005. Functional role of phosphodiesterase 3 in cardiomyocyte apoptosis: implication in heart failure. *Circulation*, 111(19):2469–2476.
- Dodge-Kafka, K.L., Langeberg, L., & Scott, J.D. 2006. Compartmentation of cyclic nucleotide signaling in the heart: the role of A-kinase anchoring proteins. *Circulation Research*, 98(8):993–1001.
- Downey, J.M., & Cohen, M.V. 2006. Reducing infarct size in the setting of acute myocardial infarction. *Progress in Cardiovascular Diseases*, 48(5):363–371.

- du Toit, E.F., Rossouw, E., Salie, R., Opie, L.H., & Lochner, A. 2005. Effect of sildenafil on reperfusion function, infarct size, and cyclic nucleotide levels in the isolated rat heart model. *Cardiovascular Drugs and Therapy*, 19:23–31.
- Durst, R., Danenberg, H., Gallily, R., Mechoulam, R., Meir, K., et al. 2007. Cannabidiol, a nonpsychoactive cannabis constituent, protects against myocardial ischemic reperfusion injury. *American Journal of Physiology Heart and Circulatory Physiology*, 293:3602–3607.
- Fehrer, J.J., Briggs, F.N., & Hess, M.L. 1980. Characterization of cardiac sarcoplasmic reticulum from ischemic myocardium: comparison of isolated sarcoplasmic reticulum with unfractionated homogenates. *Journal of Molecular and Cellular Cardiology*, 12:427–432.
- Feng, Y., Chen, F., Yin, T., Xia, Q., Liu, Y., et al. 2015. Pharmacologic effects of cannabidiol on acute reperfused myocardial infarction in rabbits: evaluated with 3.0T cardiac magnetic resonance imaging and histopathology. *Journal of Cardiovascular Pharmacology*, 66(4):354-363.
- Finegold, J.A., Asaria, P., & Francis, D.P. 2013. Mortality from ischaemic heart disease by country, religion, and age: statistics from World Health Organisation and United Nations. *International Journal of Cardiology*, 168(2):934-945.
- Fischer, Y., Rose, H., & Kammermeier, H. 1991. Highly insulin-responsive isolated rat heart muscle cells yielded by a modified isolation method. *Life Sciences*, 49:1679–1688.
- Fischmeister, R., Castro, L.R.V., Abi-Gerges, A., Rochais, F., Jurevicius, J., et al. 2006. Compartmentation of cyclic nucleotide signaling in the heart: the role of cyclic nucleotide phosphodiesterases. *Circulation Research*, 99(8):816–828.
- Fischmeister, R., Mery, P., Pavione, C., & Pecker, F. 1995. Erythro-9-(2-hydroxy-3-nonyl)adenine inhibits cyclic GMP-stimulated phosphodiesterase in isolated cardiac myocytes. *Molecular Pharmacology*, 1:121–130.
- Formukong, E.A., Evens, A.T., & Evans, F.J. 1989. The inhibitory effects of cannabinoids, the active constituents of cannabis sativa L. on human and rabbit platelet aggregation. *The Journal of Pharmacy and Pharmacology*, 41:705–709.
- Francis, S.H. 2010. The role of cGMP-dependent protein kinase in controlling cardiomyocyte cGMP. *Circulation Research*, 107(10):1164–1166.
- Francis, S.H., Blount, M.A., & Corbin, J.D. 2011. Mammalian cyclic nucleotide phosphodiesterases: molecular mechanisms and physiological functions. *Physiological Reviews*, 91(2):651–690.
- Gao, Y., Lv, J., Lin, Y., Li, X., Wang, L., et al. 2014. Effects of β -adrenoceptor subtypes on cardiac function in myocardial infarction rats exposed to fine particulate matter (PM_{2.5}). *BioMed Research International*, 1–22.

- Gauthier, C., Leblais, V., Kobzik, L., Trochu, J., Khandoudi, N., et al. 1998. The negative inotropic effect of β_3 -adrenoceptor stimulation is mediated by activation of a nitric oxide synthase pathway in human ventricle. *The Journal of Clinical Investigation*, 102(7):1377–1384.
- Gebremedhin, D., Lange, A.R., Campbell, W.B., Hillard, C.J., & Harder, D.R. 1999. Cannabinoid CB1 receptor of cat cerebral arterial muscle functions to inhibit L-type Ca^{2+} channel current. *The American Physiological Society*, 276:2085–2093.
- Geisbuhler, T.P., Schwager, T.L., & Ervin, H.D. 2002. 3-Isobutyl-1-methylxanthine (IBMX) sensitizes cardiac myocytes to anoxia. *Biochemical Pharmacology*, 63(11):2055–2062.
- Glass, M., & Felder, C.C. 1997. Concurrent stimulation of cannabinoid CB1 and dopamine D2 receptors augments cAMP accumulation in striatal neurons: evidence for a G_s linkage to the CB1 receptor. *The Journal of Neuroscience*, 17(14):5327–5333.
- Götz, K.R., Sprenger, J.U., Perera, R.K., Steinbrecher, J.H., Lehnart, S.E., et al. 2014. Transgenic mice for real-time visualization of cGMP in intact adult cardiomyocytes. *Circulation Research*, 114(8):1235–1245.
- Hanoune, J., & Defer, N. 2001. Regulation and role of adenylyl cyclase isoforms. *Annual Reviews Pharmacology Toxicology*, 41:145–174.
- Hausenloy, D.J., & Yellon, D.M. 2003. The mitochondrial permeability transition pore: its fundamental role in mediating cell death during ischaemia and reperfusion. *Journal of Molecular and Cellular Cardiology*, 35(4):339–341.
- Hausenloy, D.J., & Yellon, D.M. 2011. The therapeutic potential of ischemic conditioning: an update. *Nature Reviews*, 8(11):619–629.
- Hausenloy, D.J., & Yellon, D.M. 2013. Myocardial ischemia-reperfusion injury: a neglected therapeutic target. *The Journal of Clinical Investigation*, 123(1):92–100.
- Hearse, D.J. 1977. Reperfusion of the ischemic myocardium. *Journal of Molecular and Cellular Cardiology*, 9(8):605–616.
- Hepburn, C.Y. 2014. PhD thesis: studies investigating the mechanism of the cardioprotective effects of cannabidiol. 1 – 231.
- Hillard, C.J. 2000. Endocannabinoids and vascular function. *The Journal of Pharmacology and Experimental Therapeutics*, 294(1):27–32.
- Ho, J.C.S., Wu, S., Kam, K.W.L., Sham, J.S.K., & Wong, T.M. 2002. Effects of pharmacological preconditioning with U50488H on calcium homeostasis in rat ventricular myocytes subjected to metabolic inhibition and anoxia. *British Journal of Pharmacology*, 137:739–748.
- Howlett, A.C., Barth, F., Bonner, T.I., Cabral, G., Casellas, P., et al. 2002. International union of pharmacology. XXVII. Classification of cannabinoid receptors. *Pharmacological Reviews*, 54(2):161–202.

- Hu, Y., Chen, X., Pan, T., Neo, K.L., Lee, S.W., et al. 2008. Cardioprotection induced by hydrogen sulfide preconditioning involves activation of ERK and PI3K/Akt pathways. *European Journal of Physiology*, 455:607–616.
- Huang, M.H., Wu, Y., Nguyen, V., Rastogi, S., McConnell, B.K., et al. 2011. Heart protection by combination therapy with esmolol and milrinone at late-ischemia and early reperfusion. *Cardiovascular Drugs and Therapy*, 25(3):223–232.
- Imahashi, K., Pott, C., Goldhaber, J.I., Steenbergen, C., Philipson K.D., & Murphy, E. 2005. Cardiac-specific ablation of the Na⁺-Ca²⁺ exchanger confers protection against ischemia/reperfusion injury. *Circulation Research*, 97:916-921.
- Ishikawa, Y., & Homcy, C.J. 1997. The adenylyl cyclases as integrators of transmembrane signal transduction. *Circulation Research*, 80(3):297-304.
- Isidori, A.M., Cornacchione, M., Barbagallo, F., Di Grazia, A., Barrios, F., et al. 2015. Inhibition of type 5 phosphodiesterase counteracts β 2-adrenergic signalling in beating cardiomyocytes. *Cardiovascular Research*, 106(3):408–420.
- Johnson, W.B., Katugampola, S., Able, S., Napier, C., & Harding, S.E. 2012. Profiling of cAMP and cGMP phosphodiesterases in isolated ventricular cardiomyocytes from human hearts: comparison with rat and guinea pig. *Life Sciences*, 90:328–336.
- Kabaeva, Z., Zhao, M., & Michele, D.E. 2008. Blebbistatin extends culture life of adult mouse cardiac myocytes and allows efficient and stable transgene expression. *American Journal of Physiology - Heart and Circulatory Physiology*, 294:H1667–H1674.
- Kamentsky, L., Jones, T., Fraser, A., Bray, M., Logan, D., et al. 2011. Improved structure, function, and compatibility for CellProfiler: modular high-throughput image analysis software. *Bioinformatics*, 27(8):1179–1180.
- Kass, D.A. 2012. Cardiac role of cyclic-GMP hydrolyzing phosphodiesterase type 5: from experimental models to clinical trials. *Current Heart Failure Reports*, 9(3):192–199.
- Kilgore, K.S., & Lucchesi, B.R. 1993. Reperfusion injury after myocardial infarction: the role of free radicals and the inflammatory response. *Clinical Biochemistry*, 26(5):359–370.
- Kirstein, M., Rivet-Bastide, M., Hatem, S., Bénardeau, A., Mercadier, J., et al. 1995. Nitric oxide regulates the calcium current in isolated human atrial myocytes. *The Journal of Clinical Investigation*, 95(2):794–802.
- Knight, W., & Yan, C. 2013. Therapeutic potential of PDE modulation in treating heart disease. *Future Medicinal Chemistry*, 5(14):1607–1620.
- Krylatov, A.V., Ugdyzhekova, D.S., Bernatskaya, N.A., Maslov, L.N., Mekhoulam, R., et al. 2001. Activation of type II cannabinoid receptors improves myocardial tolerance to arrhythmogenic

- effects of coronary occlusion and reperfusion. *Bulletin of Experimental Biology and Medicine*, 131(6):523–525.
- Kukreja, R.C., Ockaili, R., Salloum, F., Yin, C., Hawkins, J., et al. 2004. Cardioprotection with phosphodiesterase-5 inhibition - a novel preconditioning strategy. *Journal of Molecular and Cellular Cardiology*, 36:165–173.
- Kukreja, R.C., Salloum, F., Das, A., Ockaili, R., Yin, C., et al. 2005. Pharmacological preconditioning with sildenafil: basic mechanisms and clinical implications. *Vascular Pharmacology*, 42:219–232.
- Kumar, P., Francis, G.S., & Tang, W.H.W. 2009. Phosphodiesterase 5 inhibition in heart failure: mechanisms and clinical implications. *Nature Reviews*, 6:349–355.
- Lamontagne, D., Lépicier, P., Lagneux, C., & Bouchard, J.F. 2006. The endogenous cardiac cannabinoid system: a new protective mechanism against myocardial ischemia. *Arch Mal Coeur Vaiss*, 99(3):242–246.
- Lasukova, O.V., Maslov, L.N., Crawford, D., Barth, F., Krylatov, A.V., et al. 2008. Role of cannabinoid receptors in regulation of cardiac tolerance to ischemia and reperfusion. *Biology Bulletin*, 35(4):404–410.
- Lee, D.I., & Kass, D.A. 2012. Phosphodiesterases and cyclic GMP regulation in heart muscle. *Physiology*, 27:248–258.
- Leineweber, K., Bohm, M., & Heusch, G. 2006. Cyclic adenosine monophosphate in acute myocardial infarction with heart failure: slayer or savior? *Circulation*, 114(5):365–367.
- Lohse, M.J., Engelhardt, S., & Eschenhagen, T. 2003. What is the role of β -adrenergic signaling in heart failure? *Circulation Research*, 93(10):896–906.
- Louch, W.E., Sheehan, K.A., & Wolska, B.M. 2011. Methods in cardiomyocyte isolation, culture, and gene transfer. *Journal of Molecular and Cellular Cardiology*, 51(3):288–298.
- Löwe, H., & Jacobsohn, E. 1992. Protection of the hypoxic myocardium by the bispyridine derivatives AWD 122-14 and milrinone: studies on isolated, working right rabbit hearts. *In Vitro*, 47(6):452–455.
- Mamas, M.A., & Terrar, D.A. 1998. Differential sensitivity to cannabidiol of the two components of delayed rectifies potassium currents in guinea pig isolated ventricular myocytes. *British Journal of Pharmacology*, 123:319.
- Maurice, D.H., Palmer, D., Tilley, D.G., Dunkerley, H.A., Netherton, S.J., et al. 2003. Cyclic nucleotide phosphodiesterase activity, expression, and targeting in cells of the cardiovascular system. *Molecular Pharmacology*, 64(3):533–546.
- McConnachie, G., Langeberg, L.K., & Scott, J.D. 2006. AKAP signaling complexes: getting to the heart of the matter. *Trends in Molecular Medicine*, 12(7):317–323.

- Mechoulam, R., Peters, M., Murillo-Rodriguez, E., & Hanus, L.O. 2007. Cannabidiol – recent advances. *Chemistry and Biodiversity*, 4:1678-1692.
- Mendizabal, V.E., & Adler-Graschinsky, E. 2007. Cannabinoids as therapeutic agents in cardiovascular disease: a tale of passions and illusions. *British Journal of Pharmacology*, 151:427–440.
- Miller, C.L., & Yan, C. 2010. Targeting cyclic nucleotide phosphodiesterase in the heart: therapeutic implications. *Journal of Cardiovascular Translational Research*, 3(5):507–515.
- Mokni, W., Keravis, T., Etienne-Selloum, N., Walter, A., Kane, M.O., et al. 2010. Concerted regulation of cGMP and cAMP phosphodiesterases in early cardiac hypertrophy induced by angiotensin II. *PLoS ONE*, 5(12):1–15.
- Mongillo, M., Mcsorley, T., Evellin, S., Sood, A., Lissandron, V., et al. 2004. Fluorescence resonance energy transfer – based analysis of cAMP dynamics in live neonatal rat cardiac myocytes reveals distinct functions of compartmentalized phosphodiesterases. *Circulation Research*, 95:67–76.
- Mongillo, M., Tocchetti, C.G., Terrin, A., Lissandron, V., Cheung, Y., et al. 2006. Compartmentalized phosphodiesterase-2 activity blunts β -adrenergic cardiac inotropy via an NO/cGMP-dependent pathway. *Circulation Research*, 98:226–234.
- Montecucco, F., Lenglet, S., Braunersreuther, V., Burger, F., Pelli, G., et al. 2009. CB2 cannabinoid receptor activation is cardioprotective in a mouse model of ischemia/reperfusion. *Journal of Molecular and Cellular Cardiology*, 46(5):612–620.
- Murphy, E., & Steenbergen, C. 2008. Ion transport and energetics during cell death and protection. *Physiology (Bethesda)*, 23(2):115–23.
- Nikolaev, V.O., Bünemann, M., Schmitteckert, E., Lohse, M.J., & Engelhardt, S. 2006. Cyclic AMP imaging in adult cardiac myocytes reveals far-reaching β 1-adrenergic but locally confined β 2-adrenergic receptor-mediated signaling. *Circulation Research*, 99(10):1084–1091.
- Niu, X., Watts, V.L., Cingolani, O.H., Sivakumaran, V., Leyton-Mange, J.S., et al. 2012. Cardioprotective effect of beta-3 adrenergic receptor agonism: role of neuronal nitric oxide synthase. *Journal of the American College of Cardiology*, 59(22):1979–1987.
- Ockaili, R., Salloum, F., Hawkins, J., & Kukreja, R.C. 2002. Sildenafil (viagra) induces powerful cardioprotective effect via opening of mitochondrial K_{ATP} channels in rabbits. *American Journal of Physiology Heart and Circulatory Physiology*, 283:H1263–H1269.
- Omori, K., & Kotera, J. 2007. Overview of PDEs and their regulation. *Circulation Research*, 100(3):309–327
- Pacher, P., Batkai, S., & Kunos, G. 2005. Blood pressure regulation by endocannabinoids and their receptors. *Neuropharmacology*, 48(8):1130–1138.

- Pertwee, R.G. 2008. The diverse CB1 and CB2 receptor pharmacology of three plant cannabinoids: Δ^9 -tetrahydrocannabinol, cannabidiol and Δ^9 -tetrahydrocannabivarin. *British Journal of Pharmacology*, 153:199–215.
- Piper, H.M., Meuter, K., & Schäfer, C. 2003. Cellular mechanisms of ischemia-reperfusion injury. *Annals of Thoracic Surgery*, 75:S644–S648.
- Rao, Y.J., & Xi, L. 2009. Pivotal effects of phosphodiesterase inhibitors on myocyte contractility and viability in normal and ischemic hearts. *Acta Pharmacologica Sinica*, 30(1):1–24.
- Rechtman, M.P., van der Zyp, A., & Majewski, H. 2000. Amrinone reduces ischaemia-reperfusion injury in rat heart. *European Journal of Pharmacology*, 402:255–262.
- Reimer, K.A., & Ideker, R.E. 1987. Myocardial ischemia and infarction: anatomic and biochemical substrates for ischemic cell death and ventricular arrhythmias. *Human Pathology*, 18(5):462–475.
- Rhee, M., Bayewitch, M., Avidor-Reiss, T., Levy, R., & Vogel, Z. 1998. Cannabinoid receptor activation differentially regulates the various adenylyl cyclase isozymes. *Journal of Neurochemistry*, 71(4):1525–1534.
- Roy, V. 2007. Autacoids : angiotensin, plasma kinins. In *Pharmacology*, 1–35.
- Ruiz-Meana, M., Insete, J., Fernandez-Sanz, C., Hernando, V., Miro-Casas, E., et al. 2011. The role of mitochondrial permeability transition in reperfusion-induced cardiomyocyte death depends on the duration of ischemia. *Basic Research in Cardiology*, 106:1259–1268.
- Salloum, F.N., Ockaili, R.A., Wittkamp, M., Marwaha, V.R., & Kukreja, R.C. 2006. Vardenafil: a novel type 5 phosphodiesterase inhibitor reduces myocardial infarct size following ischemia/reperfusion injury via opening of mitochondrial K_{ATP} channels in rabbits. *Journal of Molecular and Cellular Cardiology*, 40:405–411.
- Salloum, F.N., Takenoshita, Y., Ockaili, R.A., Daoud, V.P., Chou, E., et al. 2007. Sildenafil and vardenafil but not nitroglycerin limit myocardial infarction through opening of mitochondrial K_{ATP} channels when administered at reperfusion following ischemia in rabbits. *Journal of Molecular and Cellular Cardiology*, 42:453–458.
- Salloum, F.N., Yin, C., Xi, L., & Kukreja, R.C. 2003. Sildenafil induces delayed preconditioning through inducible nitric oxide synthase-dependent pathway in mouse heart. *Circulation Research*, 92:595–597.
- Saltman, A.E., Gaudette, G.R., Levitsky, S., & Krukenkamp, I.B. 2000. Amrinone preconditioning in the isolated perfused rabbit heart. *Annals of the New York Academy of Sciences*, 70:609–613.
- Sanada, S., Kitakaze, M., Papst, P., Asanuma, H., Node, K., et al. 2001. Cardioprotective effect afforded by transient exposure to phosphodiesterase III inhibitors: the role of protein kinase A and p38 mitogen-activated protein kinase. *Circulation*, 104:705–710.

- Schneider, C.A., Rasband, W.S., & Eliceiri, K.W. 2012. NIH Image to ImageJ: 25 years of image analysis. *Nat Methods*, 9:671–675.
- Senzaki, H., Smith, C.J., Juang, G.J., Isoda, T., Mayer, S.P., et al. 2001. Cardiac phosphodiesterase 5 (cGMP-specific) modulates β -adrenergic signaling in vivo and is down-regulated in heart failure. *The FASEB Journal*, 15(10):1718–1726.
- Sesti, C., Florio, V., Johnson, E.G., & Kloner, R.A. 2007. The phosphodiesterase-5 inhibitor tadalafil reduces myocardial infarct size. *International Journal of Impotence Research*, 19(1):55–61.
- Shibata, I., Cho, S., Yoshitomi, O., Ureshino, H., Maekawa, T., et al. 2013. Milrinone and levosimendan administered after reperfusion improve myocardial stunning in swine. *Scandinavian Cardiovascular Journal*, 47(1):550–57.
- Shin, S., Kim, T., Lee, H., Kang, J.H., Lee, J.Y., et al. 2014. The switching role of β -adrenergic receptor signalling in cell survival or death decision of cardiomyocytes. *Nature Communications*, 5:1–13.
- Shmist, Y.A., Goncharov, I., Eichler, M., Shneyvays, V., Isaac, A., et al. 2006. Delta-9-tetrahydrocannabinol protects cardiac cells from hypoxia via CB2 receptor activation and nitric oxide production. *Molecular and Cellular Biochemistry*, 283:75–83.
- Spear, J.F., Prabu, S.K., Galati, D., Raza, H., Anandatheerthavarada, H.K., et al. 2007. β 1-Adrenoreceptor activation contributes to ischemia-reperfusion damage as well as playing a role in ischemic preconditioning. *American Journal of Physiology Heart and Circulatory Physiology*, 292(5):H2459–H2466.
- Stapleton, M.T., & Allshire, A.P. 1998. Modulation of rigor and myosin ATPase activity in rat cardiomyocytes. *Journal of Molecular and Cellular Cardiology*, 30:1349–1358.
- Steffens, S., & Pacher, P. 2012. Targeting cannabinoid receptor CB2 in cardiovascular disorders: promises and controversies. *British Journal of Pharmacology*, 167:313–323.
- Takashi, E., Wang, Y., & Ashraf, M. 1999. Integrative physiology activation of mitochondrial K_{ATP} channel elicits late preconditioning against myocardial infarction via protein kinase C signaling pathway. *Circulation Research*, 85:1146–1153.
- Takimoto, E. 2012. Cyclic GMP-dependent signaling in cardiac myocytes. *Circulation Journal*, 76(8):1819–1825.
- Takimoto, E., Champion, H.C., Belardi, D., Moslehi, J., Mongillo, M., et al. 2005. cGMP catabolism by phosphodiesterase 5A regulates cardiac adrenergic stimulation by NOS3-dependent mechanism. *Circulation Research*, 96(1):100–109.
- Thomas, A., Baillie, G.L., Phillips, A.M., Razdan, R.K., Ross, R.A., et al. 2007. Cannabidiol displays unexpectedly high potency as an antagonist of CB1 and CB2 receptor agonists *in vitro*. *British Journal of Pharmacology*, 150(5):613–623.

- Tomita, H., Nazmy, M., Kajimoto, K., Yehia, G., Molina, C.A., et al. 2003. Inducible cAMP early repressor (ICER) is a negative-feedback regulator of cardiac hypertrophy and an important mediator of cardiac myocyte apoptosis in response to β -adrenergic receptor stimulation. *Circulation Research*, 93(1):12–22.
- Ufer, C., & Germack, R. 2009. Cross-regulation between β 1- and β 3-adrenoceptors following chronic β -adrenergic stimulation in neonatal rat cardiomyocytes. *British Journal of Pharmacology*, 158:300–313.
- Ugdyzhkova, D.S., Bernatskaya, N.A., Stefano, J.B., Graier, V.F., Tam, S.W., et al. 2001. Endogenous cannabinoid anandamide increases heart resistance to arrhythmogenic effects of epinephrine: role of CB1 and CB2 receptors. *Bulletin of Experimental Biology and Medicine*, 131(3):251–253.
- Vandecasteele, G., Verde, I., Rücker-Martin, C., Donzeau-Gouge, P., & Fischmeister, R. 2001. Cyclic GMP regulation of the L-type Ca^{2+} channel current in human atrial myocytes. *Journal of Physiology*, 533:329–340.
- Vandenwijngaert, S., Pokreisz, P., Hermans, H., Gillijns, H., Pellens, M., et al. 2013. Increased cardiac myocyte PDE5 levels in human and murine pressure overload hypertrophy contribute to adverse LV remodeling. *PLoS ONE*, 8(3):1–9.
- Wagner, J.A., Varga, K., & Kunos, G. 1998. Cardiovascular actions of cannabinoids and their generation during shock. *Journal of Molecular Medicine*, 76(12):824–836.
- Walsh, S.K., Hepburn, C.Y., Kane, K.A., & Wainwright, C.L. 2010. Acute administration of cannabidiol *in vivo* suppresses ischaemia-induced cardiac arrhythmias and reduces infarct size when given at reperfusion. *British Journal of Pharmacology*, 160:1234–1242.
- Watson, D.C., Sargianou, M., Leivaditis, V., & Anagnostopoulos, C. 2013. Beta2-adrenergic activation via administration of atenolol/formoterol combination increases contractility and coronary blood flow in isolated rat hearts. *Hellenic Journal of Cardiology*, 54:341–347.
- Watts, V.L., Sepulveda, F.M., Cingolani, O.H., Ho, A.S., Niu, X., et al. 2013. Anti-hypertrophic and anti-oxidant effect of beta3-adrenergic stimulation in myocytes requires differential neuronal NOS phosphorylation. *Journal of Molecular and Cellular Cardiology*, 62:8–17.
- Webster, I., du Toit, E.F., Huisamen, B., & Lochner, A. 2012. The effect of creatine supplementation on myocardial function, mitochondrial respiration and susceptibility to ischaemia/reperfusion injury in sedentary and exercised rats. *Acta Physiology*, 206:6–19.
- Wechsler, J., Choi, Y.H., Krall, J., Ahmad, F., Manganiello, V.C., et al. 2002. Isoforms of cyclic nucleotide phosphodiesterase PDE3A in cardiac myocytes. *Journal of Biological Chemistry*, 277(41):38072–38078.

- Weeks, J.L., Zoraghi, R., Beasley, A., Sekhar, K.R., Francis, S.H., et al. 2005. High biochemical selectivity of tadalafil, sildenafil and vardenafil for human phosphodiesterase 5A1 (PDE5) over PDE11A4 suggests the absence of PDE11A4 cross-reaction in patients. *International Journal of Impotence Research*, 17(1):5–9.
- Wei, G., Zhou, J., Wang, B., Wu, F., Bi, H., et al. 2007. Diastolic Ca^{2+} overload caused by $\text{Na}^+/\text{Ca}^{2+}$ exchanger during the first minutes of reperfusion results in continued myocardial stunning. *European Journal of Pharmacology*, 572:1–11.
- Wen, J.F., Cui, X., Jin, J.Y., Kim, S.M., Kim, S.Z., et al. 2004. High and low gain switches for regulation of cAMP efflux concentration: distinct roles for particulate GC- and soluble GC-cGMP-PDE3 signaling in rabbit atria. *Circulation Research*, 94:935–943.
- Wills, L.P., Trager, R.E., Beeson, G.C., Lindsey, C.C., Peterson, Y.K., et al. 2012. The β_2 -adrenoceptor agonist formoterol stimulates mitochondrial biogenesis. *The Journal of Pharmacology and Experimental Therapeutics*, 342(1):106–118.
- Xiao, R., Avdonin, P., Zhou, Y., Cheng, H., Akhter, S.A., et al. 1999. Coupling of β_2 -adrenoceptor to G_i proteins and its physiological relevance in murine cardiac myocytes. *Circulation Research*, 84:43–52.
- Xin, P., Zhu, W., Li, J., Ma, S., Wang, L., et al. 2010. Combined local ischemic postconditioning and remote preconditioning recapitulate cardioprotective effects of local ischemic preconditioning. *American Journal of Physiology Heart and Circulatory Physiology*, 298(6):H1819–H1831.
- Yanaka, N., Kurosawa, Y., Minami, K., Kawai, E., & Omori, K. 2003. cGMP-phosphodiesterase activity is up-regulated in response to pressure overload of rat ventricles. *Bioscience, Biotechnology and Biochemistry*, 67(5):973–979.
- Yeung, H.M., Kravtsov, G.M., Ng, K.M., Wong, T.M., & Fung, M.L. 2007. Chronic intermittent hypoxia alters Ca^{2+} handling in rat cardiomyocytes by augmented $\text{Na}^+/\text{Ca}^{2+}$ exchange and ryanodine receptor activities in ischemia-reperfusion. *American Journal of Cell Physiology*, 292:2046–2056.
- Yu, Q., Si, R., Zhou, N., Zhang, H., Guo, W., et al. 2008. Insulin inhibits β -adrenergic action in ischemic/reperfused heart: a novel mechanism of insulin in cardioprotection. *Springer*, 13(2):305–317.
- Zaccolo, M., & Movsesian, M.A. 2007. cAMP and cGMP signaling cross-talk: role of phosphodiesterases and implications for cardiac pathophysiology. *Circulation Research*, 100(11):1569–1578.
- Zaccolo, M. 2006. Phosphodiesterases and compartmentalized cAMP signalling in the heart. *European Journal of Cell Biology*, 85(7):693–697.

- Zaccolo, M., Cesetti, T., Di Benedetto, G., Mongillo, M., Lissandron, V., et al. 2005. Imaging the cAMP-dependent signal transduction pathway. *Biochemical Society Transactions*, 33:1323–1326.
- Zaccolo, M., Di Benedetto, G., Lissandron, V., Mancuso, L., Terrin, A., et al. 2006. Restricted diffusion of a freely diffusible second messenger: mechanisms underlying compartmentalized cAMP signalling. *Biochemical Society Transactions*, 34(4):495–497.
- Zaccolo, M., Magalhães, P., & Pozzan, T. 2002. Compartmentalisation of cAMP and Ca²⁺ signals. *Current Opinion in Cell Biology*, 14(2):160–166.
- Zhang, M., Koitabashi, N., Nagayama, T., Rambaran, R., Feng, N., et al. 2008. Expression, activity, and pro-hypertrophic effects of PDE5A in cardiac myocytes. *Cellular Signalling*, 20(12):2231–2236.
- Zoller, O., Rhyn, P., & Zimmerli, B. 2000. High-performance liquid chromatographic determination of Δ^9 -tetrahydrocannabinol and the corresponding acid in hemp containing foods with special regard to the fluorescence properties of Δ^9 -tetrahydrocannabinol. *Journal of Chromatography A*, 872:101–110.
- Zoratti, C., Kipmen-Korgun, D., Osibow, K., Malli, R., & Graier, W.F. 2003. Anandamide initiates Ca²⁺ signaling via CB2 receptor linked to phospholipase C in calf pulmonary endothelial cells. *British Journal of Pharmacology*, 140:1351–1362.
- Zucchi, R., Poddighe, R., Mariani, M., & Ronca, G. 1990. Effect of amrinone in the working rat heart: influence of ischaemic damage, adenosine and calcium. *Drugs under Experimental and Clinical Research*, 16(4):187–195.